TRANSMISSION DYNAMICS OF MOSQUITO-BORNE DISEASES: MODELING, ANALYSIS, PREDICTION AND CONTROL

YIYUAN WANG

A DISSERTATION SUBMITTED TO
THE FACULTY OF GRADUATE STUDIES
IN PARTIAL FULFILMENT OF THE REQUIREMENTS
FOR THE DEGREE OF
DOCTOR OF PHILOSOPHY

GRADUATE PROGRAM IN MATHEMATICS AND STATISITICS
YORK UNIVERSITY
TORONTO, ONTARIO

December 2018

Abstract

Mosquito-borne diseases (MBD), such as West Nile virus (WNV), dengue, and Zika virus, have become a significant global health burden for human society. Complex factors, including weather conditions, anthropogenic land use and vector-virus-host interactions, greatly affect the mosquito abundance and distribution, and the disease transmission process. In this dissertation, I will investigate the mosquito population dynamics and transmission dynamics of MBDs, and explore how these factors play roles in the MBDs. Particularly, we use WNV and *Culex* mosquitoes (WNV vectors) in the Region of Peel, Ontario, Canada, as an example for this study.

We first study single species population models for the mosquito and the bird respectively. For mosquitoes, we take into account the contribution of the mosquito feeding preference to the oviposition and the intraspecific competition among preadult mosquitoes. For birds, we summarize the impacts of bird species, migration and age states on the transmission of WNV and explore the influence of WNV on bird populations.

Then we establish a model to track the number of mosquitoes collected in a trap, pre-

dict mosquito trap counts and real adult mosquito population in an effective trapping zone. We consider the trapping mechanism of a CDC light trap and collecting procedure, and show how weather, mosquito and host selecting behaviors affect the trap counts.

To explore the transmission dynamics of WNV, we develop a single-season mosquito-bird model considering stormwater management ponds, temperature and precipitation. We reveal that moderate temperature and precipitation, weaker intraspecific competition will increase the mosquito population and consequently the potential for an outbreak. This work can be used to guide WNV programs in local health units where monitoring standing water and larviciding is often used to control mosquito populations and the spread of WNV.

To investigate backward bifurcation, threshold dynamics and outbreak recurrence mechanisms, we propose improved mosquito-bird compartment models. We define a new risk index to characterize the potential risk of WNV infections. We also develop the risk assessment criteria, which can be helpful to determine the risk level if there is an outbreak. Our evaluation results are generally consistent with results based on the minimum infection rate.

Acknowledgements

I would like to express my sincere gratitude to my supervisor Professor Huaiping Zhu, whose encouragement, guidance and support from the initial to the final level enabled me to develop an understanding of the subject.

My sincere thanks also go to the committee members: Professor Neal Madras and Professor Jane Heffernan, for their insightful comments and encouragement, but also for the question which incented me to widen my research from various perspectives.

I am also heartily thankful to my parents for their love, understanding and support throughout my doctoral studies and my life.

Last but not least, I offer my regards and blessings to all of those who encouraged and supported me in any respect during the completion of the dissertation.

Table of Contents

List of Tables

List of Figures

1 Introduction

1.1 Mosquito-borne diseases

Mosquito-borne diseases (MBDs) are diseases caused by parasites, viruses and bacteria including Chikungunya virus, dengue virus, Eastern Equine Encephalitis virus (EEEV), Japanese Encephalitis (JE) virus, La Crosse Encephalitis virus (LACV), Malaria, St. Louis Encephalitis virus (SLEV), West Nile virus (WNV), Yellow Fever and Zika virus diseases (Zika). Diseases are transmitted by the bite of an infected mosquito from one human or animal to another (World Health Organization (2017), Centers for Disease Control and Prevention (2016b)).

MBDs have made a substantial contribution to the global burden for human society; around 700 million people get infected each year and over a million die from MBDs (Caraballo and King (2014)). Transmission and distribution of MBDs are determined by mosquito species, transmission cycles, demographic and social factors. For most MBDs, there is no vaccine against human infections and no specific treatment for diseases. Trans-

mission, symptoms, distribution and treatment of Chikungunya, dengue virus, WNV and other seven MBDs are presented in Table 1.1.

Table 1.1: Mosquito-borne diseases (Centers for Disease Control and Prevention (2016b), Centers for Disease Control and Prevention (2018), Public Health Ontario (2014), Bennett et al. (2008), Kopp et al. (2013), World Health Organization (2016))

Chikungunya virus	
Transmission	Transmitted between people by *Aedes aegypti* and *Aedes albopictus* mosquitoes
Symptoms	Fever and joint pain (most common symptoms), muscle pain, headache, nausea, fatigue and rash
Distribution	Africa, Asia, Europe, and the Indian and Pacific Oceans, Americas
Treatment	No vaccine to prevent or medicine to treat chikungunya virus infection
Dengue virus	
Transmission	Transmitted between people by *Aedes aegypti* and *Aedes albopictus* mosquitoes

Symptoms	High fever and at least two of the following: severe headache and eye pain (behind eyes), joint pain, muscle and/or bone pain, rash, mild bleeding manifestation (e.g., nose or gum bleed, petechiae, or easy bruising), low white cell count
Distribution	The tropics and subtropics, Asia, the Pacific, the Americas, Africa, and the Caribbean
Treatment	No specific medication for treatment of a dengue infection

Eastern Equine Encephalitis virus (EEEV)

Transmission	maintained in a cycle involving *Culiseta melanura* mosquitoes and avian hosts; horses and humans (transmitted by *Aedes*, *Coquillettidia*, and *Culex* species) are dead-end hosts.
Symptoms	No apparent illness for most persons infected with EEEV; severe cases of EEE (involving encephalitis, an inflammation of the brain) beginning with the sudden onset of headache, high fever, chills, and vomiting, then may progress into disorientation, seizures, or coma.
Distribution	United States (most cases occurring in the Atlantic and Gulf Coast states) and southeastern Canada

Treatment	No human vaccine against EEEV infection or specific treatment for EEE
Japanese Encephalitis (JE)	
Transmission	Circulating between *Culex* species mosquitoes (particularly *Culex tritaeniorhynchus* mosquitoes) and vertebrate hosts, mainly pigs and wading birds; humans are incidental or dead-end hosts.
Symptoms	Most human infections are asymptomatic or mild symptoms (fever and headache), a small percentage of infections develop inflammation of the brain (encephalitis), with symptoms including sudden onset of headache, high fever, disorientation, coma, tremors and convulsions.
Distribution	Asia and the western Pacific, primarily in rural agricultural areas and periurban settings
Treatment	JE vaccine is available, there is no specific treatment for JE. patient.
La Crosse Encephalitis virus (LCEV)	
Transmission	maintained in a cycle between *Aedes triseriatus* (the eastern treehole mosquito) and vertebrate hosts (especially small mammals such as chipmunks and squirrels) in deciduous forest habitats; humans are incidental or dead-end hosts.

Symptoms	No apparent symptoms for many human infections; initial symptoms of the illness include fever, headache, nausea, vomiting, and tiredness; some develop severe neuroinvasive disease often involving encephalitis and including seizures, coma, and paralysis.
Distribution	North America (the upper Midwestern and mid-Atlantic and southeastern states in the US)
Treatment	No vaccine against LACV infection or specific treatment for LACV infection
Malaria	
Transmission	Transmitted between people by *Anopheles* mosquitoes
Symptoms	Very sick with high fevers, shaking chills, and flu-like illness
Distribution	Mostly in poor, tropical and subtropical areas of the world
Treatment	Most drugs used in treatment are active against the parasite forms in the blood.
St. Louis Encephalitis virus (SLEV)	
Transmission	circulating between *Culex* species mosquitoes and birds; humans and other mammals are dead-end hosts.

Symptoms	No apparent illness for most human infections; clinical infections range in severity from mild nonspecific febrile illnesses to meningitis or encephalitis.
Distribution	America and Argentina
Treatment	No vaccines to prevent nor medications to treat SLEV

West Nile virus (WNV)

Transmission	Maintained in a cycle between birds and *Culex* mosquitoes (in particular *Cx. Pipiens* and *Cx. Restuans*); human and other mammals are dead-end hosts.
Symptoms	No symptoms for most (around 80%) human infections, about 20% of human infections develop West Nile fever with symptoms including fever, headache, tiredness, and body aches, nausea, vomiting, occasionally with a skin rash (on the trunk of the body) and swollen lymph glands. The symptoms of severe diseases (also called neuroinvasive diseases, such as West Nile encephalitis or meningitis or West Nile poliomyelitis) include a headache, high fever, neck stiffness, stupor, disorientation, coma, tremors, convulsions, muscle weakness, and paralysis.
Distribution	Africa, Asia, Australia, the Middle East, Europe and North America

Treatment	No WNV vaccines are licensed for use in humans, there is no specific treatment for WNV disease.
Yellow Fever	
Transmission	Transmitted to people primarily by *Aedes* or *Haemagogus* species mosquitoes
Symptoms	Illness ranging from a fever with aches and pains to severe liver disease with bleeding and yellowing skin (jaundice)
Distribution	Tropical and subtropical areas of Africa and South America
Treatment	A safe and effective yellow fever vaccine has been available for more than 80 years, while there is no medicine to treat or cure the infection.
Zika virus diseases (Zika)	
Transmission	Transmitted to people primarily from the bite of an infected Aedes species mosquitoes (*Ae. aegypti* and *Ae. albopictus*); Zika can be passed through sex; Zika can be passed from a pregnant woman to her fetus.
Symptoms	No symptoms or generally mild symptoms include fever, rash, headache, joint pain, conjunctivitis (red eyes), muscle pain. Infection during pregnancy can cause a birth defect (microcephaly) and other severe fetal brain defects.

Distribution	Africa, the Americas, Asia and the Pacific
Treatment	No vaccine to prevent or medicine to treat Zika

Due to globalization, environmental and other complex factors such as unplanned urbanization, the emerging and reemerging of MBDs have become more and more frequent. For instance, climate warming can influence pathogen transmission, extending and transmission season, intensifying the transmission severity and leading diseases to emerge in regions and countries where they were previously unknown. Since 2014, major outbreaks of Chikungunya, dengue, malaria, yellow fever and Zika have occurred in many countries, causing human suffering from diseases, resulting in human deaths and overwhelming health systems (World Health Organization (2017)).

Thus it is of great significance to study and understand the transmission dynamics of MBDs, the threshold conditions for triggering an outbreak (emerging) and mechanisms of recurrence (reemerging) of MBDs. The major MBDs of public health importance in Ontario is WNV and we will use WNV in the Region of Peel, Ontario, Canada, as an example for the study.

1.2 West Nile virus

West Nile virus is primarily a bird pathogen and a mosquito-borne arbovirus belonging to the genus Flavivirus, and not all species of mosquitoes are responsible for the transmission of WNV: only WNV vector mosquito species are capable of carrying and transmitting WNV. The female mosquito gets infected by feeding on the blood of birds carrying the virus and then transmits the virus to humans and other animals through the bite. Humans and other mammals are dead-end hosts whereby they can become infected, while they do not spread the infection. WNV is the most widely distributed emerging arbovirus. It was first isolated in a woman in the West Nile district of Uganda in 1937 and it is now widespread in Africa, Asia, Australia, the Middle East, Europe and North America (World Health Organization (2016), Rappole (2000), Campbell et al. (2002)). In North America, since the first case was detected in New York city in 1999, the virus spread rapidly throughout the continent and it appeared in Ontario in 2001 (Nash et al. (2001), Toronto and Region Conservation Authority (2014)).

In Ontario, the number of human infection cases fluctuates from year to year, driven by complex factors including vector-virus-host interactions, international commerce and travel, biological factors (such as the abundance of WNV vector mosquitoes, migration of birds and distribution of hosts) and climate factors (Kramer et al. (2008), Epstein (2001)). The incidence and distribution of WNV will be driven and altered by global warming and

the accompanying alteration in weather patterns. Factors other than weather and climate will contribute to outbreaks of WNV as well. Local environmental conditions and anthropogenic land use can enhance the potential for mosquito breeding in urban settings, such as the stormwater management pond (Epstein (2001)).

Most human infections with WNV are subclinical leading to no symptoms but approximately 20% of human infections will develop West Nile fever with symptoms of fever, headache, body aches, nausea, and vomiting etc. Some severe cases result in neurological disease (World Health Organization (2016)). However, there is no specific treatment or vaccine for West Nile virus infection in humans. Infected people with mild symptoms usually recover themselves. For serious cases, treatment with supportive therapies, such as fluids, medication and breathing, are necessary. Considering that WNV is most commonly transmitted to humans by mosquitoes, the best method to reduce the risk of WNV infection is mosquito control, and the mosquito surveillance becomes essential to monitor the mosquito abundance and virus activities (World Health Organization (2016), Government of Canada (2015)).

Mosquito control manages the abundance of mosquitoes to reduce their damage to human health. The mosquito typically goes through four stages of its life cycle, the first three aquatic stages (egg, larva, pupa) occur in water and the last aerial stage is adult. Based on the features of the mosquito life cycle, different practices are applied to control

the mosquito population. The priority one is monitoring mosquito abundance, including monitoring abundance of larvae and adult mosquitoes. With monitoring and surveillance data, public health needs to evaluate the WNV activities in a particular area, assess the risk of infection, predict and catch an early warning signal for a potential outbreak, and decides if, when, where and how to reduce the risk of infection by education and community outreach or using mosquito control measures, such as source reduction (elimination of mosquito breeding grounds), biocontrol (the use of mosquito natural enemies), larviciding and adulticiding (Campbell et al. (2002), Florida Coordinating Council on Mosquito Control (1998), Government of Canada (2018)).

In Ontario, the Toronto and Region Conservation Authority (TRCA) has launched a WNV Monitoring Program in the Greater Toronto Area (GTA) since 2003. The program is to conduct WNV mosquito larvae monitoring and surveillance for the presence of WNV vector mosquitoes in selected natural wetlands and stormwater management ponds (SWMP) on TRCA lands, where *Culex pipiens* and *Culex restuans* are two principal vectors of WNV, in particular *Culex pipiens* – an urban mosquito species (Kilpatrick et al. (2005), Hamer et al. (2009), Toronto and Region Conservation Authority (2014)). Larval mosquito surveillance and monitoring was undertaken in 36 wetlands and 9 SWMP over the last 5 years. The program results reveal that the majority of the mosquito larvae collected in natural wetlands are non-vectors for WNV, while the mosquitoes collected

from SWMP are principally vector species and the predominant vector species was *Culex pipiens*.

Like other health units in Ontario, the Region of Peel Public Health has been running a mosquito surveillance program since 2001. This program aims at monitoring adult mosquito abundance associated with WNV, determining the level of WNV activity among these species and using this information to access the risk for transmitting the virus to humans and make decisions in the prevention and control of WNV (Molaei et al. (2006)). Adult mosquitoes will continue to be collected weekly from mosquito traps at 31 fixed locations throughout the Region of Peel, with a minimum of one trap per ward across Peel, from mid-June to early October. In the program, CDC (Centre for Disease Control) light traps are operated (Brown et al. (2008), Region of Peel (2012)).

1.3 Current modeling and literature review

Mathematical models for mosquito abundance and the transmission of WNV have been studied extensively (Lewis et al. (2006a), Shaman and Day (2007), Shaman et al. (2006), Wan and Zhu (2014), and others). To simulate the population dynamics of immature and adult *Culex* mosquitoes in the Northeastern US, Gong et al. (2011) developed climate-based models and revealed a strong correlation between the timing of early population increases and decreases in late summer. Also, a predictive statistical model for WNV

mosquito abundance was proposed by Wang et al. (2011). In this model, the influence of weather conditions (temperature and precipitation) on mosquito populations was investigated and it came to the conclusion that WNV vector population on any day could be predicted with mean degree-days $> 9^oC$ over the 11 preceding days and precipitation 35 days before.

To describe the evolution of the virus, a difference equation model incorporating pesticide spraying was formulated in Thomas and Urena (2001), whose results indicated the virus can be eliminated by a specific amount of spraying. Wonham et al. (2004) proposed a single-season ordinary differential equation model on WNV transmission and showed that mosquito control would prevent the WNV outbreak, while bird control would have the opposite reaction. Lewis et al. (2006b) presented a comparative study of the discrete and continuous time model and showed that the basic reproduction number calculation was largely determined by assumptions on mosquito feeding efficiency. Cruz-Pacheco et al. (2005) established a mathematical model for the WNV transmission in the mosquito-avian population, combined with experimental and field data, damped oscillations approaching the bird endemic value was shown in numerical simulations. Bowman et al. (2005) developed a dynamical model in a mosquito-bird-human community to assess mosquito reduction strategies and personal protection against WNV. Fan et al. (2010) established a delay differential equation model with temperature for the WNV transmission in the mosquito-

avian population, and the results illustrated that the maturation time, as well as the vertical transmission in mosquitoes, affects peaks of the infectious mosquitoes substantially. Besides these dynamical model, Ruiz et al. (2010) applied spatial and statistical modeling techniques to show that spatial and temporal patterns of mosquito infection in an area of northeastern Illinois are quite influenced by changing weather conditions.

To study the occurrence of the WNV outbreak, Castillo-Chavez and Song (2004) illustrated conditions for the occurrence of a backward bifurcation in dynamical models and claimed that only reducing the basic reproduction number to less than one was not enough to eliminate a disease owing to the backward bifurcation. Jiang et al. (2009) suggested that it was worth considering the initial state of WNV rather than only the basic reproduction number to study the prevalence of WNV. Wan and Zhu (2010) concluded that backward bifurcation in WNV transmission model in mosquito-avian population could lead to the existence of a sub-threshold condition of the outbreak of the virus; moreover, the higher WNV induced mortality rate of avian host determined the existence of backward bifurcation. Blayneh et al. (2010) developed a WNV transmission model among mosquitoes, birds and humans, the results also indicated that due to the backward bifurcation, R_0 less than unity might not always be sufficient to control WNV. Abdelrazec et al. (2014) studied a WNV transmission dynamical model among mosquitoes and two reservoir hosts (corvids and non-corvids) and concluded that estimation of the epidemic of WNV was more accu-

rate when classifying the birds into different species and including other mammals, and verified that higher death rate of birds due to WNV could explain the phenomenon of the backward bifurcation.

1.4 Objectives of the research

The overall goal of this dissertation is to investigate the dynamics of mosquito abundance and transmission of MBDs. Considering biological factors (such as host feeding preferences of mosquitoes, migration of birds), environmental factors (such as temperature, precipitation and SWMP) and vector-virus-host interactions, we propose mosquito population models and transmission models to predict the vector abundance, to analyze the influence of environmental factors on the mosquito population and the transmission, to evaluate the potential risk of the occurrence of the outbreaks, and to control mosquito and the disease spread. In particular, this research study is carried out using *Culex* mosquitoes and WNV in the Region of Peel, Ontario, Canada, as an example.

In Chapter 1, we present the background of MBDs, particularly WNV, and current mosquito population models and WNV transmission models. Then we focus on single species population models for mosquitoes and birds in Chapter 2. We incorporate the host feeding preference of mosquitoes and migrations of birds in our models, and analyze the dynamics of these single species population models.

In Chapter 3, based on the adult mosquito trapped count surveillance data and daily weather data, we first define an effective trapping zone of a CDC light trap and establish a model to describe the mosquito reproduction and development, and to depict the mechanism of mosquitoes being collected by traps. We show how weather, mosquito and host selecting behaviours affect the total mosquito population in the effective trapping zone as well as the trap counts, where parameters are estimated based on partial surveillance data. Our models can be used to predict the true mosquito abundance of the region rather than the trap counts only.

Then we develop a system of ordinary differential equations to model the impact of SWMP as well as weather conditions on the transmission of WNV between mosquito and bird populations in a single season in Chapter 4. The idea on the incorporation of SWMP impact is achieved by applying the intraspecific competition: the abundance of larvae is closely related to intraspecific competition, and intraspecific competition is associated with standing water – the habitat of larvae, furthermore, the standing water comes from the water in SWMP. We analyze the existence and stability of equilibrium points of the models and apply daily temperature and precipitation in the GTA into our model. The numerical simulations display that a smaller intraspecific competition rate leads to a larger mosquito population and more infectious birds and mosquitoes. Additionally, an excess of rainfall will control the vector population and reduce the peak value of infectious vectors

and birds.

In Chapter 5, we propose improved mosquito-bird transmission models to study the outbreak threshold dynamics and recurrence mechanisms using dynamical systems and bifurcation theory. We develop a novel risk index and the risk assessment criteria to characterize the potential risk of infections and an early warning for an outbreak. For the risk index, it's a more comprehensive tool compared to infection rate to evaluate the local WNV activity patterns. For the risk assessment criteria, it can be used to determine the risk level for the occurrence of a WNV outbreak, even if the basic reproduction number is less than one. We extend our results by applying the risk assessment criteria to the GTA, and the evaluation results are consistent with the results based on the minimum infection rate (MIR). In Chapter 6, we conclude the dissertation and provide future work.

2 Dynamical models for single species population

2.1 Mosquito population model

To delineate the reproduction of mosquitoes in models, a constant birth rate, i.e., per capita recruitment rate of mosquitoes r_m, has been adopted by numerous studies, such as Shaman and Day (2007), Shaman et al. (2006), Wan and Zhu (2010), Wonham et al. (2004) and Abdelrazec et al. (2014). In Rubel et al. (2008), the birth rate is represented by the scaled biting rate that describes the reciprocal of the mosquito gonotrophic cycle. To depict the restriction of the blood meal resource for mosquito reproduction, Wan and Zhu (2014) and Fan et al. (2010) used a Ricker function $r_m = rMe^{-\alpha M}$ (M is the population of female mosquitoes), where the blood resource is reflected by an independent parameter α rather than hosts themselves. In this chapter, we consider the influence of mosquito feeding preferences on the mosquito population model.

2.1.1 Mosquito feeding preference

Host feeding preferences vary among mosquito species: some mosquito species are generalists and express opportunistic feeding behaviour, while others are specialists and feed preferentially on selected hosts (Rizzoli et al. (2015), Burkett-Cadena et al. (2008), Farajollahi et al. (2011)).

Host preference of mosquitoes is affected by both intrinsic (a genetic basis) and extrinsic factors. Many species express inherent traits in host preference, such as a preference for birds or mammals, which cannot be predicted based upon the extrinsic determinants alone (Hassan et al. (2003), Kilpatrick et al. (2006a), Kilpatrick et al. (2006b)). Nonetheless, the inherent host preference can be overridden by environmental circumstances such as season, mosquito nutritional state (e.g., physiological factors (hunger) and physical abundance of available hosts), host behaviour (like defensive behaviour) or mosquito learning over time (Takken and Verhulst (2013), Hassan et al. (2003), Hamer et al. (2011), Thiemann et al. (2011), Savage et al. (2007), Rizzoli et al. (2015)). The reason to explain this phenomenon is that the principal strategy of the mosquito is to safeguard reproduction, for which blood source is required. Under such circumstances, mosquitoes will lower their host preference threshold and may feed on a non-preferred host (Chilaka et al. (2012)).

Many *Culex* species have a preference for feeding on birds, and birds availability plays a significant role in *Culex* species feeding. The abundance of birds often fluctuates

throughout the year due to migration. When the availability of the preferred host declines, *Culex* species may switch to other hosts, like humans and other mammals (Kilpatrick et al. (2006b), Simpson et al. (2012), Takken and Verhulst (2013), Thiemann et al. (2011)).

For example, *Cx. nigripalpus* switches from birds to deer between winter and summer (Edman and Taylor (1968), Takken and Verhulst (2013)). *Cx. tarsalis* in California feeds on mammals as well in the winter rather than just feeding on birds in the summer (Simpson et al. (2012), Thiemann et al. (2011), Takken and Verhulst (2013)). For *Cx. pipiens*, its feeding patterns change over the season even though its genetic predisposition does not change (Kilpatrick et al. (2007)).

Host feeding preferences influence the transmission of diseases in a more complex way. Some *Culex* species, such as *Cx. pipiens*, prefer feeding on specific birds (Kilpatrick et al. (2006b)). This preference plays a crucial role in the peak and intensity of WNV in *Culex* mosquitoes and in modelling WNV transmission dynamics and predicting outbreaks (Farajollahi et al. (2011), Simpson et al. (2012), Rizzoli et al. (2015)). A good understanding of feeding preferences can provide a deeper insight into bites distribution on hosts and the maintenance and transmission of WNV and other pathogens (Thiemann et al. (2011)). Shifting from preferred avian hosts to mammals including humans can increase WNV transmission to humans (Kilpatrick et al. (2006b)), and this increasing WNV transmission to humans will stop when humans, dead-end hosts, become a large propor-

tion of hosts, making the transmission inefficient (Farajollahi et al. (2011), Takken and Verhulst (2013)).

Hence, *Culex* mosquitoes shifting feeding preference on humans can both exacerbate and suppress the transmission of WNV to humans, with the net effect based on other aspects of transmission such as vector abundance and competence, and host competence (Kilpatrick et al. (2007)). Contrasted with WNV, humans are amplification hosts of some pathogens, such as dengue virus and malaria, and vectors of these viruses feeding on humans will increase both exposure of humans and the probability of an epidemic (Kilpatrick et al. (2007), Townson and Nathan (2008), Farajollahi et al. (2011)). The influence of mosquito feeding preference in WNV transmission is quite complicated and worth taking into account to well study the transmission dynamics and evaluate the risk of human infection.

2.1.2 Model formulation

Generally, female mosquitoes bite hosts and extract the blood to develop and nourish eggs. Based on this biological feature, the birth rate (or named the oviposition rate) r_m depends on the per capita biting rate of mosquitoes b_m, conversion rate of each bite c (the number of eggs developed from a bite), and the number of available hosts H providing blood meals for female mosquitoes to oviposit (Reisen et al. (2006b)). Therefore, we

describe mosquito birth rate $r_m = r(b_m, c, H)$ as a function of b_m, c and H.

In general, for the per capita birth rate $r(b_m, c, H)$, we can assume

(A1) $r(b_m, c, H) \geq 0$ for $b_m > 0,\ c > 0,\ H \geq 0$ and $\lim_{H\to 0^+} r(b_m, c, H) = (b_m, c, 0) = 0$ and $\lim_{H\to\infty} r(b_m, c, H) = r_1$, where r_1 is the maximum per capita birth rate due to the sufficient hosts providing plentiful blood resources. If no host provides blood meals for mosquito, no egg will be laid for reproduction.

(A2) $\frac{\partial r(b_m,c,H)}{\partial H} \geq 0$. The more hosts are available for female mosquitoes, the more blood resources support mosquitoes laying more eggs. When the population of available hosts is sufficient large, more hosts will not promotes the reproduction of eggs, since bites have reached saturation.

(A3) $\frac{\partial r(b_m,c,H)}{\partial b_m} > 0$, $\lim_{b_m\to 0^+} r(b_m, c, H) = 0$ and $\lim_{b_m\to\infty} r(b_m, c, H) = r_1$. The per capita birth rate of mosquitoes is an increasing function of b_m, which is bounded by 0 and r_1 for any $H > 0$, $c > 0$.

(A4) $\frac{\partial r(b_m,c,H)}{\partial c} > 0$, $\lim_{c\to 0^+} r(b_m, c, H) = 0$ and $\lim_{c\to\infty} r(b_m, c, H) = r_1$. The per capita birth rate of mosquitoes is an increasing function of c, which is bounded by 0 and r_1 for any $H > 0$, $b_m > 0$.

Here $r(b_m, c, H)$ is a more general form. If hosts are sufficiently in abundance, it is reasonable to assume that r_m is constant. That means the constant birth rate is a limit state

of the general birth rate $r(b_m, c, H)$ when hosts are greatly abundant.

According to assumptions **(A1)** - **(A4)**, different functions can be applied to formulate the recruitment rate. For instance,

(E1) $r(b_m, c, H) = \frac{r_1 c b_m H}{a + c b_m H}$ for all $r_1,\ b_m,\ c,\ a > 0$.

(E2) $r(b_m, c, H) = \frac{r_1 c b_m H^2}{a + c b_m H^2}$ for all $r_1,\ b_m,\ c,\ a > 0$.

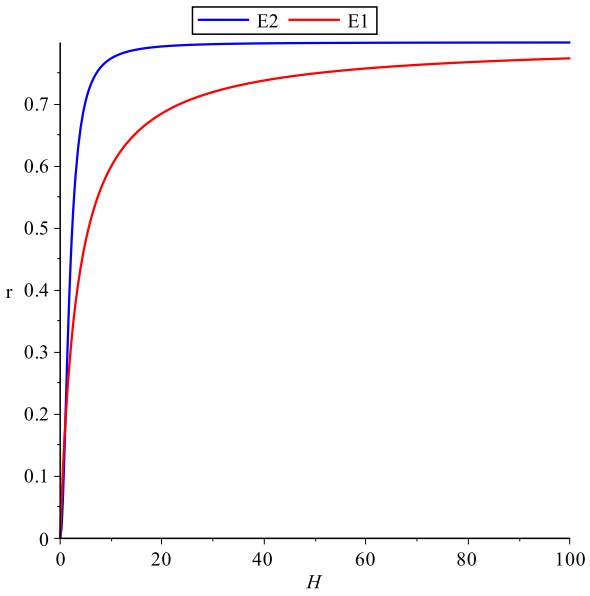

Figure 2.1: Two cases of mosquito birth rate $r(b_m, c, H)$

Based on the life cycle of the mosquito, the mosquito can be divided into the aquatic stage (also named the preadult mosquito encompassing egg, larva and pupa) and aerial stage (adult). We will consider intraspecific competition among preadult mosquitoes. Intraspecific competition is an interaction in population ecology, the effects of intraspecific

competition are density dependent (Begon et al. (2006)). Members of the same species compete for limited resources required for survival and development (Amundsen et al. (2007)). Particularly for insects, density-dependent competition among juveniles is usually related to increased juvenile mortality, delayed maturity and reduced adult size (Agnew et al. (2002)). Competition among larvae is an influential factor in regulating the growth of mosquito populations Agnew et al. (2000). For instance, *Culex pipiens* experience density-dependent reductions in growth and survival at the larval stage (Rajagopalan et al. (1976), Mpho et al. (2000), Reiskind et al. (2004), Agnew et al. (2000)).

The logistic growth equation is used to model intraspecific competition in biological systems. It depicts the reciprocal relation between the carrying capacity and the intraspecific competition rate (Tsoularis and Wallace (2002)). For *Culex* mosquitoes, the intraspecific competition rate can be assumed to be relevant to any element of competition like the size of standing water and the density of nutrients, and competitive interactions are within and between both female and male mosquitoes (Agnew et al. (2000)).

To formulate the model, we let $L(t)$ and $M(t)$ be the population of preadult mosquitoes and female adult mosquitoes at time t respectively, and the proportion of the female mosquitoes is p. Mosquito birth rate $r(b_m, c, H)$ can be chosen as **(E1)**, **(E2)** or other functions satisfying assumptions **(A1)** - **(A4)**. The preadult mosquitoes and female adults per capita mortality rate are d_l and d_m respectively. The intraspecific competition rate

among preadult mosquitoes is κ and mosquitoes per capita maturation rate from aquatic stage to adult is δ. Also, we denote the population of available hosts as H that can be birds, humans or other mammals. Then mosquito population is modelled as

$$\begin{cases} \frac{dL(t)}{dt} = r(b_m, c, H)M(t) - \delta L(t) - d_l L(t) - \kappa L(t)^2, \\ \frac{dM(t)}{dt} = p\delta L(t) - d_m M(t). \end{cases} \tag{2.1}$$

Table 2.1: Parameters in the mosquito population model (2.1)

Par.	Interpretation	Range (day^{-1})	Ref.
b_m	Female adult mosquitoes per capita biting rate	$(0.2 - 0.75)$	Abdelrazec et al. (2014)
c	Per bite conversion rate (the number of eggs developed from a bite)		
$r(b_m, c, H)$	Mosquitoes per capita birth rate	$(0.036 - 42.5)$	Wonham et al. (2004)
δ	Mosquitos per capita maturation rate from preadult to adult	$(0.051 - 0.093)$	Wonham et al. (2004)

d_l	Preadult mosquitoes per capita mortality rate	$(0.213 - 16.9)$	Wonham et al. (2004)
κ	Intraspecific competition rate of preadult mosquitoes	$(0 - 1)$	
p	Proportion of females in all preadult mosquitoes	$(0 - 1)$	
d_m	Female adult mosquitoes per capita mortality rate	$(0.016 - 0.07)$	Wonham et al. (2004)

If $r(b_m, c, H) < \frac{(d_l+\delta)d_m}{p\delta}$, model (2.1) has a trivial equilibrium point $E_0 = (0, 0)$ which is locally stable. If $r > \frac{(d_l+w)d_m}{p\delta}$, in addition to an unstable trivial equilibrium E_0, system (2.1) also has a locally stable positive equilibrium point $E_1 = (\frac{r(b_m,c,H)p\delta-d_l d_m-d_m\delta}{d_m\kappa}$, $\frac{p\delta[r(b_m,c,H)p\delta-d_l d_m-d_m\delta]}{d_m^2\kappa})$. In biological view, a relative low birth rate, less than $\frac{(d_l+\delta)d_m}{p\delta}$, leads to the mosquito dying out. Contrarily, a large birth rate, greater than $\frac{(d_l+\delta)d_m}{p\delta}$, will sustain mosquito population to a stable state E_1. As the birth rate of mosquitoes increases along with the population of available host increasing, sufficient host populations providing enough blood resource can ensure the survival of mosquitoes. Intraspecific competition exerts an opposite effect for the growth and development of mosquitoes; when the intraspecific competition is fierce (κ is quite large), the immature mosquito population will

decrease, resulting in the reduction of total mosquitoes.

2.2 Bird population model including WNV circulation

Usually, because that infected mosquitoes do not recover before dying naturally and do not die of WNV (Bowman et al. (2005)), WNV is not incorporated into the mosquito population model. However, for avian hosts, WNV has a non-negligible influence on their populations. Different species of birds have different competence in transmitting and amplifying the disease. Some infected birds develop high levels of the virus in their bloodstream. For example, American crow (*Corvus brachyrhynchos*) has a high reservoir competence to spread the virus (Hamer et al. (2009)). Cruz-Pacheco et al. (2005) also estimated the basic production number for several species of birds and Abdelrazec et al. (2014) illuminated that avian species diversity in the transmission system is worth considering for more accurate epidemic estimation. Here we summarize the contribution of bird species (corvids and non-corvids), migration and age stages (nestlings, hatch-year birds and adult birds) to the transmission of WNV, and we build and analyze a population model of birds considering the horizontal transmission.

2.2.1 The impact of bird species, migration and age stages on WNV transmission

In North America, more than 300 species of birds are found involved in WNV (Abdelrazec et al. (2014)). Members of the family Corvids (crows, jays and ravens) are especially important because they develop severe illness and their extremely elevated viremias effectively amplify WNV and increase transmission rates to epidemic levels (Reisen et al. (2006a). Reed et al. (2003)). Also particularly high mortality rates or relatively strong population declines, associated with WNV, have been noted in corvids (Reed et al. (2003), Petersen and Marfin (2002), Work et al. (1955). Komar et al. (2003a), McLean (2006), Koenig et al. (2007)). In the Region of Peel, Ontario from 2003 to 2005, the great majority of WNV positive dead birds are corvids (Zimmer (2005), Abdelrazec et al. (2014)). For a long time after WNV was discovered in North America in 1999, the mortality rate of corvid species had been the hallmark of the ongoing epidemic and served to assess infection risk (Campbell et al. (2002), Kipp et al. (2006)). While recent years, some regions are no longer collecting dead birds for testing since WNV is well established and mortality in birds is not an effective indicator of infection any more (Centers for Disease Control and Prevention (2015c)). Only considering the corvids who have high mortality rates is not enough, we should also take into account non-corvids with lower WNV induced mortality rates.

Other than mosquito bites (or in the absence of mosquitoes), birds can become in-

fected by WNV via a variety of routes and the potential of maintaining the transmission cycle may differ in different species (World Health Organization (2016)). One possible route is that some birds consume infected prey items such as insects, other birds and small mammals. Viremia usually occurs after ingesting infected organisms, and this may affect the incidence of WNV infection for raptors (Nemeth et al. (2006)). Another route may be the direct transmission (horizontal transmission) between certain bird species (McLean et al. (2001), Langevin et al. (2001), Komar et al. (2003a), Kipp et al. (2006), Reisen et al. (2009)). Birds are involved in transmission by close contacts with other infected birds, in the absence of mosquito-borne transmission (Komar et al. (2003a)). This horizontal transmission is a result of emitting particles in oral or cloacal secretions, which may contaminate food and water, or may directly contact another susceptible organism (Kipp et al. (2006)). Also, this contact transmission occurs in communal roosting populations during the breeding season (Komar et al. (2003a)).

The seasonal bird migration is a spectacular phenomenon of nature. In Western Hemisphere, each autumn approximately 5 billion birds, over 300 species, migrate from North America to Central and South America (Gill (1994), Reed et al. (2003)). With the strongly seasonal climate of North America, abundant breeding habitat and food supplies are accessible for these bird species in the spring and summer, but are not available to sustain birds' year-round requirements. Thus these birds breed in Canada and the United States and

spend the winter in warmer regions including the West Indies, Central and South America (Reed et al. (2003)).

Bird migration plays a critical role in the geographic spread of WNV and establishment of new endemic foci at great distances from where an infection was acquired. Migratory birds have been highly linked with serving as transport agents to spread WNV (Reed et al. (2003), Rappole (2000), Dusek et al. (2009), Peterson et al. (2003), McLean (2006)), and the outbreak sites of WNV coincides with major birds migratory routes (Reed et al. (2003), World Health Organization (2016)). In North America, the temporal and spatial pattern and rapidity of continental spread of WNV matched the semiannual migratory movements of a huge number of birds (McLean (2006)). Migratory birds flying back and forth between Central/South America and Canada/the United State in the fall and spring can be the best explanation for the westward movement of WNV in Canada and the United States (Gubler (2007)).

For migratory birds, most long-distance migrants consist of a series of shorter flights. From the viewpoint of WNV transmission, stopovers during the migrants are important since they give more possibilities for the close intermingling of species (Gill (1994), Wheye et al. (1988), Reed et al. (2003)). Certainly, the starting place and the terminal of migrants are also significant for the spread of the disease. WNV antibodies have been sampled in both migratory and non-migratory bird species on wintering and breeding grounds

(Farfán-Ale et al. (2004), Komar et al. (2001), Komar et al. (2003b), Dusek et al. (2009)). Around 300 native and exotic, free-ranging and captive bird species have been tested positive for WNV in the United States (McLean (2006), Centers for Disease Control and Prevention and others (2015)).

Understanding migration patterns for hundreds of bird species is largely conducive to predict and control the spread of WNV by wild birds in North American. Nevertheless, patterns of migration for wild birds between species are highly complex and clearly describing patterns for all these species seems unreachable. Even for the same species, the patterns differ for distinct populations (Reed et al. (2003)). Thus, different migration patterns should be based on different bird populations.

In addition to bird species and migration, determining the host competence on different age stages (nestlings, hatch-year and adult birds) can be of great help for studying the transmission of WNV (Kilpatrick et al. (2007)). It has been revealed that hatch-year birds are as key amplifiers and transmitters of WNV, which is associated with increasing human infection risk (Hamer et al. (2008), VanDalen et al. (2013)). Serological results only from hatch-year birds were considered reliable and were used to confirm infected bird cases during sampling years (Komar et al. (2003a), Nemeth et al. (2009), Levine et al. (2017)).

Hatch-year birds, particularly nestlings, may be especially important to WNV amplification and other avian arbovirus transmissions (Caillout et al. (2013b), Caillout et al.

(2013a)). Nestlings represent the immunologically naive avian population, spend lots of their time in a fixed location and may be greatly attractive to mosquitoes since they accumulate and give off a large amount of carbon dioxide and heat (Caillout et al. (2013b), Loss et al. (2009), Caillout et al. (2013a)). Nestlings are seemingly more susceptible to mosquito bites than adults because of being confined to nests, lacking the protective feather coverage of adults, an inability to avoid mosquitoes attack through a flight, exposing weak defensive behavior, or other factors (Caillout et al. (2013b), Griffing et al. (2007), Loss et al. (2009), Caillout et al. (2013a), Lindgren et al. (2009), Loss et al. (2009)).

Additionally, compared to adult birds, nestlings have an increased duration or intensity of viremia, which may largely contribute to mosquito infection (Mahmood et al. (2004), Loss et al. (2009)). Also, the antibody prevalence of adult birds is higher than juveniles' (Hamer et al. (2008), Lampman et al. (2013)) and juveniles have a higher antibody decay rate than adults (McKee et al. (2015)). In turn, WNV has an important influence on some nestlings, mortality among nestlings of Black-crowned night herons may be because of WNV to some degree (Reisen et al. (2009)). Furthermore, Griffing et al. (2007) suggested that early-breeding-season nestling birds may suffer less risk of exposure to arbovirus since the prevalence of the viruses rise in the late season. At the end of the nesting season, a reduction in nestling hosts makes few remaining nestlings experience quite greater mosquito burden, which increases vector abundance by increasing mosquitoes per capita

biting rates (Caillout et al. (2013b), Caillout et al. (2013a)). After avian dispersal from nests, WNV vector species shifts hosts from birds to humans and other mammals, leading to increased human WNV incidence (Hamer et al. (2009), Kilpatrick et al. (2006b), Caillout et al. (2013b)).

However, some other work showed that nestlings play a limited or no role in WNV transmission (Loss et al. (2009), Caillout et al. (2013a)). Mosquito landing rates on adult American robins were higher and landing rates on nestlings were reduced due to parental brooding (Griffing et al. (2007)).

For hatch-year birds excluding nestlings, i.e., first-year birds that have fledged the nest, they were found vital to WNV amplification in the Chicago, IL area in 2005-2006; the appearance of first-year birds, providing a large population of susceptible hosts, coincides with WNV amplification (Loss et al. (2009), Hamer et al. (2008)). Other than above findings, Ringia et al. (2004) found that antibodies to WNV in adult and hatch-year birds did not differ significantly.

The different conclusions on the role of nestlings, hatch-year and adults birds in WNV transmission may be a result of differences in temporal and spatial factors of studies/samples, in bird species or environmental conditions.

2.2.2 Model formulation

We develop a bird population model including WNV circulation. The bird population can be any species and the recruitment rate r_b can be any kind of inputs like the birth or migration of birds or both. Let $B_s(t)$, $B_i(t)$ and $B_r(t)$ be the population of susceptible, infected and recovery birds at time t respectively. We denote η_b as the horizontal transmission rate from infected birds to susceptible birds, then this transmission term is $\eta_b B_s(t) B_i(t)$. The mortality rate and recovery rate associated with WNV is μ_b and γ_b respectively. Aside from the bird recruitment, natural death of the bird demographic is also included. Then the bird population model is

$$\begin{cases} \frac{dB_s(t)}{dt} = r_b - \eta_b B_s(t) B_i(t) - d_b B_s(t), \\ \frac{dB_i(t)}{dt} = \eta_b B_s(t) B_i(t) - \mu_b B_i(t) - \gamma_b B_i(t) - d_b B_i(t), \\ \frac{dB_r(t)}{dt} = \gamma_b B_i(t) - d_b B_r(t) \end{cases} \tag{2.1}$$

Table 2.2: Parameters in the bird population model (2.1)

Par.	Interpretation	Range (day^{-1})	Ref.
r_b	Recruitment rate of birds	$(800 - 1100)$	Abdelrazec et al. (2014)
d_b	Birds per capita natural death rate	$(10^{-4} - 10^{-3})$	Abdelrazec et al. (2014)

μ_b	Birds per capita mortality rate due to WNV	$(0.2 - 0.3)$	Abdelrazec et al. (2014)
γ_b	Birds per capita recovery rate from WNV	$(0 - 0.1)$	Abdelrazec et al. (2014)
η_b	WNV transmission probability from birds to birds		

Bird population system (2.1) has up to two equilibria. If the basic reproduction number $R_0 = \frac{r_b \eta_b}{d_b(\mu+\gamma+d_b)} < 1$, a unique and locally stable disease free equilibrium point (DFE) $E_0 = (\frac{r_b}{d_b}, 0, 0)$ exists. If $R_0 > 1$,in addition to an unstable DFE E_0, a positive equilibrium $E_1 = (\frac{\mu_b+\gamma_b+d_b}{\eta_b}, \frac{r_b\eta_b - d_b(\mu_b+\gamma_b+d_b)}{\eta_b(\mu_b+\gamma_b+d_b)}, \frac{\gamma_b[r_b\eta_b - d_b(\mu_b+\gamma_b+d_b)]}{\eta_b d_b(\mu_b+\gamma_b+d_b)})$ exits and it is locally stable.

3 Estimating population sizes for *Culex* mosquitoes using the weekly CDC light trap counts

3.1 Introduction

Certain species of mosquitoes play a crucial role in transmitting and spreading of mosquito-borne diseases (MBDs). They carry and transmit diseases from one human or animal to another, causing significant human death each year (World Health Organization (2018)). Currently, over ten major MBDs are transmitted by more than eleven mosquito species (Centers for Disease Control and Prevention (2016b)). There is currently no specific treatment or vaccine for most of MBDs including West Nile Virus (WNV), dengue and Zika. For all the MBDs, vector control is recognized as the most effective method, and it is of paramount importance to control mosquito in limiting or reducing the endemic of MBDs and the risk of human infections (World Health Organization (2016), Government of Canada (2015), Hemingway and Ranson (2000), Qi et al. (2008)).

Culex mosquitoes have been one of the major vectors of arbovirus. They are accepted as the principal vectors of WNV, they are also responsible for carrying and transmitting other viruses, such as Japanese encephalitis, Venezuelan equine encephalitis, Filariasis (Service (2008)). Even for Zika virus, an emerging MBD that was declared a global emergency by the World Health Organization, it is recently reported that *Cx. quinquefasciatus* can be a potential vector for Zika virus (Centers for Disease Control and Prevention (2016a), Guedes et al. (2017), Dodson and Rasgon (2017)). Many female *Culex* species prefer feeding on birds, and the abundance of birds often fluctuates throughout the year due to migration. When the availability of the preferred host declines, *Culex* species may switch to other hosts, like humans or other mammals (McLaughlin and Focks (1990), Kilpatrick et al. (2007), Service (2008), Kilpatrick et al. (2006b), Hamer et al. (2009), Burkett-Cadena et al. (2008), Kilpatrick et al. (2006a), Hassan et al. (2003), Takken and Verhulst (2013), Rizzoli et al. (2015), Thiemann et al. (2011), Hamer et al. (2011), Savage et al. (2007), Chilaka et al. (2012)).

With the emerging of WNV in Southern Ontario, public health units in Ontario have set up mosquito surveillance programs to monitor the abundance and distribution of mosquito species, in particular, *Culex* mosquitoes. The mosquito surveillance program can monitor changes in mosquito populations, detect mosquito-borne diseases, evaluate the level of virus activity (local virus severity), monitor the emerging of new invasive species of

mosquitoes, decide whether control efforts are needed and determine what control measures need to be conducted (Region of Peel (2011), Michigan Mosquito Control Association (2018), Moore et al. (1993)).

Like other health units in Ontario, the Region of Peel Public Health has been running a mosquito surveillance program since 2001. Adult mosquitoes are collected weekly from mid-June to early October from mosquito traps at 31 fixed locations. The trapping season may change depending on the weather and surveillance results. Mosquitoes are trapped and collected using CDC (Centre for Disease Control) light traps (Region of Peel (2011), Region of Peel (2006), Region of Peel (2015), Region of Peel (2016), Region of Peel (2013), Region of Peel (2002)).

The CDC light traps are widely used to capture live mosquitoes in arbovirus studies (Centers for Disease Control and Prevention (2015a)). By mimicking hosts, the trap emits carbon dioxide and light, as baits to attract host-seeking female adult mosquitoes, then the mosquitoes are typically sucked into a net or holder (Region of Peel (2011), Region of Peel (2006), Lines et al. (1991), Newhouse et al. (1966), Brown et al. (2008), Mboera et al. (1998), Burkett et al. (2001), Reisen et al. (2000), McLaughlin and Focks (1990), Kilpatrick et al. (2007)). In the Region of Peel, traps are set up in the afternoon (2:00 pm) and then mosquitoes are collected from traps the following morning (9:00 am) (Karki et al. (2016)). Collected mosquitoes are placed in a container with dry ice to kill them and

are packed and shipped to a laboratory service provider for counting, speciation and PCR viral testing (Region of Peel (2015), Region of Peel (2016), Region of Peel (2013)).

As shown in Fig. 3.1 for the trap counts for the period of 2003 until 2015, the trap counts vary between different traps in the same year (Fig. 3.1(a)), and counts can change dramatically in different years for the same trap (Fig. 3.1(b)). The weekly trap counts supply a rough measurement for mosquito abundance, and the PCR viral test results give a reasonable risk level of WNV in the region. For the case in Peel, Wang et al. (2011) used trap counts and developed a predictive statistical model incorporating temperature and precipitation for mosquito abundance.

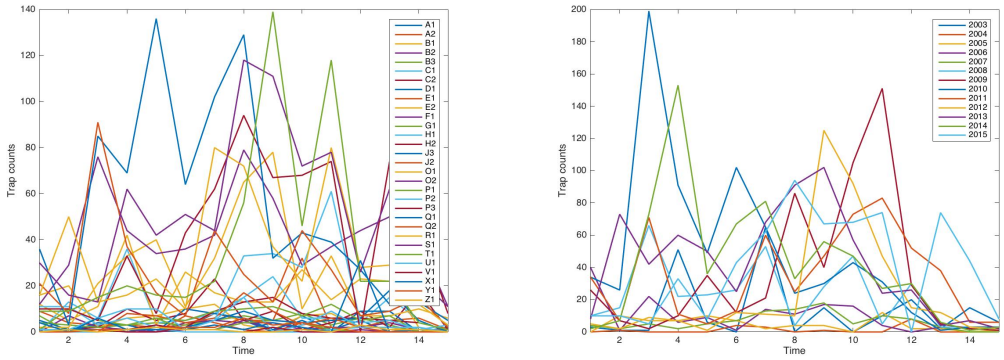

(a) Trap counts for different traps in 2015

(b) Trap counts for a same trap in different years (2003-2015)

Figure 3.1: Variations of trap count data for different traps or in different years

To estimate mosquito population size, it was usually implemented through mark-release-

recapture (MRR) experiments. Based on the principle of the Fisher-Ford method, Cianci et al. (2013) applied a logistic regression model to MRR data to estimate mosquito populations. Villela et al. (2017) designed Bayesian biodemographic models to fit MRR data to estimate abundance. In Epopa et al. (2017), authors carried out sequential MRR experiments and estimated mosquito population size using MRR data and Bayesian analyses of the Fisher-Ford model.

Besides population estimation models based on MRR data, other numerous models have been proposed to investigate the development and population dynamics of mosquitoes. Climate-dependent matrix population models were developed to describe *Culex pipens* and *Aedes vexans* and other mosquito population dynamics (Lončarić and Hackenberger (2013), Schaeffer et al. (2008)). To simulate the population dynamics of immature and adult *Culex* mosquitoes in the Northeastern US, Gong et al. (2011) developed climate-based models and revealed a strong correlation between the timing of early population increases and decreases in late summer.

Nonetheless, as far as we know, there is no available work taking into account the trapping mosquito mechanism in a dynamical model. Even if some work has used trap counts in their modeling studies, the results are just a prediction of average mosquito abundance rather than the real population of a region. Furthermore, trapping counts from the surveillance program are closely related to and influenced by many climatic and environmental

complex factors, for instance, temperature, precipitation, wind patterns, the locations of traps, the behavior, availability and distribution of blood-meal hosts, and the mosquito feeding preferences. All these contribute to technical difficulties of estimating the population size.

In this work, we will define an effective trapping zone (ETZ) of a CDC light trap. Then we will propose a predictive population dynamical model for mosquitoes. We will incorporate the trapping mechanism of a CDC light trap and collecting procedure in the model. Moreover, the role of blood meal hosts and mosquito biting feeding preference will be considered. Based on weekly surveillance trap counts data and local daily weather data, we estimate parameters involved in the model, then predict total mosquito population in the ETZ as well as mosquito trap counts.

3.2 Method

First, we define an effective trapping zone (ETZ) for a trap. ETZ is needed for calculating real mosquito abundance by our predictive model. Inputting trap counts provides the total mosquito population of the ETZ rather than only the information provided by trap counts.

In an ETZ, we will establish a general dynamical trap count model by treating the trap as a special human host for *Culex* mosquitoes, incorporating feeding preference, reproduc-

tion and development of *Culex* mosquitoes in the zone, and the trapping mechanism of the trap. All these contribute to estimating the total number of mosquitoes in the ETZ using trap counts.

To characterize and predict weekly trap counts and the *Culex* mosquito population in an ETZ in the Region of Peel, we will modify the general model and propose a specific model for the Region of Peel. In particular, we will classify the blood meals hosts in the Region of Peel into humans, non-humans (including birds and other mammals), and regard the CDC light traps as fake humans (mimic humans to attract mosquitoes). For *Culex* females, they have different feeding preferences on these different types of hosts, meanwhile, the available number of different types of hosts will shift mosquitoes feeding preferences. Also, we consider the impact of local weather factors, the temperature and precipitation are main factors impacting the development of *Culex* mosquitoes and considered in the model. By using the daily local weather data and weekly mosquito trap counts from the surveillance program, we can estimate the parameters involved. We test and verify the models using historical data, and predict trap counts and population sizes of *Culex* mosquitoes in an ETZ.

3.2.1 Effective trapping zone of a CDC light trap

The effective trapping zone (ETZ) of a CDC light trap can be considered as a circular zone with radius R_{ETZ}. Generally, mosquito development and abundance are influenced by weather factors, such as temperature, precipitation, humidity and wind, in time and space (Region of Peel (2016), Mullen and Durden (2009), Wang et al. (2017), Shaman and Day (2007), Rubel et al. (2008), De Meillon et al. (1967), Gong et al. (2011)). Driven by weather conditions, more mosquitoes will be trapped when there are more adults host-seeking mosquitoes. Also, the population of mosquitoes in the trapping zone and mosquito trap counts reach their peaks around the same time (same day). The peak value (occurring at time t_p) of total female *Culex* mosquitoes in the trapping zone is denoted as M_{total_p}; at the same time t_p, the number of collected mosquitoes is $M_{collect_p}$.

For a trap, we assume that it can effectively capture all female *Culex* mosquitoes in the circular area with radius R_{trap} and the trap at the center. R_{trap} is closely related to mosquito flight capacity, which is greatly influenced by landscape structure, meteorological conditions and wind (Greenberg et al. (2012), Ciota et al. (2012), Hamer et al. (2014), Cianci et al. (2013), Villela et al. (2017)). When seeking a blood meal, female mosquitoes fly about 25 feet or less off the ground and field trials show that relocating traps distances of only 25 feet (7.62 m) can significantly change the number of mosquitoes collected (Service (1980), Reisen et al. (2006b)).

We further assume that the population of female *Culex* mosquitoes are proportional to the size of their living areas, with the relationship

$$\frac{M_{collect_p}}{\pi R_{trap}^2} = \frac{M_{total_p}}{\pi R_{ETZ}^2}. \tag{3.1}$$

Derived from (3.1), the radius of the ETZ of a trap is

$$R_{ETZ} = \sqrt{\frac{M_{total_p}}{M_{collect_p}}} R_{trap}. \tag{3.2}$$

R_{ETZ} is proportional to R_{trap}. Therefore the area of the effective trapping zone (ETZ) of a trap is

$$A_{ETZ} = \pi R_{ETZ}^2 = \frac{M_{total_p}}{M_{collect_p}} \pi R_{trap}^2. \tag{3.3}$$

Increasing the total mosquito population M_{total_p}, the radius R_{trap} or decreasing the collected mosquitoes $M_{collect_p}$ leads to an increase in the radius of the effective trapping zone and increasing the area of the ETZ.

3.2.2 A general model

The life cycle of *Culex* mosquitoes goes through two stages: aquatic (including eggs, larvae and pupae) and aerial adult. Adult mosquitoes will be attracted and captured by traps. Let $L(t)$ be the population of female aquatic-stage *Culex* mosquitoes at time t, $M_{total}(t)$ be total female adult mosquitoes at time t, and $M_{collect}(t)$ be the number of collected female adult mosquitoes at time t.

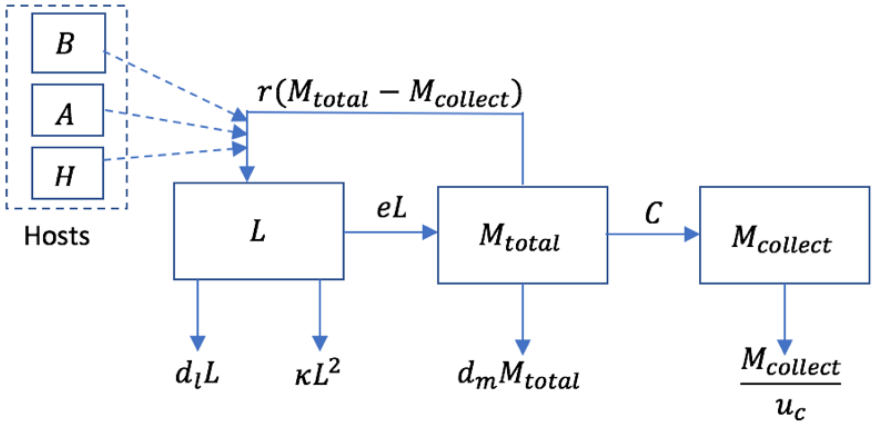

Figure 3.2: Flow chart of the model. Hosts (B, A, H) provide blood meals for female adults (outside a trap) to reproduce offspring, the immature mosquitoes develop into adults, and some adults are captured by the trap.

In an ETZ, only female adult mosquitoes outside a trap $(M_{total}(t) - M_{collect}(t))$ can produce offspring. The function and capability of a trap for trapping mosquitoes can be measured by the amount of carbon dioxide and light emitted. We treat the amount of these emissions as the population of mimicked fake hosts, that is, the higher the capability is, the more fake hosts the trap can mimic.

We also consider *Culex* mosquitoes feeding preferences among the diversity of host species. From Fig. 3.2, eL, $d_l L$ and κL^2 are outputs of the compartment L due to maturation, mortality and intraspecific competition respectively. Total adult mosquitoes decrease due to natural mortality $d_m M$ and a proportion of adults to be captured by a trap

$C(M_{total}, B, A, H)$. The trap will be emptied with collection rate $\frac{M_{collect}(t)}{u_c}$. Then a general model to describe female *Culex* mosquito development and mechanism of trapping and collecting is

$$\begin{cases} \frac{dL(t)}{dt} = r(b,c,B,H,A)[M_{total}(t) - M_{collect}(t)] - eL(t) - d_l L(t) - \kappa L_t^2, \\ \frac{dM_{total}(t)}{dt} = eL(t) - d_m M_{total}(t) - g(t)C(M_{total}(t), B, A, H), \\ \frac{dM_{collect}(t)}{dt} = g(t)C(M_{total}(t), B, A, H) - f(t)\frac{M_{collect}(t)}{u_c}, \end{cases} \tag{3.4}$$

where $g(t)$ and $f(t)$ are indicator functions: $g(t)$ is defined as (3.12) to indicate on which day to set a trap and $f(t)$ is defined as (3.13) to indicate on which day to collect trapped mosquitoes.

Mosquito feeding preferences, reproduction rate $r(b, c, B, H, A)$, mosquitoes being trapped rate $C(M_{total}(t), B, A, H)$ and collected rate $\frac{M_{collect}(t))}{u_c}$ are derived in the following subsections 3.2.2.1 - 3.2.2.4. The definitions and values of the parameters used in the model (3.4) are summarized in Table 3.1.

Table 3.1: Parameters in the general model (3.4)

Par.	Interpretation
b	Female adult mosquitoes per capita biting rate
c	Egg production rate per bite
B	Bird population of a given region providing real blood meal resource

H Human population of a given region providing real blood meal resource

A Other mammal population of a given region providing real blood meal resource

p_1 Genetic feeding preference on birds

p_2 Genetic feeding preference on other mammals

p_3 Genetic feeding preference on humans

p_4 Genetic feeding preference on fake hosts

p_B Actual feeding preference on birds

p_A Actual feeding preference on other mammals

p_H Actual feeding preference on humans

p_F Actual feeding preference on fake hosts

q_B The probability that a bite on birds is efficient (the probability of a successful bite on birds)

q_A The probability that a bite on other mammals is efficient

q_H The probability that a bite on humans is efficient

q_c The probability of mosquitoes attracted by a trap is successfully captured

$\hat{B}$ The number of birds at which actual feeding preference on birds is equal to genetic one

$\hat{A}$	The number of other mammals at which actual feeding preference on mammals is equal to genetic one
$\hat{H}$	The number of humans at which actual feeding preference on humans is equal to genetic one
r	Female mosquitoes per capita reproduction (egg-laying) rate, also denoted as $r(b, c, B, A, H)$ (3.11) as it is related to mosquito biting rate, egg production rate per bite and host populations
e	Female mosquitoes per capita maturation rate from aquatic stages to adult
d_l	Female preadult mosquitoes per capita mortality rate
κ	Intraspecific competition rate of female preadult mosquitoes
d_m	Female adult mosquitoes per capita mortality rate
C	Female mosquitoes being trapped rate, also denoted as $C(M_{total}, B, A, H)$ as it is related to total mosquito and host populations
u_c	The time taken to collect trapped mosquitoes

3.2.2.1 *Culex* Mosquito Feeding preferences

Based on previous chapters, *Culex* mosquitoes usually exhibit host feeding preferences. If the population of available preferred hosts declines, they may change their preferences on other hosts. We will consider this characteristic of mosquitoes in our model.

We define *Culex* mosquito biting rate b as the average number of bites per mosquito per day (day, used as the unit of time for the modeling). Mosquitoes inherent preferences (without influence by environmental factors) for feeding on hosts are reflected by the probability of a bite distributed to available hosts. For each bite, a genetic preference on birds, other mammals, humans, and fake hosts (represented by a trap) are the probability p_1 (birds), p_2 (other mammals), p_3 (humans) and p_4 (fake hosts) respectively with $0 < p_i < 1 (i = 1, 2, 3, 4)$ and $\sum_{i=1}^{4} p_i = 1$.

Host abundance is an important extrinsic factor influencing *Culex* mosquito feeding preferences. We will combine genetic preferences (intrinsic determinants) and host abundance (extrinsic determinant) to give actual preferences exhibited by female *Culex* mosquitoes. The priority is to sort genetic preference based on degrees of preference. Obviously, the first biting choice is birds and it can be assumed for the rest satisfying $p_1 > p_2 > p_3 > p_4$ (McLaughlin and Focks (1990), Service (2008), Kilpatrick et al. (2007), Kilpatrick et al. (2006b), Hamer et al. (2009), Burkett-Cadena et al. (2008), Kilpatrick et al. (2006a), Hassan et al. (2003), Takken and Verhulst (2013), Rizzoli et al. (2015), Thiemann et al. (2011), Hamer et al. (2011), Savage et al. (2007)). We define actual preferences on birds, other mammals, humans, and fake hosts are p_B, p_A, p_H and p_F with $0 < p_B, p_A, p_H, p_F < 1$ and $p_B + p_A + p_H + p_F = 1$.

Based on the characteristics of *Culex* mosquito feeding preferences (McLaughlin and

Focks (1990), Service (2008), Kilpatrick et al. (2007)), we also assume that 1) actual preference on birds p_B is a function of bird population B, and the genetic preference on birds p_1 does not depend on B, and $\hat{B}$ is the particular value of B that satisfies $p_B(\hat{B}) = p_1$; 2) p_B is increasing, particularly, p_B will be less than p_1 if the number of birds B is less than $\hat{B}$; 3) actual preference on birds is zero if there is no bird. The relationship between p_B and p_1 is

$$p_B = w(B, \hat{B})p_1, \tag{3.5}$$

different functions satisfying assumptions 1) - 3) can be applied to formulate $w(B, \hat{B})$, for instance,

$$\begin{aligned} &1) w(B, \hat{B}) = \frac{B}{\hat{B}}, \\ &2) w(B, \hat{B}) = \log_{(\hat{B}+1)}(B+1). \end{aligned} \tag{3.6}$$

The next preferred host are other mammals. Except birds, the sum of the rest of the actual preferences is $(1 - p_B)$. The ratio of inherent preference on other mammals A among non-birds $(A + H + F)$ is $\frac{p_2}{p_2+p_3+p_4}$. We assume that actual preference p_A is equal to $(1 - p_B)\frac{p_2}{p_2+p_3+p_4}$ (without extrinsic influences) when other mammals A is $\hat{A}$, p_A will less than $(1 - p_B)\frac{p_2}{p_2+p_3+p_4}$ if the number of other mammals A is less than $\hat{A}$, and the relationship between them is

$$p_A = w(A, \hat{A})(1 - p_B)\frac{p_2}{p_2 + p_3 + p_4}. \tag{3.7}$$

Similarly, $w(A, \hat{A})$ can be

$$1)w(A, \hat{A}) = \frac{A}{\hat{A}}, \tag{3.8}$$

$$2)w(A, \hat{A}) = \log_{(\hat{A}+1)}(A+1).$$

For humans and fake hosts, they will share the rest of the actual preferences $(1 - p_B - p_A)$. We still assume that when the population of human H is $\hat{H}$, the ratio of actual preference between humans and other hosts is equal to the intrinsic one, meaning $p_H : p_F = p_3 : p_4$. If the human population H is less than $\hat{H}$, p_H will be less than preference $(1 - p_B - p_A)\frac{p_3}{p_3+p_4}$ determined by intrinsic factor. The relationship between p_H and p_3 is

$$p_H = w(H, \hat{H})(1 - p_B - p_A)\frac{p_3}{p_3 + p_4}, \tag{3.9}$$

Again, $w(H, \hat{H})$ can be

$$1)w(H, \hat{H}) = \frac{H}{\hat{H}}, \tag{3.10}$$

$$2)w(H, \hat{H}) = \log_{(\hat{H}+1)}(H+1).$$

Then mosquito actual feeding reference on fake hosts is $p_F = (1 - p_B - p_A - p_H)$.

3.2.2.2 Per capita reproduction rate $r(b, c, B, A, H)$

Not every bite of mosquitoes is efficient. A bite on birds is efficient/successful with probability q_B; similarly, the probability that a bite is efficient on humans and other mammals are q_H and q_A respectively.

The average number of bites per mosquito per day b, multiplied by the actual feeding preference p_B and a successful biting probability q_B, is efficient average bites of a mosquito on birds per day bp_Bq_B. In the same manner, a mosquito succeeds biting other mammals and humans in average bp_Aq_A, bp_Hq_H times per day, respectively.

Apparently, only by biting real hosts (including birds, other mammals and humans) can female mosquitoes produce offspring. Bites on all real hosts per mosquito is $(bp_Bq_B + bp_Aq_A + bp_Hq_H)$, simplifying as $b(p_Bq_B + p_Aq_A + p_Hq_H)$. After taking blood meals, female adults use nutrients (such as proteins) obtained from the blood to carry out egg production (Takken and Verhulst (2013)). In Mullen and Durden (2009), the mosquito egg-laying rate is delineated by a scaled mosquito biting rate (i.e., a scaling factor times biting rate). Here we use c to represent egg production rate per bite. With $b(p_Bq_B + p_Aq_A + p_Hq_H)$ bites, the number of eggs laid by a mosquito is $cb(p_Bq_B + p_Aq_A + p_Hq_H)$, which is females per capita reproduction rate, i.e.,

$$r(b, c, B, H, A) = cb(p_Bq_B + p_Aq_A + p_Hq_H). \tag{3.11}$$

3.2.2.3 Adult mosquitoes being trapped rate $C(M_{total}, B, A, H)$

If mosquitoes get close to a trap and bite fake hosts (mimicked by the trap), they may be captured by a trap. First, we decide the number of mosquitoes biting fake hosts. With $M_{total}(t)$ female mosquito individuals, total bites on fake hosts is $M_{total}(t) \times bp_F$ per day.

Combining the definition of the biting rate b, the number of mosquitoes attracted by a trap per day is $\frac{M_{total}(t)\times bp_F}{b} = p_F M_{total}(t)$.

Not every mosquito attracted by a trap will be successfully captured, as they struggle against traps. We assume that the probability of mosquitoes successfully captured is $q_c (0 \leq q_c \leq 1)$. Let $C(M_{total}, B, A, H)$ denote the rate of adult mosquitoes being trapped. Then the form of $C(M_{total}, B, A, H)$ can be one of following:

1) $C(M_{total}, B, A, H) = q_c p_F M_{total}(t)$. A linear increasing trapped rate with mosquito density is assumed.

2) $C(M_{total}, B, A, H) = \frac{q_c \bar{M}_c p_F M_{total}(t)}{a + p_F M_{total}(t)}$, which is an increasing function that saturates. That is without successfully trapping probability q_c, mosquitoes that a trap can hold has a finite positive limit $\bar{M}_c$ as M_{total} approaches infinity. The space of a trap is limited and cannot contain an infinite number of mosquitoes.

Traps are not operated every day, we need to modify the mosquitoes trapped term $C(M_{total}(t))$ to reflect this discontinuity. We introduce function $g(t)$, which is a sign function in the form

$$g(t) = \begin{cases} 1, & if\ a\ trap\ is\ operated\ on\ t^{th}\ day, \\ 0, & otherwise. \end{cases} \tag{3.12}$$

Particularly, if traps are set daily, we just set $g(t) = 1$ for all t in (3.12).

3.2.2.4 Trapped mosquitoes being collected rate

To incorporate the process of mosquito collection in a dynamical model, we add an output representing collection for $M_{collect}(t)$ compartment. In particular, we set up a time point as a start of one day, for example, we set 9:00 am as the point. $M_{collect}(t)$ is the mosquito population at time 9:00 am on the t^{th} day. We trap mosquitoes on the i^{th} day (one day) means we trap mosquitoes from 9:00 am on the i^{th} day to next day 9:00 am. Under this set-up, if we collect mosquito on the i^{th} day, with collection starting at 9:00 am on the i^{th} day. We assume it takes u_c day ($u_c \times 24$ hours) to collect mosquitoes, u_c is short and during this period no mosquitoes enter the trap. Then the mosquito population in a trap decreases from $M_{collect}(t)$ to 0 during u_c day. This change rate (trapped mosquitoes being collected rate) should be $\frac{0-M_{collect}(t)}{u_c}$, a trap is empty after each collection. Again, we introduce the function $f(t)$ to describe on which day to collect mosquitoes (to empty a trap)

$$f(t) = \begin{cases} 1, & if\ mosquitoes\ being\ collected\ on\ t^{th}\ day, \\ \\ 0, & otherwise. \end{cases} \tag{3.13}$$

3.2.3 A specific model for the Region of Peel

In the Region of Peel, mosquitoes are trapped and collected weekly. Specifically, traps are operated at 2:00pm on one afternoon and mosquitoes are collected at 9:00 am next

morning in each week (trapping for 19 hours). Here we use the 24-hour mode to approximate the 19-hours, since the period (9:00 am-2:00 pm on the same day) is a short time frame when female *Culex* mosquitoes are least likely to bite (Rozendaal (1997)). Thus, we modify $f(t)$ in the general model (3.4) and obtain the following model for the Peel region

$$\begin{cases} \frac{dL(t)}{dt} = r(b,c,B,H,A)[M_{total}(t) - M_{collect}(t)] - eL(t) - d_l L(t) - \kappa L_t^2, \\ \frac{dM_{total}(t)}{dt} = eL(t) - d_m M_{total}(t) - g(t)C(M_{total}(t), B, A, H), \\ \frac{dM_{collect}(t)}{dt} = g(t)C(M_{total}(t), B, A, H) - g(t-1)\frac{M_{collect}(t)}{u_c}, \end{cases} \tag{3.14}$$

where $g(t)$ is the form (3.12) representing when to set a trap, $f(t) = g(t-1)$ represents that mosquitoes are collected from the trap on the next day. If a trap is set on the i^{th} day, $g(t) = 1$ when $t = i$, then $f(t+1) = g(t) = 1$, that is, collection is operated on the $(i+1)^{th}$ day. Thus it is reasonable to use $g(t-1)$ (to replace $f(t)$) to indicate that mosquitoes in this trap are collected next day.

Temperature and precipitation have profound effects on mosquito abundance in time and space (Mullen and Durden (2009)). Temperature is influential on the *Culex* mosquito biting rate, maturation and mortality rate (Gong et al. (2011), Rubel et al. (2008), De Meillon et al. (1967), Otero et al. (2006), Dohm et al. (2002), Møller (2013), Service (1980), Reisen et al. (2006b)). Precipitation influences the intraspecific competition among preadult mosquitoes by changing the abundance and type of aquatic habitats (Shaman and Day (2007)). Based on our previous work and research (Wang et al. (2017), Gong et al. (2011),

Rubel et al. (2008), De Meillon et al. (1967), Otero et al. (2006)), we adopt temperature (T) and precipitation (P)-dependent functions in the following:

$$
\begin{aligned}
b(T) &= \frac{0.344}{1 + 1.231\exp(-0.184(T-20))}, \\
e(T) &= \frac{(T+273.15)exp(\frac{47.42(T-25)}{T+273.15})}{1192.6[1+exp(\frac{59.6(T-25.45)}{T+273.15})]}, \\
d_l(T) &= 1 - S_l\exp[-(\frac{T-T_l}{Var_{Tl}})^2], \\
d_m(T) &= 1 - S_m\exp[-(\frac{T-T_m}{Var_{Tm}})^2], \\
\kappa(P) &= \frac{(1+\rho)\bar{\kappa}}{1+\rho\exp[-(\frac{P-P_l}{Var_{Pl}})^2]}.
\end{aligned}
\tag{3.15}
$$

Replacing constant parameters in the model (3.14) by (3.15), we obtain a system driven by temperature and precipitation. Then we do numerical simulations to show how to predict total female *Culex* mosquitoes in a region based on trapped mosquitoes. Weather data (temperature and precipitation) is from June to October in 2015 gathered from Toronto Pearson International Airport Station Government of Canada (2011). The maturation rate e depends on the arithmetic mean of previous 11 days' temperature and other weather-dependent parameters depend on daily weather data Wang et al. (2017). Trapped *Culex* mosquitoes are collected from a trap located in the Region of Peel.

3.3 Results

We first qualitatively analyze a corresponding continuous system of (3.4) by equalization. Then we carry out numerical simulations to analyze the dynamics of the model.

3.3.1 Model analysis

Before numerically analyzing the dynamics of the system (3.4), it is instructive to qualitatively analyze its continuous system by equalization. In specific, the processes of trapping and collecting mosquitoes once a week is averaged to seven days of a week, that is, mosquitoes are trapped and data are collected every day (in this case, $f(t) = g(t) = 1$). Then this continuous system is

$$\begin{cases} \frac{dL(t)}{dt} = r(b, c, B, H, A)[M_{total}(t) - M_{collect}(t)] - eL(t) - d_l L(t) - \kappa L_t^2, \\ \frac{dM_{total}(t)}{dt} = eL(t) - d_m M_{total}(t) - C(M_{total}(t), B, A, H), \\ \frac{dM_{collect}(t)}{dt} = C(M_{total}(t), B, A, H) - \frac{M_{collect}(t)}{u_c}, \end{cases} \tag{3.1}$$

For the system (3.1), all compartments need to be non-negative for all time t and all parameters should be positive. Then the model is mathematically and ecologically well-posed and studied in the invariant region:

$$D = \{(L, M_{total}, M_{collect}) \in \mathbb{R}^3 | L, M_{total}, M_{collect} \geq 0\}. \tag{3.2}$$

For simplification, we use r to represent $r(b, c, B, H, A)$, then the analysis is carried out in the following two cases.

3.3.1.1 Linear female mosquitoes being trapped rate

The system (3.1) with linear being trapped rate $C(M_{total}, B, A, H) = q_c p_F M_{total}(t)$ has up to two nonnegative equilibrium points.

Trivial equilibrium point

The model has a trivial equilibrium which is denoted by $E_0 = (0, 0, 0)$. The stability of E_0 depends on the basic offspring number Q_0:

$$Q_0 = \frac{er(1 - q_c p_F u_c)}{(e + d_l)(d_m + q_c p_F)}, \tag{3.3}$$

it presents the average expected number of alive newborn mosquitoes produced by a single female mosquito during its life time. Ecologically, it is interpreted as the fraction of newborn immature mosquitoes survived and emerged into adults $\frac{er}{e+d_l}$, multiplied by the successful survival and not being captured by a trap $\frac{1-q_c p_F u_c}{d_m+q_c p_F}$.

Theorem 3.3.1. *The trivial equilibrium E_0 of the system (3.1) with linear female mosquitoes being trapped rate is locally asymptotically stable if $Q_0 < 1$, and unstable if $Q_0 > 1$.*

Proof. The Jacobian matrix of the system (3.1) at E_0 is

$$J(E^-) = \begin{bmatrix} -e - d_l & r & -r \\ e & -d_m - q_c p_F & 0 \\ 0 & q_c p_F & -\frac{1}{u_c} \end{bmatrix}, \tag{3.4}$$

with the corresponding characteristic equation

$$\lambda^3 + a_2\lambda^2 + a_1\lambda + a_0 = 0, \tag{3.5}$$

where

$$\begin{aligned} a_2 &= e + d_l + d_m + q_c p_F + \frac{1}{u_c}, \\ a_1 &= \frac{1}{u_c}(e + d_l + d_m + q_c p_F) + (e + d_l)(d_m + q_c p_F) - er, \\ a_0 &= \frac{1}{u_c}(e + d_l)(d_m + q_c p_F)(1 - Q_0). \end{aligned} \tag{3.6}$$

Applying the Routh-Hurwitz criteria, E_0 is locally asymptotically stable if

$$a_2 > 0, a_0 > 0 \ \& \ a_1 a_2 - a_0 > 0. \tag{3.7}$$

Rewriting $a_1 a_2 - a_0$, we have

$$\begin{aligned} a_1 a_2 - a_0 = (e + d_l + d_m + q_c p_F) u_c a_0 + \frac{1}{u_c^2}[(e + d_l + d_m + q_c p_F) u_c + 1][e \\ + d_l + d_m + q_c p_F (1 - e r u_c^2)]. \end{aligned} \tag{3.8}$$

It is apparent that $a_2 > 0$ since all parameters are positive. When $Q_0 < 1, a_0 > 0$, and combining with $1 - eru_c^2 > 0$ (based on the magnitudes of the parameters in Table 3.3),

we also obtain $a_1a_2 - a_3 > 0$. Thus, the trivial equilibrium E_0 is locally asymptotically stable if $Q_0 < 1$.

If $Q_0 > 1$, then $a_0 < 0$, the characteristic equation (3.5) has roots with positive real part. Hence, E_0 is unstable. □

Non-trivial equilibrium point

If $Q_0 > 1$, the system (3.1) also has a positive equilibrium $E_1 = (L_1, M_{total_1}, M_{collect_1})$ with $M_{total_1} = \frac{e[er(1-q_cp_Fu_c)-(e+d_l)(d_m+q_cp_F)]}{\kappa(d_m+q_cp_F)^2}$, $L_1 = \frac{d_m+q_cp_F}{eM_{total_1}}$, $M_{collect_1} = q_cp_Fu_cM_{total_1}$.

Theorem 3.3.2. *The equilibrium point E_1 of the system (3.1) is locally asymptotically stable if $Q_0 > 1$.*

Proof. The Jacobian matrix of the system (3.1) at E_1 is

$$J(E^-) = \begin{bmatrix} \frac{er(q_cp_Fu_c-1)+u_ca_0}{z} & r & -r \\ e & -z & 0 \\ 0 & q_cp_F & -\frac{1}{u_c} \end{bmatrix}, \tag{3.9}$$

where $z = d_m + q_cp_F$ and a_0 is represented in (3.6). The characteristic equation associated to matrix (3.9) is

$$\lambda^3 + b_2\lambda^2 + b_1\lambda + b_0 = 0, \tag{3.10}$$

where

$$b_2 = \frac{1}{zu_c}[z(zu_c+1) + eru_c(1-q_cp_Fu_c) - a_0u_c^2], \tag{3.11}$$
$$b_1 = \frac{1}{zu_c}[er + z^2 - (erq_cp_F + a_0)u_c(zu_c+1)],$$
$$b_0 = -a_0.$$

Again, we use Routh-Hurwitz criteria to investigate the stability of E_1. E_1 is locally asymptotically stable if

$$b_2 > 0, b_0 > 0 \ \& \ b_1b_2 - b_0 > 0, \tag{3.12}$$

in specific,

$$\begin{aligned} b_1b_2 - b_0 =& \frac{1}{(z^2u_c^2}\{u_c^3a_0^2(zu_c+1) - u_ca_0[2zu_cd_m + 2zq_cp_Fu_c(1-eru_c^2) \\ &+ 2eru_c(1-q_cp_Fu_c) + zu_c^2(er+z^2+z)] + [q_cp_F(1-eru_c^2) \\ &+ u_c(er+z^2) + d_m][zq_cp_F(1-eru_c^2) + zd_m + er(1-q_cp_Fu_c)]\}. \end{aligned} \tag{3.13}$$

By the definition of Q_0 (3.3) and Theorem 3.3.1, $1 - q_cp_Fu_c > 0 \ \& \ a_0 < 0$ whenever $Q_0 > 1$. Also, all parameters are positive and $1 - eru_c^2 > 0$ (which has been shown in Theorem 3.3.1), then all conditions of (3.12) are satisfied, thus, the equilibrium point E_1 is locally asymptotically stable. □

3.3.1.2 Nonlinear female mosquitoes being trapped rate

Any nonnegative equilibrium of the system (3.1) with nonlinear female mosquitoes being trapped rate $C(M_{total}, B, A, H) = \frac{q_c \bar{M}_c p_F M_{total}(t)}{a + p_F M_{total}(t)}$ can be expressed as $\tilde{E} = (\tilde{L}, \tilde{M}_{total}, \tilde{M}_{collect})$ satisfying

$$\begin{aligned} &\tilde{M}_{total}(k_3 \tilde{M}_{total}^3 + k_2 \tilde{M}_{total}^2 + k_1 \tilde{M}_{total} + k_0) = 0, \\ &\tilde{L} = \frac{d_m(a + p_F \tilde{M}_{total})\tilde{M}_{total} + q_c \tilde{M}_c p_F \tilde{M}_{total}}{e(a + p_F \tilde{M}_{total}}, \\ &\tilde{M}_{collect} = \frac{u_c q_c \tilde{M}_c p_F \tilde{M}_{total}}{a + p_F \tilde{M}_{total}}, \end{aligned} \tag{3.14}$$

where

$$\begin{aligned} &k_3 = \kappa d_m^2 p_F^2, \\ &k_2 = p_F[2\kappa d_m(a d_m + q_c \bar{M}_c p_F) + e p_F(d_l d_m + d_m e - e r)], \\ &k_1 = \kappa(a d_m + q_c \bar{M}_c p_F)^2 + e q_c \bar{M}_c p_F^2(u_c e r + d_l + e) + 2ae p_F(d_l d_m + d_m e - e r), \\ &k_0 = ae[(d_l + e)(a d_m + q_c \bar{M}_c p_F) - e r(a - u_c q_c \bar{M}_c p_F)]. \end{aligned} \tag{3.15}$$

Trivial equilibrium point

The system (3.1) with nonlinear trapped rate has a trivial equilibrium point $E_0 = (0, 0, 0)$ and we calculate the basic offspring number Q_0:

$$Q_0 = \frac{e r(a - q_c \bar{M}_c p_F u_c)}{(e + d_l)(a d_m + q_c \bar{M}_c p_F)}. \tag{3.16}$$

Theorem 3.3.3. *The trivial equilibrium E_0 of the system (3.1) with nonlinear female mosquitoes being trapped rate is locally asymptotically stable if $Q_0 < 1$, and unstable if $Q_0 > 1$.*

Proof. The Jacobian matrix of the system (3.1) at E_0 is

$$J(E_0) = \begin{bmatrix} -(e+d_l) & r & -r \\ e & -(d_m + \frac{q_c \bar{M}_c p_F)}{a} & 0 \\ 0 & \frac{q_c \bar{M}_c p_F}{a} & -\frac{1}{u_c} \end{bmatrix}, \tag{3.17}$$

with the eigenvalues satisfying the characteristic equation

$$\lambda^3 + \hat{a}_2\lambda^2 + \hat{a}_1\lambda + \hat{a}_0 = 0, \tag{3.18}$$

where

$$\begin{aligned} \hat{a}_2 =& e + d_l + d_m + \frac{q_c \bar{M}_c p_F}{a} + \frac{1}{u_c}, \\ \hat{a}_1 =& \frac{1}{u_c}(e + d_l + d_m + q_c p_F) + \frac{1}{a u_c}\{[(e+d_l)u_c + 1](a d_m + q_c \bar{M}_c p_F q_c p_F) \\ & + a(e+d_l)\} - er, \\ \hat{a}_0 =& \frac{1}{a u_c}(e+d_l)(a d_m + q_c \bar{M}_c p_F)(1 - Q_0). \end{aligned} \tag{3.19}$$

Applying the Routh-Hurwitz criteria, E_0 is locally asymptotically stable if

$$\hat{a}_2 > 0, \hat{a}_0 > 0 \ \& \ \hat{a}_1\hat{a}_2 - \hat{a}_0 > 0, \tag{3.20}$$

where

$$\begin{aligned}\hat{a}_1\hat{a}_2 - \hat{a}_0 =& \frac{q_c\bar{M}_c p_F[e(1-ru_c)+(e+2d_l+2d_m)]}{au_c} \\ &+ \frac{(q_c\bar{M}_c p_F)^2 + a^2(e+d_l+d_m)^2}{a^2u_c} \\ &+ \frac{[q_c\bar{M}_c p_F + a(e+d_l+d_m)][u_c^2(e+d_l)(ad_m+q_c\bar{M}_c p_F)+a(1-eru_c^2)]}{a^2u_c^2}.\end{aligned} \tag{3.21}$$

$\hat{a}_2 > 0$ as all parameters are positive, and $\hat{a}_0 > 0$ when $Q_0 < 1$. By the magnitudes of the parameters in Table 3.3, we have $(1 - ru_c) > 0$ and $1 - eru_c^2 > 0$, then $\hat{a}_1\hat{a}_2 - \hat{a}_3 > 0$. Thus, the trivial equilibrium E_0 is locally asymptotically stable if $Q_0 < 1$. Contrarily, $Q_0 > 1$ contributes to $\hat{a}_0 < 0$, then characteristic equation (3.18) has roots with positive real part, and E_0 is unstable. □

Non-trivial equilibrium point

$k_3 > 0$ is due to the positivity of all parameters, and rewriting the coefficients (3.15) of the equation (3.14), we have

$$k_0 = ae(e+d_l)(ad_m + q_c\bar{M}_c p_F)(1-Q_0). \tag{3.22}$$

By Descartes' Rule of Signs, we have following situations: $S1)$ If $Q_0 < 1$, the equation (3.14) has 2 or 0 real root(s); $S2)$ If $Q_0 > 1$, the equation (3.14) has 3 or 1 real root(s). Considering the ecological reality, we only care about the existence of positive equilibria when parameters in the model (3.1) are positive.

Furthermore, if $er \leq d_l d_m + d_m e$, no positive equilibrium exists. If $er > d_l d_m + d_m e$, we reorganize $k_3 \tilde{M}_{total}^3 + k_2 \tilde{M}_{total}^2 + k_1 \tilde{M}_{total} + k_0 = 0$ in (3.14) in terms of a,

$$s_2 a^2 + s_1 a + s_0 = 0 \tag{3.23}$$

where

$$\begin{aligned} s_2 =& \tilde{M}_{total}^2 p_F^2 [\tilde{M}_{total} d_m^2 \kappa + e(d_l d_m + d_m e - er)], \\ s_1 =& \tilde{M}_{total} [2\tilde{M}_{total} \kappa d_m p_F (d_m + q_c + p_F) + e q_c p_F^2 (u_c er + d_l + e) \\ & + 2e p_F (d_l d_m + d_m e - er)], \\ s_0 =& \tilde{M}_{total} \kappa (q_c p_F + d_m)^2 + e q_c p_F (u_c er + d_l + e) + e(d_l d_m + d_m e - er). \end{aligned} \tag{3.24}$$

For the equation (3.23), if no positive root a exists when $\tilde{M}_{total} > 0$, we can conclude that there is no positive $\tilde{M}_{total}$ satisfying the the equation (3.14). Then we consider the following two cases.

Case 1: If $\tilde{M}_{total} \geq \frac{e(er - d_l d_m - d_m e)}{d_m^2 \kappa}$, then $s_2 \geq 0,\ s_1 > 0$ and $s_0 > 0$, which indicates there is no positive a satisfying (3.23).

Case 2: If $0 < \tilde{M}_{total} < \frac{e(er - d_l d_m - d_m e)}{d_m^2 \kappa}$, then $s_2 < 0$. The discriminant of (3.23)

$$\begin{aligned} s_1^2 - 4 s_2 s_0 =& \tilde{M}_{total}^2 e^2 q_c^2 p_F^4 [4\kappa r \tilde{M}_{total} ((u_c d_m + 1)) + (u_c er + d_l + e)^2] \\ >& 0, \end{aligned} \tag{3.25}$$

then equation (5.22) has two distinguished roots a.

1. If $Q_0 < 1$, $s_0 > 0$, then a unique positive parameter a exists.

2. If $Q_0 > 1$, $-\frac{e^2 p_F}{8\kappa d_m(d_m+q_c p_F)}[q_c p_F(u_c er + d_l + e) + 2(d_l d_m + d_m e - er)]^2 < s_1 < \frac{e^2 p_F^2 q_c}{\kappa d_m^3}(d_l d_m + d_m e - er)(-d_m u_c er + d_l d_m + d_m e - 2er)$. s_1 reaches the minimum when $\tilde{M}_{total} = -\frac{e}{4\kappa d_m(d_m+q_c p_F))}[q_c p_F(u_c er + d_l + e) + 2(d_l d_m + d_m e - er)]$, s_1 reaches the maximum when $\tilde{M}_{total} = \frac{e}{d_m^2 \kappa}(er - d_l d_m - d_m e)$. $s_1 < 0$ when $0 < \tilde{M}_{total} < -\frac{e}{2\kappa d_m\ (d_m+q_c p_F)}\ [q_c p_F(u_c er + d_l + e) + 2(d_l d_m + d_m e - er)]$, $s_1 > 0$ when $-\frac{e}{2\kappa d_m\ (d_m+q_c p_F)}[$ $q_c p_F\ (u_c er + d_l + e) + 2(d_l d_m + d_m e - er)] < \tilde{M}_{total} < \frac{e}{d_m^2 \kappa}(er - d_l d_m - d_m e)$.

Also $e[q_c p_F(u_c er + d_l + e) + (d_l d_m + d_m e - er)] < s_0 < -\frac{e p_F q_c}{d_m^2}[(d_l d_m + d_m e - er)(d_m + q_c p_F) - d_m er(1 + d_m u_c)]$. $s_0 < 0$ when $0 < \tilde{M}_{total} < -\frac{e}{\kappa(d_m+q_c p_F)^2)}[q_c p_F(u_c er + d_l + e) + (d_l d_m + d_m e - er)]$, $s_0 > 0$ when $-\frac{e}{\kappa(d_m+q_c p_F)^2}[q_c p_F(u_c er + d_l + e) + (d_l d_m + d_m e - er)] < \tilde{M}_{total} < \frac{e}{d_m^2 \kappa}(er - d_l d_m - d_m e)$.

Then we have that when $-\frac{e}{\kappa(d_m+q_c p_F)^2}[q_c p_F(u_c er + d_l + e) + (d_l d_m + d_m e - er)] < \tilde{M}_{total} < \frac{e}{d_m^2 \kappa}(er - d_l d_m - d_m e)$, a unique positive parameter a exists, and we summarize the results in Table 3.2.

Therefore, we obtain that positive equilibrium point(s) may exist in the following two cases: 1) positive equilibrium point(s) with $0 < \tilde{M}_{total} < \frac{e(er - d_l d_m - d_m e)}{d_m^2 \kappa}$ may exist when $er > d_l d_m + d_m e$ and $Q_0 < 1$ are satisfied; 2) positive equilibrium point(s) with $\frac{-e}{\kappa(d_m+q_c p_F)^2}[q_c p_F(u_c er + d_l + e) + (d_l d_m + d_m e - er)] < \tilde{M}_{total} < \frac{e(er - d_l d_m - d_m e)}{d_m^2 \kappa}$ may exist when $er > d_l d_m + d_m e$ and $Q_0 > 1$ are satisfied. The exact number of positive

Table 3.2: The existence of positive a depending on the sign of s_1 & s_0

$\tilde{M}_{total}$	s_1	s_0	Positive a
$\big(0, \frac{-e}{\kappa(d_m+q_cp_F)^2}[q_cp_F(u_cer+d_l+e)+(d_ld_m+d_me-er)]\big]$	<0	<0	$\nexists$
$\big(\frac{-e}{\kappa(d_m+q_cp_F)^2}[q_cp_F(u_cer+d_l+e)+(d_ld_m+d_me-er)], \frac{-e}{2\kappa(d_m+q_cp_F)^2}[q_cp_F(u_cer+d_l+e)+2(d_ld_m+d_me-er)]\big]^*$	≤ 0	>0	$\exists$
$\big(\frac{-e}{2\kappa(d_m+q_cp_F)^2}[q_cp_F(u_cer+d_l+e)+2(d_ld_m+d_me-er)], \frac{e}{d_m^2\kappa}(er-d_ld_m-d_me)\big)$	>0	>0	$\exists$

* $-\frac{e}{\kappa(d_m+q_cp_F)^2}[q_cp_F(u_cer+d_l+e)+(d_ld_m+d_me-er)] < -\frac{e}{2\kappa(d_m+q_cp_F)^2}[q_cp_F(u_cer+d_l+e)+2(d_ld_m+d_me-er)]$, since $-\frac{e}{\kappa(d_m+q_cp_F)^2}[q_cp_F(u_cer+d_l+e)+(d_ld_m+d_me-er)]-(-\frac{e}{2\kappa(d_m+q_cp_F)^2}[q_cp_F(u_cer+d_l+e)+2(d_ld_m+d_me-er)]) = -\frac{eq_cp_F}{2\kappa d_m(d_m+q_cp_F)^2} < 0.$

equilibriums needs to be considered in future work.

3.4 Sensitivity analysis, parameter estimation and numerical simulations

First, we do the sensitivity analysis of each parameter on the three output variables, the population of the preadult female, the adult female and the collected female. Then combining model (3.1) with parameters in (3.15) and weekly trapped *Culex* mosquito data, we obtained estimated values of parameters. Then adopting these estimated parameters,

we present the population of aquatic-stage females and total females in the ETZ, and the number of trapped mosquitoes and collected data.

3.4.1 Sensitivity analysis

To do the sensitivity analysis of each parameter in the system (3.1) (with a trapped rate in the form of $C(M_{total}, B, A, H) = q_c p_F M_{total}(t))$ on the three critical output variables, $L(t)$, $M_{total}(t)$ and $M_{collect}(t)$. Specifically, we evaluate partial rank correlation coefficients (PRCCs) between each input parameter and the output variable, using Latin hypercube sampling (LHS) with 3000 samples (Marino et al. (2008)). Due to the absence of available data and a priori information on the distributions of input parameters, we choose uniform distributions for each parameter with corresponding baseline and range in Table 3.3. When $g(t) = 0$ parameters related to trapping and collecting procedures have no effect on three output variables. To obtain the sensitivity analysis of these parameters on female mosquito abundance, we choose $g(t) = 1$ in the analysis. Also, we treated the reproduction rate r as one parameter rather than split it into several parameters.

Table 3.3: Parameters analyzed in sensitivity analysis (1)

Par.	Description	Baseline & Range (day^{-1})

r	The female per capita reproduction (egg-laying) rate	0.6 & $[0.036, 42.5]$
e	The female per capita maturation rate (the preadult to the adult)	0.06 & $[0.051, 0.093]$
d_l	The preadult female per capita mortality rate	0.4 & $[0.213, 16.9]$
κ	Intraspecific competition rate of the preadult female	0.005 & $[0, 1]$
d_m	The adult female per capita mortality rate	0.05 & $[0.016, 0.07]$
p_F	Actual feeding preference on fake hosts	0.3 & $[0, 0.4]$
q_c	The probability of mosquitoes being successfully captured	0.1313 & $[0, 0.8]$
u_c	The time taken to collect trapped mosquitoes	0.0035 & $[0, 0.0148]$

To address how the number of bird, human and other animal hosts affect mosquito abundance, we look deep into the reproduction procedure, decompose the reproduction rate r and carry out the sensitivity analysis of parameters c, b, B, A and H in system (3.1) (with trapped rate in the form $C(M_{total}, B, A, H) = q_c p_F M_{total}(t)$) on the critical output variables, $L(t)$, $M_{total}(t)$ and $M_{collect}(t)$. We evaluated partial rank correlation coefficients (PRCCs) between each of these input parameters and output variable, using

Latin hypercube sampling (LHS) with 3000 samples (Marino et al. (2008)); we chose uniform distributions for each parameter (corresponding baseline and range in Table (3.4) because of the absence of available data and a priori information on the distributions of input parameters.

Table 3.4: Parameters analyzed in sensitivity analysis (2)

Par.	Description	Baseline & Range (day^{-1})
c	Egg production rate per bite	2.325 & $[0.1, 6]$
b	Female adult mosquitoes per capita biting rate	0.5 & $[0.2, 0.75]$
B	The population of birds in a region	40 & $[10, 200]$
A	The population of other mammals in a region	50 & $[10, 150]$
H	The population of humans in a region	5 & $[1, 15]$

Sensitivity analysis (Fig. 3.3) shows that mosquito reproduction rate r, maturation rate e, mortality rates d_l and d_m, intraspecific competition rate κ have significant impacts (with $p - value < 0.05$) on both preadult and adult female mosquito population $L(t)$ and $M_{total}(t)$, while only slight impacts on $M_{collect}(t)$. Reversely, $M_{collect}(t)$ is sensitive to the rest of the three parameters p_F, q_c and u_c, but not for $L(t)$ and $M_{total}(t)$.

Sensitivity analysis (Fig. 3.4) indicates all of these five parameters significantly influence (with $p - value < 0.05$) preadult, adult and collected female mosquito popula-

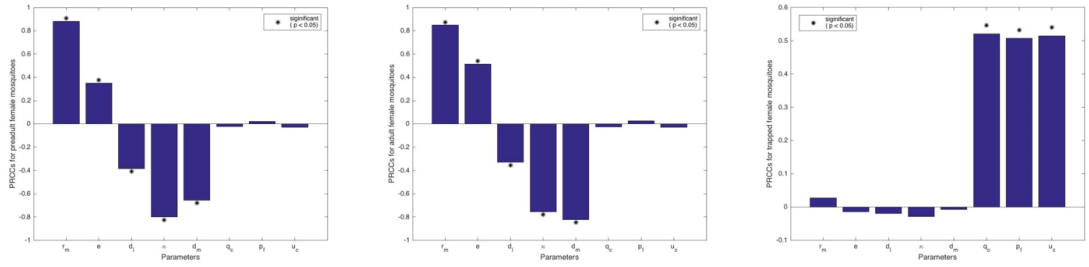

Figure 3.3: Performance of LHS/PRCC on the model (3.1) with input parameters r, e, d_l, κ, d_m, p_F, q_c and u_c. Parameters with a PRCC significantly $(p < 0.05)$ different from zero are indicated with $(*)$.

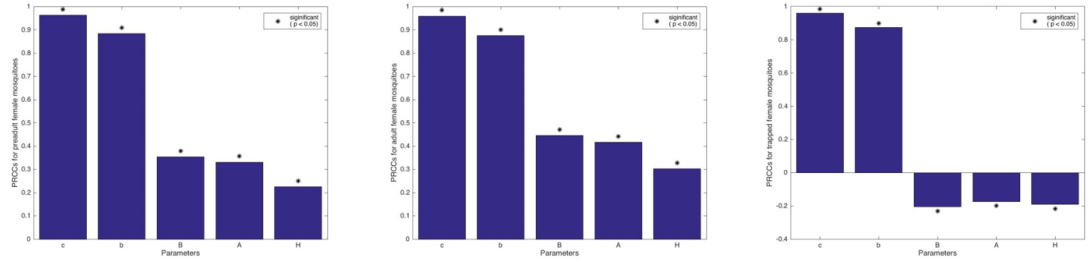

Figure 3.4: Performance of LHS/PRCC on the model (3.1) with input parameters c, b, B, A and H. Parameters with a PRCC significantly $(p < 0.05)$ different from zero are indicated with $(*)$.

tions. Egg reproduction rate per bite c and mosquito biting rate b have positive impacts on all mosquito populations, the increase of c and b results in the increase of the mosquito population. While for host populations, they affect three classes of mosquitoes in different ways. Host populations including birds (B), humans (H) and other mammals (A) positively influences preadult and adult mosquitoes and negatively influences collected mosquitoes. This is in accordance with what is expected: more host abundance (B, A, H) provides more blood meals, which promotes mosquito reproduction. More real hosts, the priority choice for host-seeking female mosquitoes, lead to fewer adults being attracted and collected by traps (fake hosts).

3.4.2 Parameter estimation

Model realities strongly depend on the assumed parameters and having an accurate estimation of parameters is critical. Since there are multiple parameters involved in the model, we first classify the parameters into groups based on their functions: one group is related to trapping and collecting process (u_c, q_c and p_F), another group is the temperature-dependent parameters.

To make use of the weekly trapping counts (data) to estimate the total number of mosquitoes in one area, the parameters u_c, q_c and p_F are fitted to the data.

For the temperature or precipitation dependent parameters, the optimal temperatures

(T_l, T_m) for survival and corresponding survival rates (S_l, S_m) of *Culex* mosquitoes are fixed no matter where they live. The variance of temperature and precipitation Var_T and Var_P is also fixed and is calculated with daily weather data. The component of reproduction rate $c(p_B q_B + p_A q_A + p_H q_H)$, denoted as $\bar{c}$, largely depends on host demographics in different locations. Also, the precipitation level P_l varies along with locations. Thus $\bar{c}$ and P_l still need to be estimated with different trap locations.

Five months' trap count data (June - October) are available to estimate unknown parameters $\bar{c}$, P_l, u_c, q_c and p_F. Here trap count data is weekly trapped female *Culex* mosquitoes obtained from a specific trap located in the Region of Peel health unit. To remove variation and fill in missing data values, we smooth trap count data. Smoothed weekly trapped count data is obtained by averaging previous, current and next week trap counts. Then the estimation is carried out by minimizing the difference between the observed trap count data and our model produced results $M_{collect}(t)$. Except parameters $\bar{c}$, P_l, u_c, q_c and p_F, other parameters are given in Table 3.5. Considering the following model validation, we only use four months' trap count data to estimate the parameters and treat remaining months as a validation set. In particular, we have five approaches to choose four months' count data to estimate parameters: A1 (June, July, August, September), A2 (June, July, August, October), A3 (June, July, September, October), A4 (June, August, September, October), A5 (July, August, September, October). For each approach, we can

obtain a corresponding set of estimated values (in Table 3.5).

Table 3.5: Values of fixed and estimated parameters

Fixed par.	S_l	S_m	T_l	T_m	ρ	$\bar{\kappa}$
Value	0.95	0.93	17	23	9	0.001

Est. par.	$\bar{c}$	P_l	u_c	q_c	p_F
Value - A1	5.825	1.125	0.01	0.675	0.2875
Value - A2	5.825	2.375	0.0002	0.925	0.2875
Value - A3	4.45	5.875	0.0027	0.8155	0.225
Value - A4	4.3876	3	0.0061	0.925	0.2875
Value - A5	5.3719	6	0.0178	0.9328	0.2876

3.4.3 Model validation

We carry out cross-validation against real trap count data. We implement the validation in five ways where we divide the original data into a training set and a validation set. These five ways correspond to five sets of estimations, i.e., W1 (training set: A1, validation set: October's), W2 (training set: A2, validation set: September's), W3 (training set: A3, validation set: August's), W4 (training set: A4, validation set: July's), W5 (training set:

A5, validation set: June's). We adopt fixed parameter values and five sets of estimated parameter values (Table 3.5) in the model (3.14) to simulate the population of female preadult, adult and trapped mosquitoes from July to October.

By comparing all simulated and real trap count data in validation sets (Fig. 3.5), we find that our simulated results can identify trends in mosquito abundance. The errors between simulated results and real data may be due to more complex factors than just temperature and precipitation.

For the third and fourth set validation W3 and W4, the error of estimations is a little larger, indicating that trap count data in July and August (the period during which mosquito abundance is increasing) is more helpful to produce an accurate estimation. In general, our model is a reasonable representation of the actual system.

3.5 Estimated female mosquito population during surveillance season

Based on the validated model (3.14), we can obtain a more accurate estimation of the mosquito population. It is apparent that if more information is used we could have more accurate estimations. We estimated parameters $\bar{c}$, P_l, u_c, q_c and p_F by using trap count data of all five months (June - October). Moreover, we have simulated the model with two different trapped rate forms. With trapped rate in the form $C(M_{total}, B, A, H) =$

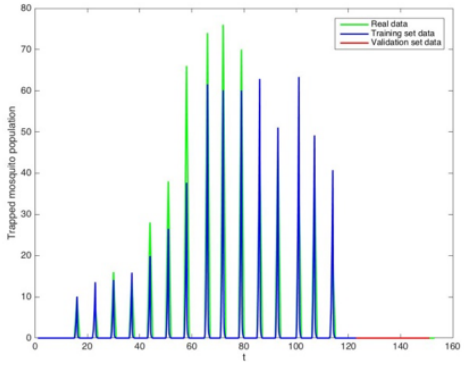

(a) W1: October's trap count data is validation set

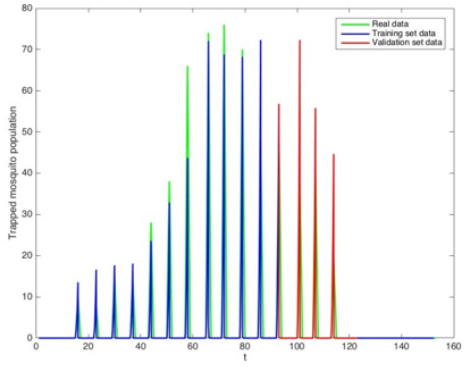

(b) W2: September's trap count data is validation set

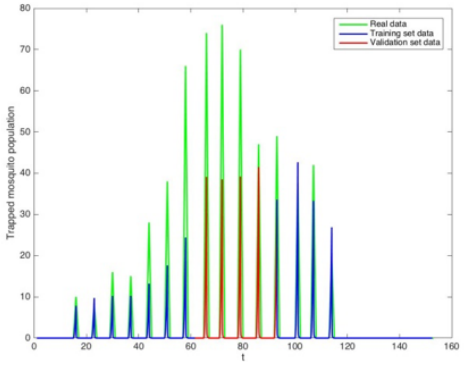

(c) W3: August's trap count data is validation set

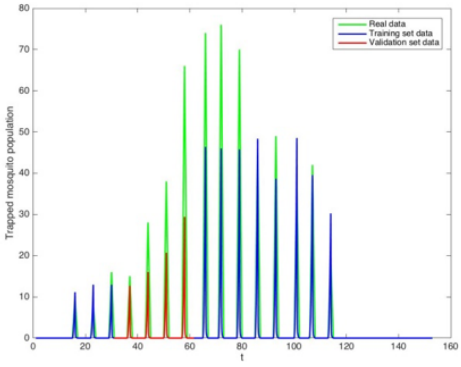

(d) W4: July's trap count data is validation set

Figure 3.5: Model validations against real trap count data with five pairs (training set & validation set) of data sets (W1, W2, W3, W4, W5).

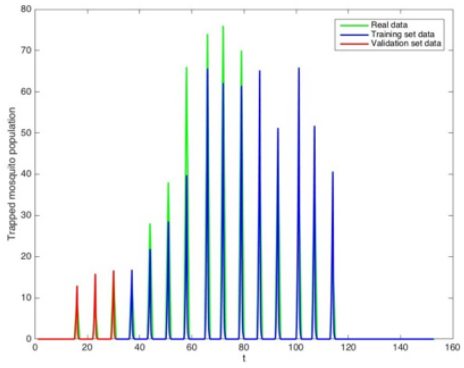

(e) W5: June's trap count data is validation set

Figure 3.5: (Cont.) Model validations against real trap count data with five pairs (training set & validation set) of data sets (W1, W2, W3, W4, W5).

$q_c p_F M_{total}(t)$, the results are shown in Fig. 3.6 and Fig. 3.7. With trapped rate in the form $C(M_{total}, B, A, H) = \frac{q_c \bar{M}_c p_F M_{total}(t)}{a + p_F M_{total}(t)}$, the results are shown in Fig. 3.8 and Fig. 3.9.

Results (Fig. 3.6 - Fig. 3.9) show that two trapped rates can be used to fit observed data of trapped *Culex* mosquitoes and to predict total *Culex* mosquito population. The changes of total *Culex* mosquito abundance with these two trapped rates reveal the same trends, only peak values are different (Fig. 3.6 vs. Fig. 3.8). Moreover, the initial size of mosquitoes (including pre-adult mosquitoes, adults and trapped mosquitoes) has a notable influence on mosquito abundance around the first month (0-30 days), nevertheless, this influence will not last until the end of October. Hence the trend of mosquito development will be affected by the population of mosquitoes at the starting point, while this effect

will weaken gradually and the trend will be determined much more by temperature and precipitation (based on the comparison of (a) and (b) in Fig. 3.6 - Fig. 3.9). These results are consistent with the growth and reproduction of mosquitoes in nature.

Effective Trapping Zone (ETZ) We apply the definition of the ETZ of a trap for the Peel region model. We adopt $R_{trap} = 7.62m$ (Curtis Dyna-fog (2013)) as an example to calculate the ETZ of a trap. With linear trapped rate, from Fig. 3.6 and Fig. 3.7, one can find t_p is around 70, $M_{collect_p} \approx 70$ and $M_{total_p} \approx 650$. Based on (3.2), the radius of effective trapping zone of the trap $R_{ETZ} = 23.22m$ and the area of this ETZ is $1693.85m^2$. Similarly, with nonlinear trapped rate and from Fig. 3.8 and Fig. 3.9, $M_{collect_p} \approx 70$ and $M_{total_p} \approx 600$, we have $R_{ETZ} = 22.31m$ and the area of this ETZ is $1563.55m^2$.

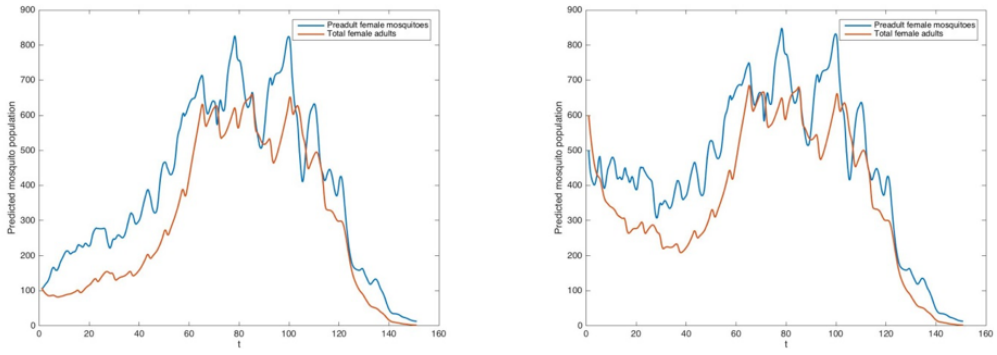

(a) (b)

Figure 3.6: Predicted total preadult female *Culex* mosquitoes and adult *Culex* females with linear trapped rate with different initial population size (a larger initial size in 3.6(b)). The unit of time is day^{-1} and the starting time point 0 representing June 1, 2015.

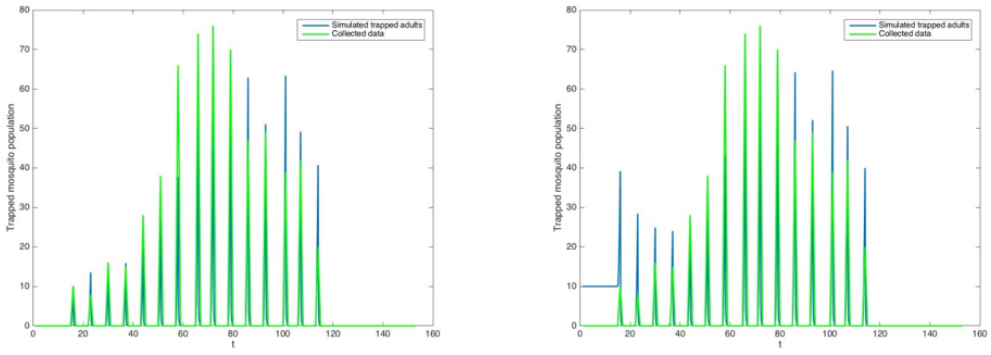

(a) (b)

Figure 3.7: Simulated trapped *Culex* mosquitoes and real collected mosquitoes with linear trapped rate with different initial population size (a larger initial size in 3.7(b)). The unit of time is day^{-1} and the starting time point 0 representing June 1, 2015.

3.6 Discussion

This research has found that the accurate estimation of the ETZ is largely dependent on R_{trap} (female *Culex* mosquitoes within R_{trap} radius can all be captured). A greater R_{trap} reflects a higher efficiency of a trap and a larger area of the zone. R_{trap} can be influenced by many factors, such as trapping mosquito capability of a CDC light trap, trap location, weather conditions (like windy or storming). For example, a strong wind will blow away mosquitoes and a consequent decrease of trapped mosquitoes, in this case, R_{trap} will be smaller compared to one with windless weather. If we have access to an accurate real

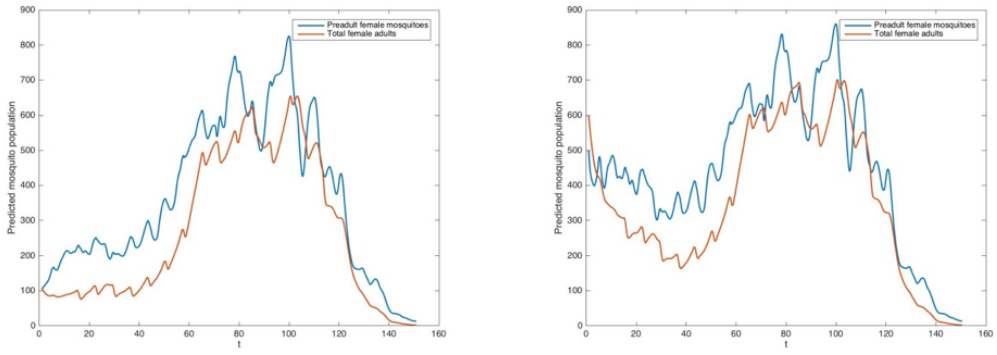

(a) (b)

Figure 3.8: Predicted total preadult female *Culex* mosquitoes and adult *Culex* females with nonlinear trapped rate with different initial population size (a larger initial size in 3.8(b)). The unit of time is day^{-1} and the starting time point 0 representing June 1, 2015.

R_{trap}, we can define an accurate ETZ and more accurately predict real mosquito population size or density in the ETZ.

Based on sensitivity analysis (Fig. 3.3), increasing the female per capita reproduction rate, maturation rate, or decreasing the preadult female per capita mortality rate, intraspecific competition rate and the adult mosquito per capita mortality rate can lead to an increase in preadult and adult population. Increasing actual mosquito feeding preference on fake hosts, the probability of mosquitoes being successfully captured and the time spent on collecting trapped mosquitoes is helpful to capture more mosquitoes.

To look into the influence of weather on the mosquito abundance, we investigate the

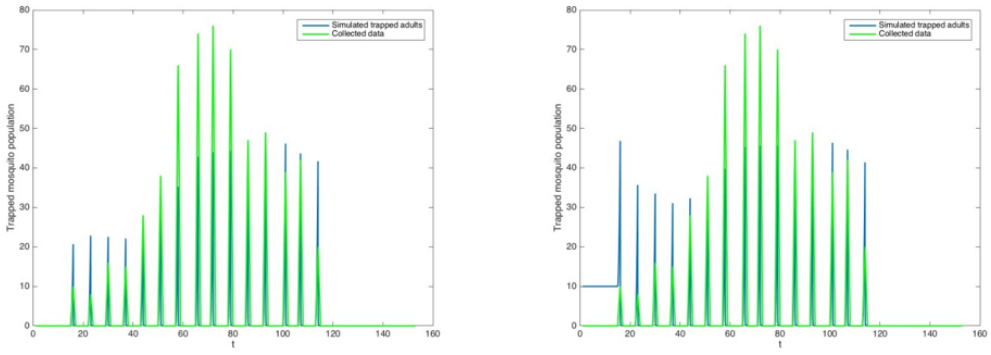

(a) (b)

Figure 3.9: Simulated trapped *Culex* mosquitoes and real collected mosquitoes with non-linear trapped rate with different initial population size (a larger initial size in 3.9(b)). The unit of time is day^{-1} and the starting time point 0 representing June 1, 2015.

variation of female mosquito populations during short periods. From Fig. 3.10 - Fig. 3.12, we find that the overall trends of predicted total preadult, adult female *Culex* mosquitoes and trapped females are in accordance with the changes of temperature. Moreover, the preadult female *Culex* mosquitoes are more sensitive to temperature, the subtle up-and-downs of preadult females agree with the fluctuation of temperature. Hence the preadult female *Culex* mosquitoes are driven by temperature, which explains that mosquito populations vary from year to year with some years having multiple peaks (since temperatures have multiple peaks) and some years the peak coming earlier. Moreover, we find that there are lags between the variation of temperature and mosquito populations (Fig. 3.10 - Fig.

3.12).

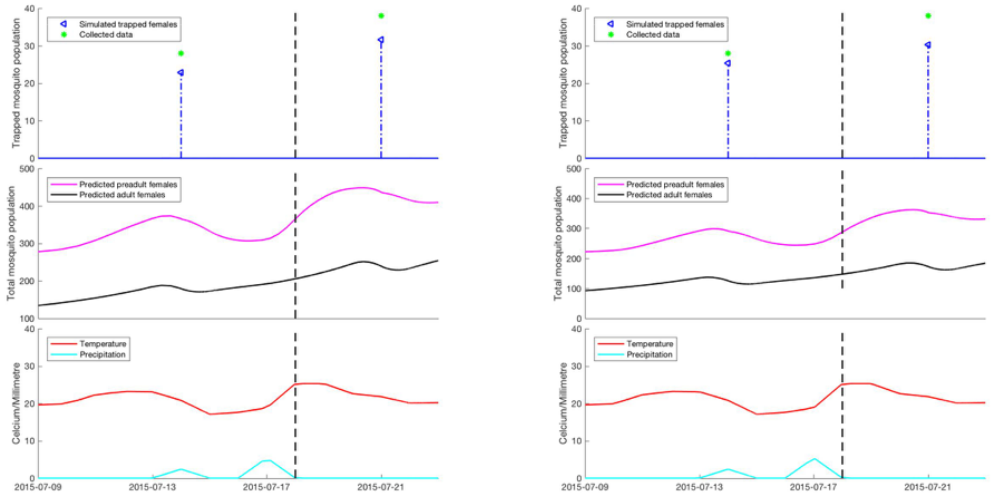

(a) (b)

Figure 3.10: Predicted total preadult, adult female *Culex* mosquitoes and trapped females over daily average temperature and precipitation during a period in mid-July. 3.10(a) with a linear trapped rate, 3.10(b) with a nonlinear trapped rate.

Based on the specific model for the Region of Peel (3.14) (where parameters are estimated based on previously known trap count data) and weather forecasts, we can predict not only weekly trap counts but also mosquito population in the ETZ.

For the traps in the Region of Peel, we use the first three-month (June-August) trap count data to estimate unknown parameters, then use the model (with the linear trapped rate or nonlinear trapped rate) and the following week (the first week of September) weather data to predict mosquito abundance. We can obtain a good prediction of fol-

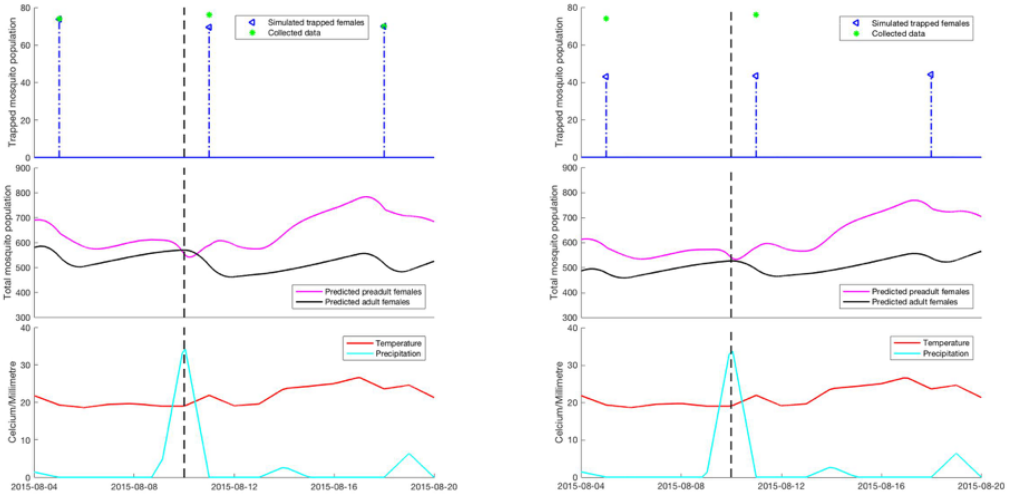

(a) (b)

Figure 3.11: Predicted total preadult, adult female *Culex* mosquitoes and trapped females over daily average temperature and precipitation during late August and early September. 3.11(a) with a linear trapped rate, 3.11(b) with a nonlinear trapped rate.

lowing week trap counts and total mosquito populations (with the linear trapped rate (Fig. 3.13(a)) or nonlinear trapped rate (Fig. 3.13(b)). Comparing predicted results (red dashed curve) of our model and observed data (corresponding green solid curve), our model can provide a relatively accurate prediction. Similarly, we can predict the total mosquito population size encompassing preadult and adult mosquitoes (dashed yellow and purple curve) in the ETZ.

This predictive model is useful for mosquito surveillance programs. It can be used to improve the accuracy of mosquito abundance estimation and provide real population data

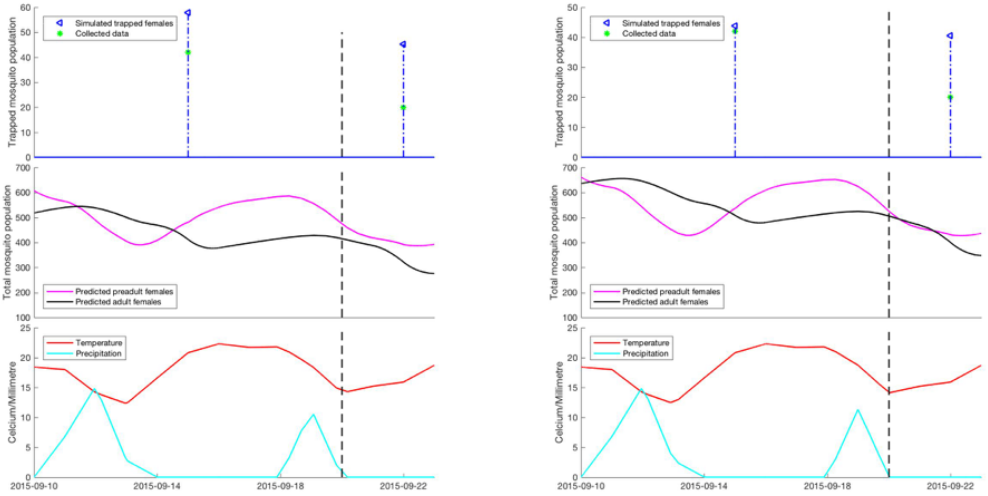

(a) (b)

Figure 3.12: Predicted total preadult, adult female *Culex* mosquitoes and trapped females over daily average temperature and precipitation in the middle of September. 3.12(a) with a linear trapped rate, 3.12(b) with a nonlinear trapped rate.

of mosquitoes in the ETZ. This more accurate information will greatly help health units to make decisions on mosquito control, to decide what actions should be taken based on predicted mosquito abundance. If the predictions indicate that a large number of mosquitoes are expected then larviciding or adultciding can be considered to rapidly and effectively control mosquitoes. The results of this model will also improve the assessment of the risk of related MBD infections. When the model predicts a higher mosquito population, media and education on individual protection from mosquito bites are also important.

In our models, female mosquitoes per capita reproduction rate $r(b, c, B, A, H)$ and fe-

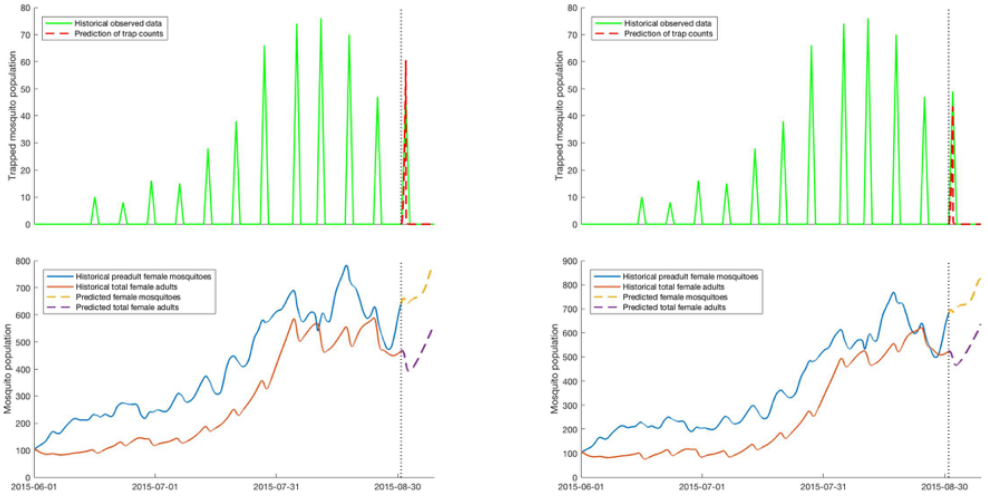

(a) (b)

Figure 3.13: Prediction of following week trap counts, total preadult and adult female mosquitoes, based on model (3.14) with corresponding weather data (weather forecasts) and 3.13(a) with a linear trapped rate, 3.13(b) with a nonlinear trapped rate.

male mosquitoes being trapped rate $C(M_{total}, B, A, H)$ are influenced and determined by the species (here we roughly classify as birds, humans and other mammals), the abundance and the distribution of hosts. With the information of hosts in different trap locations, we can calculate these two rates for corresponding locations respectively, then use them in our model to predict future real mosquito abundance considering the influence of locations, however, this has not been achieved due to the lack of information of hosts.

Although the hosts' information is not included in this work, we can use this model to estimate and obtain some information related to hosts. In this model, we used trap count

data to estimate the parameter $\bar{c}$ (a component of $r(b, c, B, A, H)$) and q_c & p_F (components of $C(M_{total}, B, A, H)$). For a region with a trap, $\bar{c}$ reveals the components structure of hosts and the mosquitoes feeding preferences in a qualitative aspect. q_c indicates the performance of the trap, a higher value of q_c characterizes a higher efficiency of the trap. p_F is the mosquito feeding preference on the trap which is treated as a fake host. Usually, p_F is between 0 and 1, since the summation of mosquito feeding preferences on all hosts is 1. If $p_F = 0$, which means compared to other hosts, fake host (a trap) has no attractiveness, female mosquitoes are surrounded by enough reals hosts and no one will come to the trap. If $p_F = 1$, which means all mosquitoes prefer and come to feed on the fake host, one possible reason is that no real hosts are available, or the emissions (like lights or carbon dioxide) given off by a trap is really strong and mosquitoes greatly like them, then the trap can entice all mosquitoes to it. These two extreme cases are too rare to happen, in general, a larger p_F means less mosquito feeding preferences on the real hosts, thus we can indirectly get mosquito feeding preferences on the real hosts based on the value of p_F.

Combining these three parameters together, it provides a better view of hosts. For instance, for two different locations, we obtain two sets of estimated values of parameters $\bar{c}$, q_c and p_F using our model, if the difference between the two sets are relatively small, then the hosts structures (the abundances and distributions) in these two locations are similar, or maybe some great diversities of hosts exist, but the influence of hosts on the mosquitoes

is similar. Hence we could also use estimations of these parameters to make a comparison of hosts in different locations.

Additionally, estimations of these parameters can help us to identify the changes of host structures. For example, at one location, we use the first three-month trap count data to fit the model to get parameter value set S1, and first four-month trap count data to get set S2. Comparing set S1 and S2, a big difference of values indicates a host demographic shifts. We can use our model to monitor the host demographic changes in this way.

For a more accurate prediction of the mosquito population, it is better to consider the host demographic change. For each new prediction, all history trap count data is used to fit parameters, then these updated fitted parameters, latest historic trap count data and weather forecast serve as model input, to output prediction result.

The mosquito surveillance program in the Region of Peel is carried out each week and the preventative actions are made based on the weekly trap count data. It is admitted that daily trap count data is more accurate and reliable than a weekly one to be used for surveillance program, hourly one is even better. However, daily or hourly trapping mechanism is not implemented when considering economics, and weekly trapping is most adopted. Then what about setting up traps biweekly? Is it still a feasible approach to obtain acceptable trap data based on biweekly trapping and collecting mechanism? To answer these questions, we modified the model for the Region of Peel and carry out numerical simu-

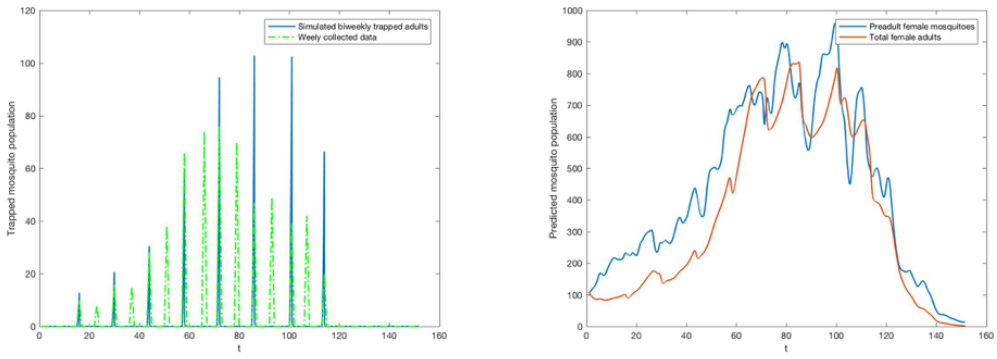

(a) (b)

Figure 3.14: Prediction of trap counts, total preadult and adult female mosquitoes, based on biweekly trapping mechanism and with linear trapped rate and corresponding weather data (weather forecasts). The unit of time is day^{-1} and the starting time point 0 representing June 1, 2015. 3.14(a) shows comparison of biweekly trap counts and weekly collected data, 3.14(b) shows prediction of mosquito abundance with biweekly trapping mechanism.

lations. Specifically, all parameters are unchanged, only traps being operated weekly is modified into being operated biweekly, that is, the nonzero $f(t)$ and $g(t)$ appear biweekly. Comparing biweekly predicated trap counts with weekly collected data (Fig. 3.14(a)), the number of collected mosquitoes biweekly is relatively more than the weekly's in the late period of surveillance period, and it delays the appearance of trap count peak and amplifies the peak values. Also, the peak values of mosquito population size (Fig. 3.14(b)) are enlarged when operating the traps biweekly (compared with Fig. 3.8(a)). Hence, biweekly

trap count data may exaggerate the mosquito population density, which may lead to unnecessary operations on mosquito control. In this situation, setting up traps biweekly cannot be an economic approach compared with weekly one, since the costs due to overpredictions of mosquito abundance can offset, or even be higher than the costs of operating trap one more time every two weeks. Therefore, setting up traps weekly is a relatively good approach for mosquito monitoring and surveillance program.

4 The impact of weather and stormwater management ponds on the transmission of West Nile virus

4.1 Introduction

West Nile virus (WNV) is the most widely distributed emerging arbovirus. In North America, the first WNV case was detected in New York City in 1999; the virus spread rapidly throughout the continent and appeared in Ontario in 2001 (Nash et al. (2001), Toronto and Region Conservation Authority (2014)). Since 2001 human infections have occurred yearly in Ontario, the number of cases varies based on the time at which WNV becomes endemic and the peak value of infections (Fig. 4.1). The variations of the annual human infection may be due to a number of complex factors including vector-virus-host interactions, the increase in urbanization and agriculture, climatic factors, and anthropogenic land use such as the stormwater management ponds (SWMP) (Kramer et al. (2008), Epstein (2001)).

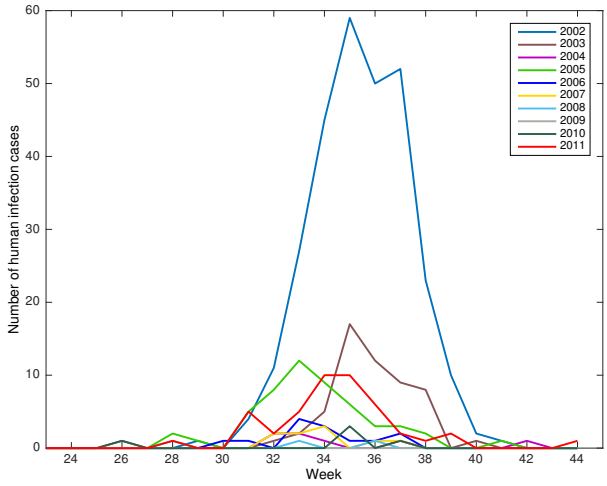

Figure 4.1: Human infections in the Greater Toronto Area from June to October, 2002-2011 (Data from Public Health Ontario)

SWMP, including wet ponds and dry ponds, are artificial ponds designed to collect, retain and filter stormwater runoff (Toronto Water (2015)). In Ontario, municipalities first began implementing wet ponds as part of their stormwater infrastructure in the late 1980s. Currently, there are over 1000 SWMP and wetlands in the Greater Toronto Area (GTA) (Toronto and Region Conservation Authority and CH2M Hill Canada Ltd. (2016)). Improperly designed, operated, and maintained SWMP can be conducive to creating standing water. Particularly for wet ponds that maintain a permanent pool of water, shallow zones of these ponds may be an attractive fertile breeding site for the female *Culex* mosquitoes. Thus the SWMP, along with temperature, precipitation and wind patterns, can contribute

to supporting the growth and development of mosquitoes that are competent WNV vectors.

The Toronto and Region Conservation Authority (TRCA) has been running a WNV mosquito larval monitoring and surveillance program in natural wetlands and SWMP on TRCA lands in the Greater Toronto Area since 2003. Their results showed that the mosquitoes collected from these SWMP were principally WNV vector species, predominantly *Culex pipiens*. SWMP can be used to predict adult mosquito emergence and the potential for human infections (Toronto and Region Conservation Authority (2014)). Research also indicates that larval abundance is related to temperature and precipitation as well (Gardner et al. (2012)).

Lots of research also has been done on mathematical modeling for mosquito abundance and the transmission of WNV (Lewis et al. (2006a), Abdelrazec et al. (2014), Fan et al. (2010), Lewis et al. (2006b)). An ordinary differential equation model in Wonham et al. (2004) showed that mosquito control can prevent a WNV outbreak. Gong et al. (2011) developed climate-based models to simulate the population dynamics of immature and adult *Culex* mosquitoes in the Northeastern US, and revealed a strong correlation between the timing of early population increases and decreases in late summer. Additionally, the influence of weather conditions on the mosquito population or infection were studied in Wang et al. (2011) and Ruiz et al. (2010).

Previous mathematical modelling has failed to take into account the SWMP impact in a

dynamical model. The purpose of this research was to develop a single-season dynamical model between mosquito and bird populations to explore the influences of SWMP and weather conditions on vector abundance and the transmission of WNV.

The better understanding of the mechanism of a WNV outbreak and having a more reliable evaluation of transmission risk will greatly help to control the spread of the virus and human infections. In our work, we will build a WNV transmission model among mosquitoes and birds. We will split mosquitoes population into two stages, furthermore, we consider the intraspecific competition of mosquitoes in the aquatic stage. We will yield new insights into the transmission of WNV and the threshold conditions of a WNV outbreak. Moreover, we will propose a novel index to assess the risk of WNV transmission.

4.2 Mosquito-bird model without weather factors

In order to explore the influence of SWMP on the mosquito population and WNV transmission, we consider the intraspecific competition and applied it in aquatic stages of mosquitoes: the abundance of preadult is closely related to intraspecific competition, and intraspecific competition is associated with standing water developed from the water in SWMP. We combined the vector mosquitoes and the host birds and established a single-season compartmental model.

4.2.1 Model formulation

Due to WNV circulating between mosquitoes and birds and being established as a seasonal epidemic in North America, we extended the mosquito-bird model in Wonham et al. (2004) and developed a single-season ordinary differential equation model on WNV transmission in the mosquito-bird population. For the mosquito population, we adopt the two-stage *Culex* mosquito model (2.1) in Chapter 2 with constant birth rate r_m, assume preadult mosquitoes includes both female and male with the sex ratio $1 : 1$ (Tejerina et al. (2009), Tun-Lin et al. (2000), Yasuno and Tonn (1970)) and competitive interactions are within and between both female and male (Agnew et al. (2000)). For intraspecific competition, we assume it is only related to the size of standing water, and other factors such as density of nutrients and oxygen are fixed. Adult female mosquitoes are classified into susceptible, exposed and infectious compartments. For avian hosts, more than 300 species of birds are involved in the WNV transmission in North America (Reed et al. (2003)). Here focusing on the effects of SWMP and for simplicity, we regard all birds as one family and classified the family into susceptible, infectious, recovered and dead compartments. In this single-season (from spring to autumn) model, it is reasonable that the demographic dynamics of mosquitoes is considered but not for birds. We further make assumptions that vertical transmission in mosquitoes and horizontal transmission in birds are small and neglected (Wonham et al. (2004)). For an accurate estimation of WNV

epidemic, we consider mammals which are dead-end hosts also providing blood meals for mosquitoes (Abdelrazec et al. (2014)). Then our model (all parameters are defined in Table 4.1) is

$$\begin{cases} \frac{dL_m}{dt} = r_m(S_m + E_m + I_m) - \delta L_m - d_l L_m - \kappa L_m^2, \\ \frac{dM_m}{dt} = \frac{1}{2}\delta L_m - \tilde{d}_m M_m, \\ \frac{dS_m}{dt} = \frac{1}{2}\delta L_m - b_m \beta_m S_m \frac{I_b}{N_b + A} - d_m S_m, \\ \frac{dE_m}{dt} = b_m \beta_m S_m \frac{I_b}{N_b + A} - kE_m - d_m E_m, \\ \frac{dI_m}{dt} = kE_m - d_m I_m, \\ \frac{dS_b}{dt} = -b_m \beta_b I_m \frac{S_b}{N_b + A}, \\ \frac{dI_b}{dt} = b_m \beta_b I_m \frac{S_b}{N_b + A} - \mu I_b - \gamma I_b, \\ \frac{dR_b}{dt} = \gamma I_b, \\ \frac{dX_b}{dt} = \mu I_b, \end{cases} \tag{4.1}$$

$L_m(t)$ = the population of preadult WNV vector mosquitoes at time t,

$M_m(t)$ = the population of male adults developed from the preadult stages at time t,

$S_m(t)$, $E_m(t)$ & $I_m(t)$ = the population of susceptible, exposed and infectious female mosquitoes respectively at time t,

$S_b(t)$, $I_b(t)$, $R_b(t)$ & $X_b(t)$ = the population of susceptible, infectious, recovered and dead birds respectively at time t,

A = the total mammals that mosquitoes feed on for blood meals,

$N_b = S_b + I_b + R_b$.

Table 4.1: Parameters in the WNV transmission model (4.1)

Par.	Interpretation	Baseline & Range (day^{-1})
r_m	Mosquitoes per capita birth rate (or oviposition rate)	0.6 $(0.036, 42.5)$ (Wonham et al. (2004))
δ	Mosquitoes per capita maturation rate from preadult stages to adult	0.06 $(0.051, 0.093)$ (Wonham et al. (2004))
d_l	Preadult mosquitoes per capita mortality rate	0.4 $(0.213, 16.9)$ (Wonham et al. (2004))
κ	Intraspecific competition rate of preadult mosquitoes	0.005 $(0, 1)$
b_m	Female adult mosquitoes per capita biting rate	0.5 $(0.2, 0.75)$ (Abdelrazec et al. (2014))
β_m	WNV transmission probability from birds to mosquitoes	0.12 $(0.02, 0.24)$ (Wonham et al. (2004))

d_m	Female adult mosquitoes per capita mortality rate	$0.05\ (0.016, 0.07)$ (Wonham et al. (2004))
$\tilde{d_m}$	Male adult mosquitoes per capita mortality rate	$0.05\ (0.016, 0.07)$ (Wonham et al. (2004))
k	Female adult mosquitoes per capita transition rate from exposed to infected	$0.09\ (0.087, 0.125)$ (Wonham et al. (2004))
β_b	WNV transmission probability from mosquitoes to birds	$0.84\ (0.8, 1.0)$ (Wonham et al. (2004))
μ	Birds per capita mortality rate due to WNV	$0.127\ (0.125, 0.2)$ (Wonham et al. (2004))
γ	Birds per capita recovery rate from WNV	$0.001\ (0, 0.2)$ (Abdelrazec et al. (2014))

4.2.2 Basic properties of the transmission model

The model (4.1) has up to two disease-free equilibrium (DFE) points. The number of DFE points is determined by the sign of $\frac{r_m\delta}{2d_m} - (d_l + \delta)$ which means the effect of intraspecific competition on the rate of change of preadult mosquito population.

If $\frac{r_m\delta}{2d_m} - (d_l + \delta) < 0$, the model has a unique equilibrium point $E_0 = (0, 0, 0, 0, 0, S_{b_0},$

$0, 0, 0)$, where S_{b_0} is any given initial density of birds. The E_0 has eigenvalues 0 (multiplicity 3), $-d_m$, $-\tilde{d}_m$, $-(d_m + k)$, $-(\mu + \gamma)$ and the roots of the equation:

$$2\lambda^2 + 2(d_l + d_m + \delta)\lambda + 2d_l d_m + 2d_m\delta - r_m\delta = 0. \tag{4.2}$$

All parameters are positive in a biological sense, all the roots of (4.2) have negative real parts, and DFE E_0 is locally stable.

If $\frac{r_m\delta}{2d_m} - (d_l + \delta) > 0$, that is besides the death and the maturation working on reducing the rate of change of L_m, intraspecific competition is also involved in playing a part, then the model (4.1) has two DFE $E_1 = (L_{m_0}, M_{m_0}, S_{m_0}, 0, 0, S_{b_0}, 0, 0, 0)$ as well as E_0, where $L_{m_0} = \frac{\frac{r_m\delta}{2d_m} - (d_l+\delta)}{\kappa}$, $M_{m_0} = \frac{\delta[\frac{r_m\delta}{2d_m} - (d_l+\delta)]}{2\tilde{d}_m\kappa}$, $S_{m_0} = \frac{\delta[\frac{r_m\delta}{2d_m} - (d_l+\delta)]}{2d_m\kappa}$ and S_{b_0} is any given initial density of birds. E_0 has a positive real part eigenvalue due to (4.2), thus E_0 is unstable. The local stability of E_1 is determined by the basic reproduction number R_0 which can be obtained from the next generation matrix for the system (4.1).

Using the notation of van den Driessche and Watmough (2002), with the infected variables (E_m, I_m, I_b) in the model (4.1), $\mathfrak{F}$ denotes the rate of new infections and $\mathfrak{V}$ denotes the rate of transfer out of each compartment,

$$\mathfrak{F} = \begin{bmatrix} b_m\beta_m S_m \frac{I_b}{N_b+A} \\ 0 \\ b_m\beta_b I_m \frac{S_b}{N_b+A} \end{bmatrix}, \mathfrak{V} = \begin{bmatrix} kE_m + d_m E_m \\ -kE_m + d_m I_m \\ \mu I_b + \gamma I_b \end{bmatrix},$$

The corresponding linearized matrices at the DFE E_1 are

$$F = \begin{bmatrix} 0 & 0 & b_m\beta_m\frac{S_{m_0}}{N_{b_0}+A} \\ 0 & 0 & 0 \\ 0 & b_m\beta_b\frac{S_{b_0}}{N_{b_0}+A} & 0 \end{bmatrix}, V = \begin{bmatrix} k+d_m & 0 & 0 \\ -k & d_m & 0 \\ 0 & 0 & \mu+\gamma \end{bmatrix}.$$

Then the basic reproduction number R_0 is defined as the spectral radius of the matrix FV^{-1},

$$R_0 = \sqrt{\frac{b_m\beta_m\frac{S_{m_0}}{N_{b_0}+A}\frac{k}{k+d_m}}{(\mu+\gamma)}\frac{b_m\beta_b\frac{S_{b_0}}{N_{b_0}+A}}{d_m}}. \tag{4.3}$$

In biological view, R_0 gives the expected number of new infections produced by a single infective mosquito or bird when introduced into a susceptible population. The first term under the square root of R_0 performs as the spread of WNV from birds to mosquitoes; the transmission probability from birds to mosquitoes ($b_m\beta_m$) multiplied by the number of initially susceptible female mosquitoes per host ($\frac{S_{m_0}}{N_{b_0}+A}$) surviving the exposed period ($\frac{k}{k+d_m}$), multiplied by the birds infectious lifespan ($\frac{1}{\mu+\gamma}$). The second term represents transmission of WNV from birds to mosquitoes, that is the transmission probability ($b_m\beta_b$) multiplied by the number of initially susceptible birds per host ($\frac{S_{b_0}}{N_{b_0}+A}$) times the adult female mosquito infectious lifespan ($\frac{1}{d_m}$). The square root in R_0 provides the geometric mean for an average individual of both species combined (Wonham et al. (2004)).

When $R_0 < 1$, E_1 is locally stable, when $R_0 > 1$, E_1 is unstable (van den Driessche and Watmough (2002)). We also find that κ, reflecting the role of SWMP, only affects the

stability of E_1. Other aspects related to SWMP, such as the surroundings and the size of a pond, still only influence κ and the stability of E_1 accordingly. Furthermore, the threshold level of the intraspecific competition related to SWMP derived from the threshold $R_0 = 1$ is

$$\kappa = \frac{b_m^2 S_{b_0} \beta_m k \beta_b \delta [r_m \delta - 2d_m(d_l + \delta)]}{4(N_{b_0} + A)^2 d_m^3 (\mu + \gamma)(k + d_m)} \doteq \kappa^*. \tag{4.4}$$

If the intraspecific competition is not strong ($\kappa < \kappa^*$), for instance, a pond is located among plants where fertilizers are applied, this pond receiving many nutrients can favor submersed aquatic vegetation and algae blooms, which create more ideal habitats for larvae and hence weaken the intraspecific competition, then E_1 is unstable and the disease introduction will lead to an outbreak. Otherwise, strong competition ($\kappa > \kappa^*$) results in controlling mosquito abundance and even preventing a WNV outbreak.

4.3 Mosquito-bird model incorporating temperature and precipitation

Environmental factors, especially temperature and precipitation, largely impact the transmission of mosquito-borne pathogens by affecting the infection rate of the virus as well as mosquito and host abundance in time and space (Mullen and Durden (2009)). To incorporate weather factors, we first identify critical input parameters of this model by

performing the sensitivity analysis. Then we extend the transmission model (4.1) into a weather-driven model, where SWMP in conjunction with precipitation determines the water habitat for larvae and the weather data from June to October gathered from Toronto Pearson International Airport Station (Government of Canada (2006)).

4.3.0.1 Sensitivity analysis

We first identify which input parameters significantly contribute to model outcomes. The identification is implemented by studying the sensitivity analysis of each parameter in system (4.1) on the two critical output variables, the population of adult mosquitoes N_m ($N_m = M_m + S_m + E_m + I_m$) and the basic reproduction number R_0 (4.3). Specifically, we evaluate partial rank correlation coefficients (PRCCs) between each input parameter and the output variable, using Latin hypercube sampling (LHS) with 3000 samples (Marino et al. (2008)). Due to the absence of available data and a priori information on the distributions of input parameters, we choose uniform distributions for each parameter with corresponding range in Table 4.1.

Sensitivity analysis (Fig. 4.2) indicates that *Culex* mosquito biting rate, oviposition rate, maturation rate, mortality rates and intraspecific competition rate significantly influence both mosquito abundance N_m and an indicator of local WNV activity level R_0, and we incorporate temperature and precipitation into these six critical input parameters to

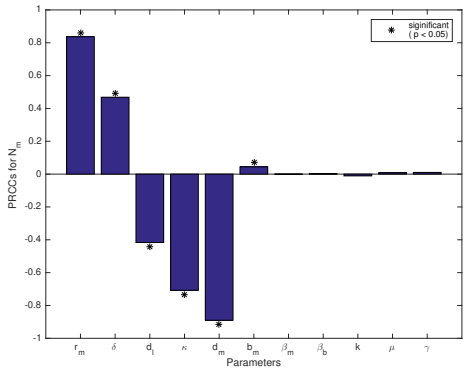

(a) PRCCs between input parameters and the outcome variable N_m

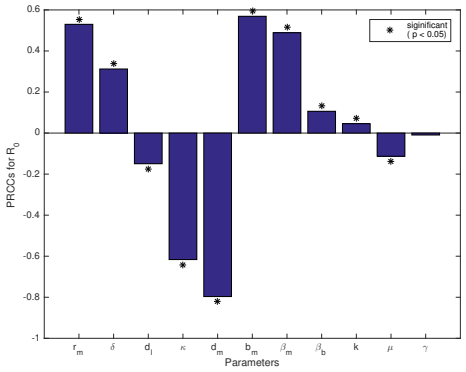

(b) PRCCs between input parameters and the outcome variable R_0

Figure 4.2: Performance of LHS/PRCC on the model (4.1). Parameters with a PRCC significantly $(p < 0.05)$ different from zero are indicated with $(*)$.

reflect the effect of weather factors.

4.3.0.2 Temperature-dependent parameters

Temperature can affect infection, dissemination, and transmission rates for lots of arboviruses, including WNV (Dohm et al. (2002)). Temporal changes in the efficacy of transmission essentially depict the seasonality of WNV activity, and this process is described in Reisen et al. (2006b) by presenting the temperature dependence of the duration of the development cycle of mosquitoes comprising blood meal as well as development and deposition of eggs, known as the gonotrophic cycle. Yasuno and Tonn (1970) reveals

that temperature variations are influential in biting activity. Reisen et al. (2006b) indicates that biting rate is the reciprocal of the gonotrophic cycle depending on the temperature. Based on this work, Rubel et al. (2008) delineates the biting rate (Fig. 4.3(a)) as

$$b_m(T) = \frac{0.344}{1 + 1.231 \exp(-0.184(T - 20))}, \tag{4.1}$$

where T is the temperature in degrees Celsius.

Beyond the biting rate relying on the temperature, the seasonality of the mosquito-population cycle is a consequence of the temperature dependent birth and mortality rates. The birth rate of *Culex* larvae, also called oviposition rate of female mosquitoes, also named as the egg-deposition rate of *Culex* mosquitoes, is developed by the scaled reciprocal of the gonotrophic cycle as logistic (S-shaped) function (Rubel et al. (2008)) (Fig. 4.3(b))

$$r_m(T) = cb_m(T), \tag{4.2}$$

where $b_m(T)$ is the biting rate defined in (4.1). A feasible way to determine the scaling factor c is that the average birth rate $\bar{r}_m(T)$ is a fixed value, for instance $c = 2.325$ if $\bar{r}_m(T) = 0.537\ day^{-1}$ (Rubel et al. (2008)).

Temperature variations also affect the duration of the immature stages significantly, which influences the maturation rate (development rate) from the preadult to the adult (De Meillon et al. (1967)). Accounting for the thermal requirements of the mosquito

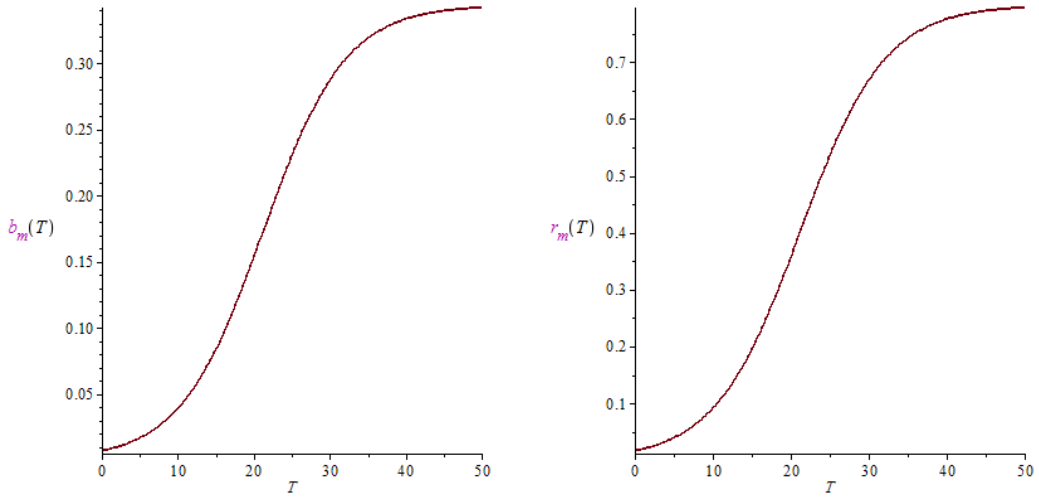

(a) $b_m(T)$ (b) $r_m(T)$

Figure 4.3: The biting rate and the birth rate of mosquitoes

development, the maturation rate of *Culex* mosquitoes (Fig 4.4(a)) is proposed by the Sharpe & DeMichele equation

$$\delta(T) = A\frac{T+273.15}{298.15}\frac{\exp[\frac{HA}{1.987}(\frac{1}{298.15}-\frac{1}{T+273.15})]}{1+\exp[\frac{HH}{1.987}(\frac{1}{TH}-\frac{1}{T+273.15})]}, \tag{4.3}$$

where four parameters $(A,\ HA,\ HH,\ TH)$ are constants which reflect the individual thermodynamic characteristics of the organism's control enzyme system and T is the temperature in units of Celsius (Sharpe and DeMichele (1977), Rueda et al. (1990)). Specifically for *Culex pipiens* and *Culex restuans* in Gong et al. (2011), four parameters are estimated as $(A,\ HA,\ HH,\ TH) = (0.25,\ 28094,\ 35362,\ 298.6)$.

Logistic function is also fitted to temperature-dependent maturation rate from the aquatic stages to adults, where the maturation rate is treated as the birth rate for adults, and the

function or the population parameters are of similar shape to larvae's, while the difference is that one order of magnitude lower than those for larval mosquitoes (Rubel et al. (2008)). Then maturation rate in logistic function form (Fig. 4.4(b)) is

$$\delta(T) = \frac{r_m(T)}{10}. \tag{4.4}$$

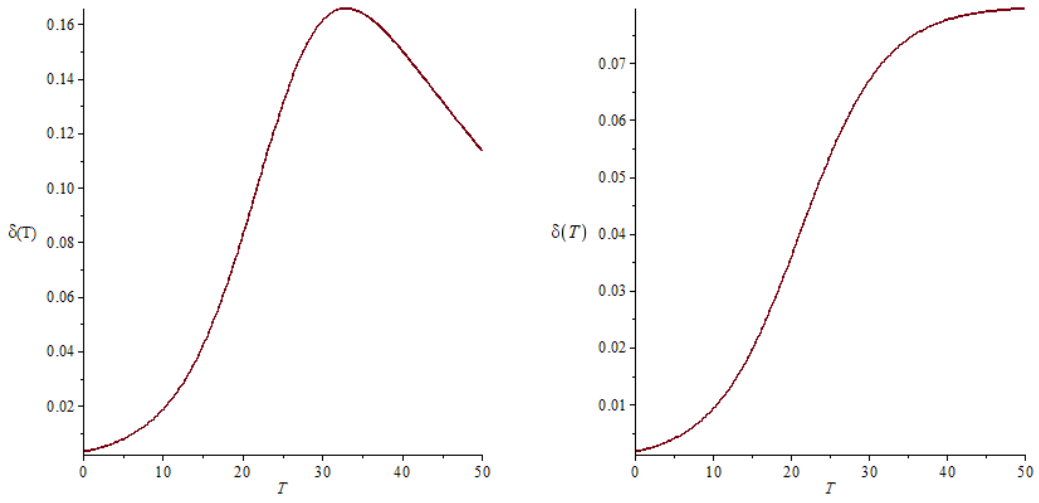

(a) $\delta(t)$ (4.3) (Gong et al. (2011))

(b) $\delta(t)$ (4.4) (Rubel et al. (2008))

Figure 4.4: The maturation rate of mosquitoes from preadult stages to adult stage in different forms

With above two forms of the maturation rate, we adopt the Sharpe & DeMichele equation (4.3) to our model. (4.3) in Gong et al. (2011) describes the maturation rate of *Culex pipiens* and *Culex restuans* associated with the temperature in New York site Freeville. (4.4) was obtained by fitting temperature data and *Culex tarsalis* data from the Coachella

and San Joaquin Valleys of California (Rubel et al. (2008), Reisen (1995)). The Coachella and San Joaquin Valleys of California is located near the Pacific coast of the southwestern US whose geographical factors and climatic conditions are different to GTA's to some degree. In contrast with valleys in California, Freeville is much closer to GTA and its weather conditions more resemble GTA's.

Temperature is as well an important determinant for the mortality rates of mosquitoes and a U-shaped function is feasible description to reflect this relation. A quadratic function was selected to describe the mortality rates of immature and adult *Culex* mosquitoes in Rubel et al. (2008). A quadratic function was used to delineate both larva and adult mortality rates with one order of magnitude difference (Fig. 4.5(c))

$$d_l(T) = 0.0025T^2 - 0.094T + 1.0257, \tag{4.5}$$

$$d_m(T) = \frac{d_l(T)}{10}. \tag{4.6}$$

In Shaman et al. (2006), the mortality rate (Fig. 4.5(b)) for larvae as well as adults varies as an empirically derived function of temperature in the form of

$$d(T) = (-4.4 + 1.31T - 0.03T^2)^{-1}, \tag{4.7}$$

where T is the temperature in degrees Celsius.

In addition to direct depiction of the temperature impact on mosquito mortality rates, temperature can affect the mortality rates through the survival rates by the relationship sur-

vival rate $= 1-$ death rate (Gong et al. (2011)). The Gaussian function is a proper choice to approximate the shape of the survival rate with respect to temperature (Otero et al. (2006)) and was backed qualitatively by field and laboratory trials (Gong et al. (2011)). In the light of this, mortality rates of the mosquitos (Fig. 4.5(a)) relative to the temperature read as

$$d_l(T) = 1 - S_l \exp[-(\frac{T - T_l}{Var_{Tl}})^2], \tag{4.8}$$

$$d_m(T) = 1 - S_m \exp[-(\frac{T - T_m}{Var_{Tm}})^2], \tag{4.9}$$

where S_l and S_m are survival rates at T_l and T_m (i.e., optimal temperature for survival of preadult and adult mosquitoes) respectively. Var_{Tl} and Var_{Tm} are variances of daily water temperature and air temperature respectively, and T, T_l and T_m are in degrees Celsius.

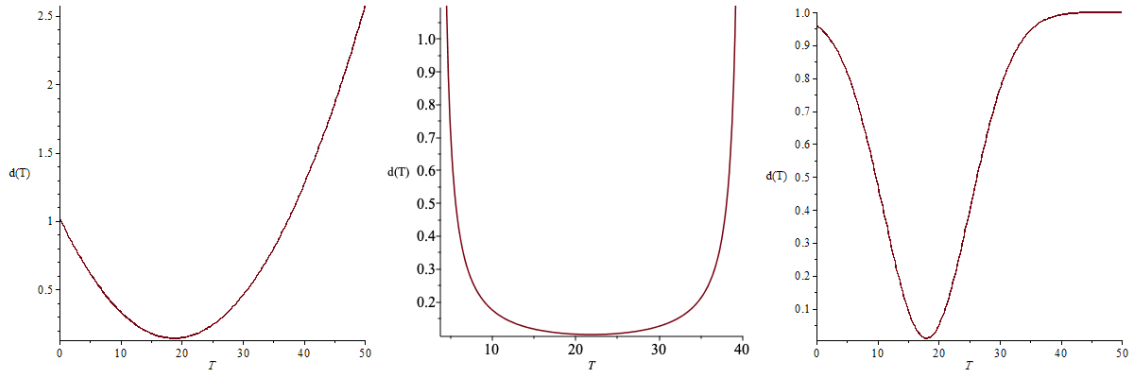

(a) (4.5) (Rubel et al. (2008)) (b) (4.7) (Shaman et al. (2006)) (c) (4.8) (Gong et al. (2011))

Figure 4.5: The mortality rate of mosquitoes in different form

Similarly, the selection of mortality rates is also based on data of geographic position

and weather conditions used for developing mortality rates in literature, we choose (4.8) accounting for the following reasons: (4.7) is employed to depict the population dynamics of *Anopheles walkeri* (Shaman et al. (2006)), which is different from the WNV vectors – *Culex* mosquitoes; (4.5) and (4.8) all applied to *Culex* species, (4.8) is our choice due to the same reason in selection of maturation rate, i.e., data used to establish (4.8) was collected in New York site Freeville with more similar geographic and weather conditions to GTA's.

4.3.1 Precipitation-dependent parameter

Precipitation influences the mosquito life cycle in two principal aspects: 1) the increased near-surface humidity related to precipitation promotes mosquito flight activity and host-seeking behavior, and 2) precipitation can change the abundance and type of aquatic habitats where mosquitoes oviposit and the subsequent development of the immature stages (Shaman and Day (2007)). In our study we primarily take into account the second influence associated with the SWMP, in particular, precipitation in conjunction with SWMP has a profound effect on the intraspecific competition rate κ (Lončarić and Hackenberger (2013)).

Some work has been done concerning the influence of precipitation on the abundance of floodwater mosquitoes such as *Aedes vexans* and *Aedes cinereus*. For instance, the pop-

ulation of *Aedes vexans* largely depends upon the availability of precipitation and floodwater pools (Miller et al. (2002)). An increase in the surface of the flooded area enlarges breeding sites and enhances egg hatching and subsequent larval survival. With *Aedes vexans* biological characteristics, the carrying capacity for larvae is improving as precipitation increases. Specifically for carrying capacity $K(WL) = K_0 K_f(WL)$, $K_f(WL)$ is carrying capacity coefficient and monotone increasing with respect to the water level and K_0 is the carrying capacity when there is no flood (Lončarić and Hackenberger (2013)).

While for the nonfloodwater species *Culex* mosquitoes, the females oviposit only upon standing water, and the eggs are not drying resistant (Lončarić and Hackenberger (2013)). Some studies of WNV systems have found positive associations between precipitation and mosquito abundance, that is higher-than-average levels of precipitation can result in mosquito outbreaks and potential disease outbreaks (Takeda et al. (2003), Landesman et al. (2007)). However other existing work indicates that an excess of precipitation may actually impose a restriction on vector production (Shaman (2002), Ruiz et al. (2010)). Apart from these, the quantitative results of Gardner et al. (2012) are consistent with the hypothesis that moderate precipitation is indispensable to provide habitats for *Culex* larvae depositing eggs and development, nevertheless, an excess of precipitation plays an opposite role on accelerating immature abundance. These distinguished conclusions may be due to various reasons, such as temporal variations, regional disparity and human factors.

Based upon larvae data from TRCA, weather data in the GTA (Government of Canada (2006)), one can find: more precipitation leading to a larger habitat for larvae does not hold all the time, since too much rain will dilute or even refresh the standing water which in turn reduces larval habitats; certainly, the moderate amount of precipitation will increase the abundance of habitats. In this case, the approximate description of the carrying capacity function relative to precipitation resembled the Gaussian function and we adopt the relation

$$K(P) = K^* K_f(P),$$

with differences that we replace the water level by daily total precipitation P, K^* is the carrying capacity with the optimal precipitation and carrying capacity coefficient $K_f(P)$ is taken a form similar to the temperature-dependent survival rate:

$$K_f(P) = \frac{1}{1+\rho}(1 + \rho \exp[-(\frac{P - P_l}{Var_{Pl}})^2]).$$

Combined the intraspecific competition rate in logistic growth equation (i.e., inverse relation between carrying capacity and intraspecific competition), we propose a precipitation-dependent instraspecific competition rate (Fig. 4.6)

$$\kappa(P) = \frac{(1+\rho)\kappa^*}{1 + \rho \exp[-(\frac{P-P_l}{Var_{Pl}})^2]} \tag{4.10}$$

where $\kappa^* = \frac{1}{K^*}$ and κ^* is the smallest intraspecific competition rate when there is optimal amount of rain P_l for larvae development, Var_{Pl} is variance of $P(t)$. $\rho > 0$ is the scaling

factor to reflect the influence degree of precipitation on κ and consequently the amplitude of variation of the κ, moreover, $(1+\rho)\kappa^*$ represents the maximum value of κ with constraint $0 < (1+\rho)\kappa^* < 1$. Both ρ and κ^* are largely dependent on the properties of SWMP itself, like the size and depth of the pond as well as the amount of precipitation.

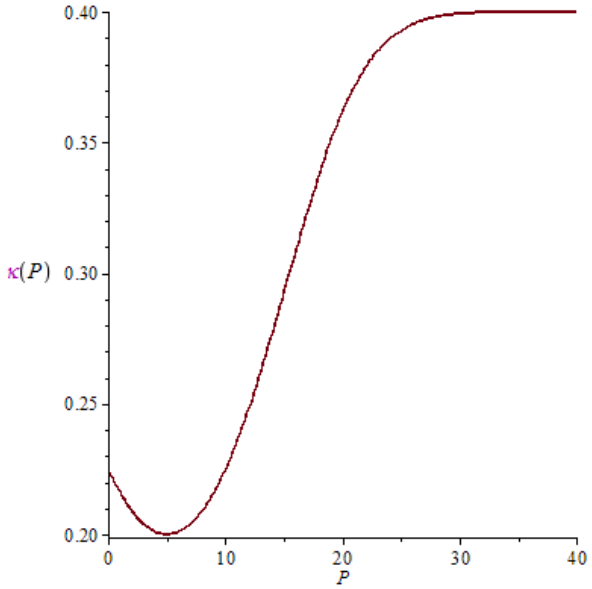

Figure 4.6: The intraspecific competition rate among preadult mosquitoes

4.3.2 Formulation of the model

To formulate the transmission model with weather factors, we assume that the mean daily temperature of breeding sites is equal to the mean daily temperature of the air because of a lack of water temperature data. Replacing parameters b_m, r_m, δ, d_l, d_m and κ in

(4.1) by $b_m(T)(4.1)$, $r_m(T)$ (4.2), $\delta(T)$ (4.3), $d_l(T)$ (4.8), $d_m(T)$ (4.9) and $\kappa(P)$ (4.10) respectively, and $\tilde{d}_m(T) = 1 - S_{\tilde{m}} \exp[-(\frac{T-T_{\tilde{m}}}{Var_{T\tilde{m}}})^2]$, then we have the following weather driven model and all parameters are defined in Table. 4.2.

$$\begin{cases} \frac{dL_m}{dt} = r_m(T)(S_m + E_m + I_m) - \delta(T)L_m - d_l(T)L_m - \kappa(P)L_m^2, \\ \frac{dM_m}{dt} = \frac{1}{2}\delta(T)L_m - \tilde{d}_m(T)M_m, \\ \frac{dS_m}{dt} = \frac{1}{2}\delta(T)L_m - b_m(T)\beta_m S_m \frac{I_b}{N_b} - d_m(T)S_m, \\ \frac{dE_m}{dt} = b_m(T)\beta_m S_m \frac{I_b}{N_b} - kE_m - d_m(T)E_m, \\ \frac{dI_m}{dt} = kE_m - d_m(T)I_m, \\ \frac{dS_b}{dt} = -b_m(T)\beta_b I_m \frac{S_b}{N_b}, \\ \frac{dI_b}{dt} = b_m(T)\beta_b I_m \frac{S_b}{N_b} - \mu I_b - \gamma I_b, \\ \frac{dR_b}{dt} = \gamma I_b, \\ \frac{dX_b}{dt} = \mu I_b. \end{cases} \tag{4.11}$$

For the model with the daily changing temperature and precipitation, we replace the fixed temperature T and precipitation P in (4.11) by $T(t)$ and $P(t)$, and simulate the transmission dynamics based on weather data (Fig. 4.7). Here the maturation rate is treated specially since it relies on the average temperature of several days, while other weather-dependent parameters only depend on the temperature or precipitation of a single day. More specifically, the maturation rate on n^{th} day is influenced by the arithmetic

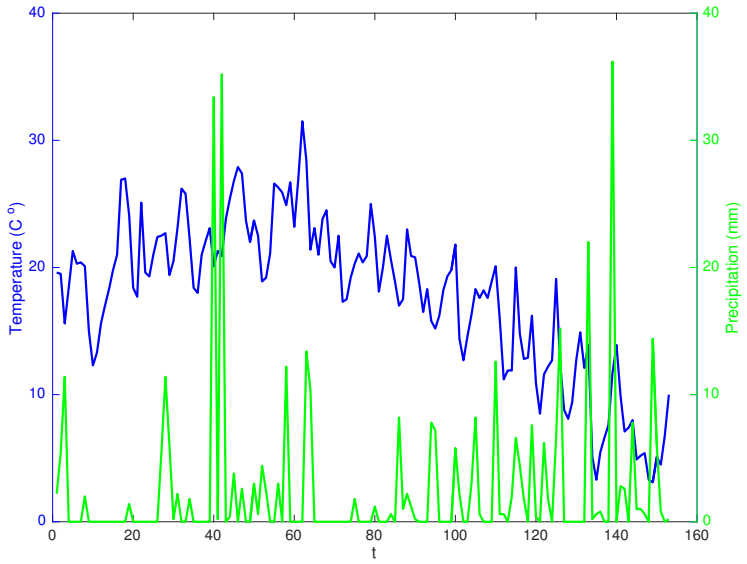

Figure 4.7: Weather variations from June to October in 2006 in the GTA

means of daily mean temperature of 11 days before the n^{th} day (Wang et al. (2011)), i.e., $\frac{1}{11}\sum_{i=n-1}^{n-11} T_i$, other parameters are only related to T_n or P_n, where T_i and P_i are the daily mean temperature and daily total precipitation on i^{th} day respectively. To determine the influence of precipitation, we select three distinguished patterns of precipitation: normal precipitation, heavy precipitation ($30mm$ more daily) and heavier precipitation ($60mm$ more daily). The three different patterns are applied to a single month – July or September, as the mosquito population, infectious mosquitoes and birds are increasing in July and decreasing in September.

Table 4.2: Temperature-dependent and precipitation-dependent parameters in the model (4.11)

Par.	Interpretation	Range
c	the scaling factor associated with biting rate	2.325 (Rubel et al. (2008))
AA	parameters related to the individual	0.25 (Gong et al. (2011))
HA	thermodynamic characteristics	28094 (Gong et al. (2011))
HH	of the organisms control	35362 (Gong et al. (2011))
TH	enzyme system	298.6 (Gong et al. (2011))
T_l	optimal temperature for survival of preadult mosquitoes[a]	17 (Gong et al. (2011))
T_m	optimal temperature for survival of female adult mosquitoes[a]	23 (Gong et al. (2011))
$T_{\tilde{m}}$	optimal temperature for survival of male adult mosquitoes[a]	23 (Gong et al. (2011))
S_l	survival rates of preadult mosquitoes with T_l	$0.6 - 0.95$ (Gong et al. (2011))

S_m	survival rates of female adult mosquitoes with T_m	$0.6 - 0.95$ (Gong et al. (2011))
$S_{\tilde{m}}$	survival rates male adult mosquitoes with $T_{\tilde{m}}$	$0.6 - 0.95$ (Gong et al. (2011))
Var_{Tl}	variance of $T(t)$[b]	
Var_{Tm}	variance of $T(t)$[b]	
$Var_{T\tilde{m}}$	variance of $T(t)$[b]	
P_l	optimal amount of precipitation	5 (Government of Canada (2006))
$\bar{\kappa}$	intraspecific competition rate when $P = P_l$	$0 - 1$[c]
$\rho > 0$	the scaling factor to reflect the amplitude of the κ[d]	
Var_{Pl}	variance of $P(t)$[d,e]	

[a] All temperature parameters are in degrees Celsius (Gong et al. (2011), Rubel et al. (2008), Rueda et al. (1990), Sharpe and DeMichele (1977)).

[b,e] Calculated with temperature and precipitation data in the GTA.

[c] Derived from reciprocal of carrying capacity ranging from 1 to any positive integer.

[d] $(1 + \rho)\bar{\kappa}$ represents the maximum value of κ with the constraint $0 < (1 + \rho)\bar{\kappa} < 1$.

For fixed temperature and precipitation, one can still obtain the basic reproduction number

$$\hat{R}_0 = \sqrt{\frac{b_m(T)\beta_m \frac{\frac{\delta(T)[\frac{r_m(T)\delta(T)}{2d_m(T)} - (d_l(T)+\delta(T))]}{2d_m(T)\kappa(P)}}{N_{b_0}} \frac{k}{k+d_m(T)} \frac{b_m(T)\beta_b}{d_m(T)}}{(\mu+\gamma)}}, \tag{4.12}$$

and the threshold $\hat{R}_0 = 1$ plays a significant role on the outbreak of the WNV.

To look deep into the influence of precipitation on $\hat{R}_0$, we have

$$\frac{\partial \hat{R}_0}{\partial P} = \frac{\partial \hat{R}_0}{\partial \kappa}\frac{\partial \kappa}{\partial P} = \frac{\partial \hat{R}_0}{\partial \kappa}\frac{2\kappa^2\rho(P-P_l)\exp[-(\frac{P-P_l}{Var_{Pl}})^2]}{Var_{pl}^2(1+\rho)\kappa^*}, \tag{4.13}$$

it is apparent that $\frac{\partial \hat{R}_0}{\partial \kappa} < 0$ and accordingly $\frac{\partial \hat{R}_0}{\partial P} > 0$ when $P < P_l$, $\frac{\partial \hat{R}_0}{\partial P} < 0$ when $P > P_l$, moreover $\lim\limits_{P\to\infty} \frac{\partial \hat{R}_0}{\partial P} = 0$. That is, $\hat{R}_0$ increases as precipitation P increases starting from 0, and once crossing the optimal value P_l, $\hat{R}_0$ begins to decrease and gradually approaches a constant. In consequence, when other factors (except P) are fixed, the closer the amount of rain gets to P_l, the higher the probability of occurrence of WNV outbreak.

Both κ^* and ρ are indicators to reflect the properties of SWMP and we investigate how each of them acts on $\hat{R}_0$. Similarly,

$$\begin{aligned}
\frac{\partial \hat{R}_0}{\partial \kappa^*} &= \frac{\partial \hat{R}_0}{\partial \kappa}\frac{1+\rho}{1+\rho\exp[-(\frac{P-P_l}{Var_{Pl}})^2]} < 0, \\
\frac{\partial \hat{R}_0}{\partial \rho} &= \frac{\partial \hat{R}_0}{\partial \kappa}\frac{\kappa^*(1-\exp[-(\frac{P-P_l}{Var_{Pl}})^2])}{(1+\rho\exp[-(\frac{P-P_l}{Var_{Pl}})^2])^2} \leq 0,
\end{aligned}$$

and $\lim\limits_{\rho\to\infty} \frac{\partial \hat{R}_0}{\partial \rho} = 0$. The increase of κ^* or ρ leads to $\hat{R}_0$ decreasing, where $\hat{R}_0$ approaches a constant when ρ is sufficient large and a special case is that $\hat{R}_0$ is a always constant

if $P = P_l$ no matter how ρ changes. Thenceforth, it may prevent the WNV outbreak occurring if κ^* or ρ (when $P \neq P_l$) is large enough.

As weather conditions changing with time, we replace the fixed temperature T and precipitation P by $T(t)$ and $P(t)$. In this case, the ordinary differential equations characterize the transmission dynamics of the WNV and population dynamics of vectors and hosts with time-dependent weather factors, numerical simulations exhibit these dynamics when actual weather is taken into consideration. Apparently, at a specific time point, the model with changing weather conditions is exactly the model (4.11).

4.4 Numerical simulations

Numerical simulations display the influence of each parameter of the system (4.1) on the outcome variables N_m and R_0, the impact of precipitation and SWMP on the transmission of WNV and the vector population, where both fixed weather conditions and time-dependent weather conditions are included.

Sensitivity analysis (Fig. 4.2) shows mosquito oviposition rate r_m, maturation rate δ, mortality rates d_l and d_m, intraspecific competition rate κ and biting rate b_m have significant impacts (with p-value < 0.05) on both mosquito population N_m and indicator of local WNV severity R_0. For other parameters, R_0 is also sensitive to WNV transmission probability β_m and β_b, bird transition rate from the exposed to the infected k and WNV induced

mortality rate μ, while these parameters have only slight impacts on N_m. Decreasing r_m, δ and b_m or increasing d_l, κ and d_m can lead to the simultaneous decrease in N_m and R_0, which is beneficial to control mosquitoes and WNV transmission.

Incorporating weather factors in these critical parameters, when weather conditions do not change with time (Fig. 4.8), too high or too low temperature or a heaver precipitation will decrease the basic reproduction number $\hat{R}_0$, leading to a lower risk of WNV. For SWMP, a larger intraspecific competition rate $\bar{\kappa}$ and a larger scaling factor ρ can make the $\hat{R}_0$ less than one, controlling the vector abundance and the WNV transmission. In Fig. 4.8(b) and 4.8(c), $\hat{R}_0 > 1$ is for a small part of parameter space, and $\hat{R}_0$ increases rapidly in these fringe conditions. That is when the intraspecific competition among preadult mosquitoes is weak, for instance with less restriction of habitats, (i.e., with sufficient standing water in the pond), more mosquitoes will be developed and involved in WNV transmission, leading to a high potential of WNV outbreak. Particularly, when the intraspecific competition barely exists, reproduction of mosquitoes will increase dramatically.

Taking the daily temperature and precipitation into consideration, the intraspecific competition will control the development of the vector and consequently hinder the transmission of WNV to some extent. In Fig. 4.9(b), a strong intraspecific competition will shrink the peak of infectious mosquitoes from around 23 to 3. A larger ρ has a slight influ-

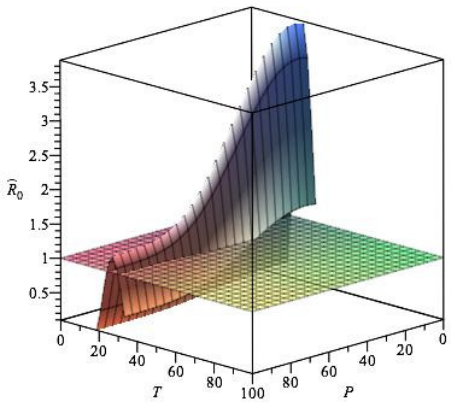

(a) Weather conditions

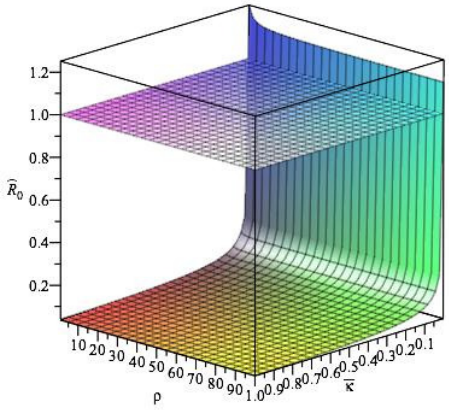

(b) SWMP properties

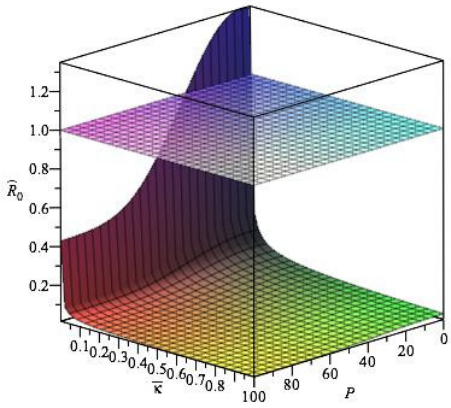

(c) Precipitation with $\bar{\kappa}$ of SWMP

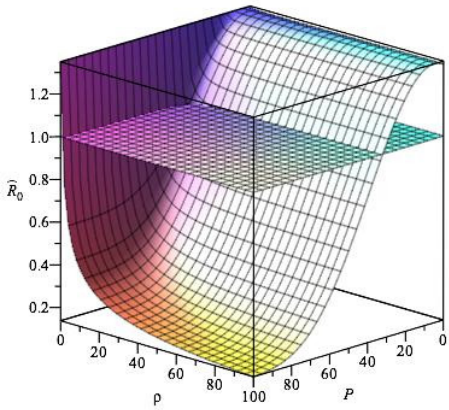

(d) Precipitation with ρ of SWMP

Figure 4.8: Variation of basic reproduction number $\hat{R}_0$ along with combinations of weather conditions or SWMP properties

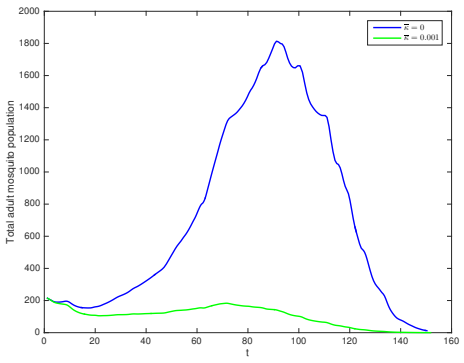

(a) The impact of $\bar{\kappa}$ on total adult mosquitoes

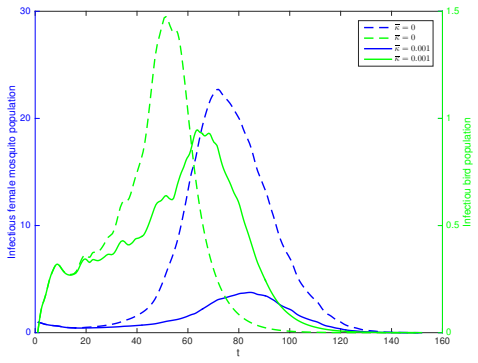

(b) The impact of $\bar{\kappa}$ on infectious female mosquitoes and birds

Figure 4.9: The impact of $\bar{\kappa}$ on the mosquito abundance and transmission of WNV

ence to decrease the vector abundance and the spread of WNV, and this influence exhibits only at the peaks of total mosquitoes, infectious birds and mosquitoes (Fig. 4.10). Fig. 4.11 indicates that an excess of precipitation can actually impose restrictions on vector production and WNV spread in the population.

4.5 Discussion

This research has demonstrated that temperature, precipitation, and intraspecific competition among preadult mosquitoes in SWMP are key factors in predicting the WNV vector abundance and the occurrence of WNV in the bird population. Then for these factors, proactive measures can be taken to control mosquitoes and the spread of WNV. The

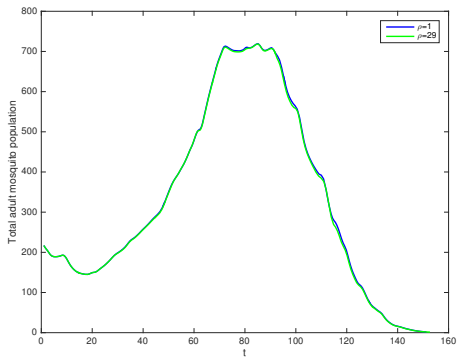

(a) The impact of ρ on total adult mosquitoes

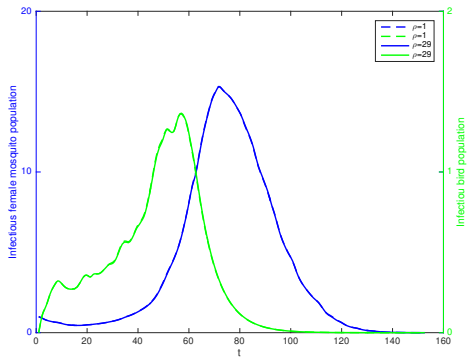

(b) The impact of ρ on infectious female mosquitoes and birds

Figure 4.10: The impact of ρ on the mosquito abundance and the transmission of WNV

measures for increasing the intraspecific competition of larvae in SWMP include clearing stagnant water in shallow regions of SWMP, preventing excess nutrients and pollutants from entering the pond, using mechanical aerators to generate water movement, introducing top feeding fish or other predators (Ladd B (2003)). Also, based on weather forecasts and our weather-driven model, the prediction of vector abundance and WNV activity will be useful for public health to make decision in the prevention and control of WNV, such as the use of larvicides and pesticides and encouraging individuals to take personal protection measures including wearing long sleeves and using an insect repellent containing DEET. Certainly, regular monitoring of the vector population in SWMP from May to September is critical to guide the choice of these prevention and control measures.

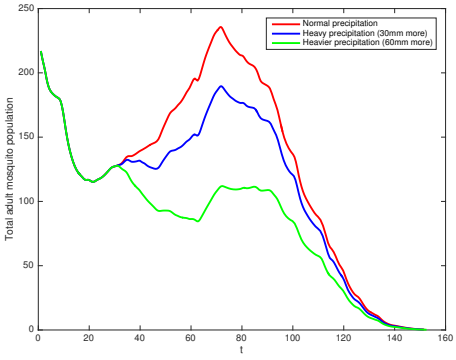

(a) Total adult mosquito population

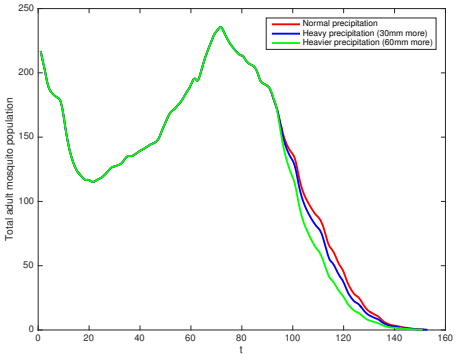

(b) Total adult mosquito population

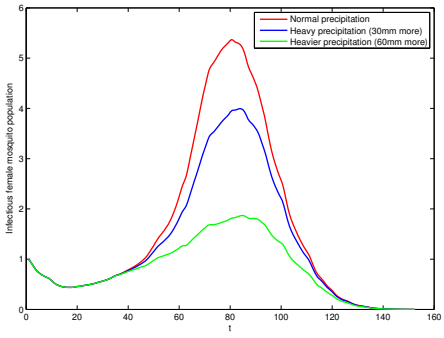

(c) Infectious female mosquito population

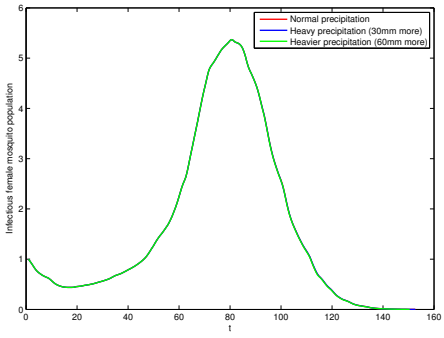

(d) Infectious female mosquito population

Figure 4.11: The impact of precipitation on the mosquito abundance and the transmission of WNV with $\bar{\kappa} = 0.0007$ & $\rho = 9$. (a), (c) and (e) are based on different patterns of precipitation in July, (b), (d) and (f) are based on different patterns of precipitation in September.

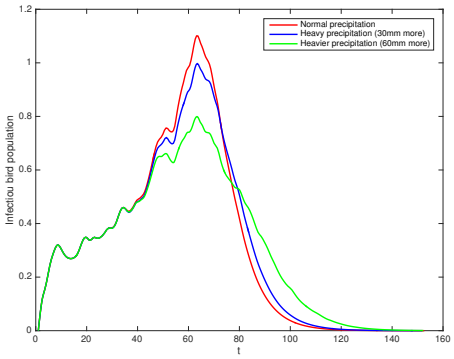

(e) Infectious bird population

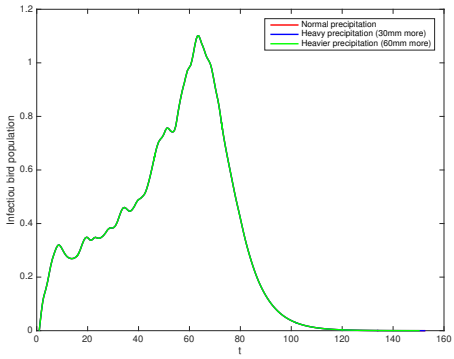

(f) Infectious bird population

Figure 4.11: (Cont.) The impact of precipitation on the mosquito abundance and the transmission of WNV with $\bar{\kappa} = 0.0007$ & $\rho = 9$. (a), (c) and (e) are based on different patterns of precipitation in July, (b), (d) and (f) are based on different patterns of precipitation in September.

In model (4.1), when the intraspecific competition is weak, with the rate less than κ^*, virus introduction can lead to an outbreak of WNV and actions to control the spread of the disease would be needed. When a rate greater than κ^* occurs, the abundance of larvae and infected mosquitoes decrease due to fierce intraspecific competition, and there are not adequate mosquitoes available to act as a vector of WNV to spread the disease. In model (4.11), the intraspecific competition varies with respect to the time-dependent precipitation. In such situation, the intraspecific competition can be stronger or weaker at different times, and one cannot simply conclude that vector populations and the WNV transmission will be persistently controlled or not since the effects of the intraspecific

competition will change over time as well.

Temperature and precipitation combined are complex. Fig. 4.8(a) depicts how weather conditions influence the occurrence of a WNV outbreak when considering a specific SWMP ($\bar{\kappa}$ and ρ are constants). With suitable temperature ($20 - 30°C$) an outbreak of WNV will occur, regardless of precipitation. While if the temperature is lower or higher than the suitable range, moderate precipitation ($0 - 30mm$) will enhance the potential occurrence of a WNV outbreak. Under the same weather conditions, habitats for SWMP can differ for egg deposition and larval development, leading to the different basic reproduction number (Fig. 4.8(b)). The intraspecific competition rate $\bar{\kappa}$ plays a principal role on $\hat{R}_0$. A larger $\bar{\kappa}$, such as a deeper pond having more adequate surface water movement, will suppress the reproduction of the mosquitoes and accordingly prevent a WNV outbreak. The effects of precipitation on SWMP and the spread of WNV is of great importance. Under moderate temperature, the interaction effects of precipitation and SWMP is depicted in Fig. 4.8(c) and Fig. 4.8(d). Moderate precipitation ($0 - 30mm$) will provide more standing water to promote the transmission of WNV; otherwise, too much precipitation, for a pond which is sensitive to precipitation, will dilute or eliminate standing water and result in the prevention of a disease outbreak.

Moderate precipitation promotes the spread of the virus and increases vector abundance (Fig. 4.11), nevertheless, excess precipitation plays a role in controlling the trans-

mission of WNV and vector abundance. The impact of precipitation is more remarkable in July, with heavier precipitation ($60mm$ or more daily), the number of total female mosquitoes will decrease rather than rise. A possible explanation is that the temperature in July is more suitable for mosquito development and the spread of disease. In September the weather cools and does not support mosquito survival. When the temperature is suitable for the development of mosquitoes, heavy precipitation suppresses the mosquito population, while moderate precipitation and suitable temperature indicates a need to monitor the mosquito abundance and reduce mosquito populations through larviciding. If the temperature is low, precipitation may have little impact on mosquito development.

Frequently monitoring and surveillance activities are needed when the temperature is warm, higher than $20°C$. Under such temperature modes, if accompanied by moderate precipitation, it is more likely to trigger the reproduction of WNV vectors and the spread of the virus in the following few days. In this situation, some control actions such as larviciding may be taken to control mosquito abundance in a timely manner. While, if precipitation is quite heavy, there may not be a need to take action to reduce larvae since heavy precipitation will dilute standing water and reduce habitats for larvae. It is worth noting that following such weather patterns, monitoring WNV larvae in SWMP is still needed due to moderate temperatures, but concentrated efforts on larviciding are likely unnecessary. Additionally, applications of aeration and larvicide in the middle of the sea-

son may be more effective than applications in the spring or fall, as the weather at this time is suitable for the development of WNV vectors.

Usually, a region has multiple SWMP and the characteristics of these ponds also play a role in the transmission of WNV. Each SWMP has an intraspecific competition rate and the harmonic mean (HM) of all these competition rates serves as a representative of all SWMP in the whole region. With the same effect of intraspecific competition rate, a larger HM contributes to decreasing larval populations and infectious mosquitoes and birds. Moreover, to increase the HM, the most effective way is to take actions on the pond in which the intraspecific competition rate is smallest. For instance, a region with several SWMP, the size of stagnant surface water, the concentration of organics, the population of predators and the existence of vegetation will differ in each pond. An economical and effective strategy to control larvae is targeting the SWMP with the weakest intraspecific competition, i.e. the pond holding more standing water with plenty of organics, free of predators and within areas of some vegetation. Applying proactive measures, such as adding top feeding fish and clearing the water body will alleviate the overall severity of WNV and mosquito population. Fig. 4.12 shows that for a region possessing three SWMP with different intraspecific competition rates, only increasing the smallest one $\bar{\kappa}_1$ of SWMP 1 from 0.00004 to 0.0002 could reduce the number of total mosquitoes and infectious vectors and hosts for the overall region.

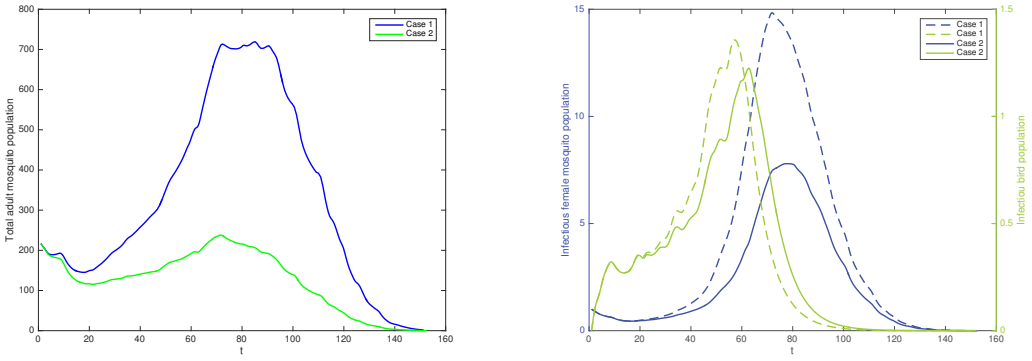

(a) Total adult mosquitoes (b) Infectious female mosquitoes and birds

Figure 4.12: Mosquito abundance and the transmission of WNV in a region with three SWMP. Case 1: SWMP 1: $\bar{\kappa}_1 = 0.00004$, SWMP 2: $\bar{\kappa}_2 = 0.0005$ & SWMP 3: $\bar{\kappa}_3 = 0.002$; Case 2: SWMP 1: $\bar{\kappa}_1 = 0.0002$, SWMP 2: $\bar{\kappa}_2 = 0.0005$ & SWMP 3: $\bar{\kappa}_3 = 0.002$.

This work provides insight into how to predict and control mosquito abundance and the transmission of WNV based on temperature, precipitation and SWMP in a region. Measures to promote intraspecific competition among preadult mosquitoes, such as refreshing the shallow regions of water in a pond and using aeration to make wave action or water movement, can be taken to reduce the mosquito population and spread of WNV.

5 Bifurcation and threshold dynamics of compartmental models for WNV

5.1 Introduction

West Nile Virus (WNV), the most widely distributed emerging arbovirus, circulates between mosquitoes and birds. WNV was first isolated in a woman in the West Nile district of Uganda in 1937 and it is now widespread in Africa, Asia, Australia, the Middle East, Europe and North America (World Health Organization (2016), Rappole (2000), Campbell et al. (2002)). In North America, WNV was first detected in New York city in 1999, then it spread and appeared in southern Ontario in 2001. Since then, infections in hosts (particularly birds and humans) occurred yearly in Ontario and phenomena presented were differently. For instance, in the Region of Peel in Ontario (Fig. 5.12), the outbreak of bird infections occurred again in 2005, three years after the first outbreak in 2002; human cases were reported in 2002 and 2003, and appeared again after the human-infection-free

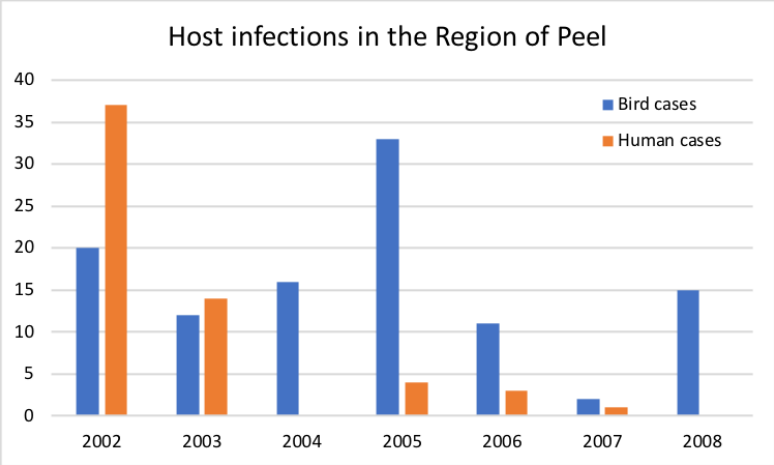

Figure 5.1: Infections in hosts in the Region of Peel, 2002-2008

year 2004. Numerous factors can contribute to the variation of the annual host infections. Notably, weather pattern alterations and climatic change will greatly influence the incidence and distribution of WNV. Other factors, including the host distribution and social characteristics of involving communities, conduce to triggering an outbreak of WNV in the Region of Peel.

The rapidly spread and the outbreaks of WNV has placed a burden on public health and healthcare systems (Nash et al. (2001), Toronto and Region Conservation Authority (2014)). All these necessitate a concerted global effort to investigate the transmission of WNV, study the mechanism of triggering mechanisms for an outbreak of WNV and combat to control and prevent its spread. Mosquito control is recognized as the most effective way to prevent mosquito-borne diseases (Wilke and Marrelli (2015)), which is

also obtained by the classical "Ross model", it showed that malaria can be controlled by reducing mosquito numbers below a certain figure (Transmission threshold) (Ross (1915), Mandal et al. (2011)).

Then WNV mosquito monitoring and surveillance programs have been run by public health. With surveillance data, public health evaluates the WNV activities in a particular area, assesses the risk of infection, predicts and catches an early warning signal for a potential outbreak, and decides if, when, where and how to reduce the risk of infection by using mosquito control measures, or education and community outreach (Government of Canada (2018)). Usually, programs incorporate the infection rate (IR) into their mosquito-based evaluation of local WNV activity patterns (Centers for Disease Control and Prevention (2015b)). The estimates of the IR are obtained in different ways such as minimum infection rate (MIR) and maximum likelihood estimation (MLE) (Gu et al. (2003), Centers for Disease Control and Prevention (2015b)), bias-corrected likelihood methods (Centers for Disease Control and Prevention (2015b)). Peel public health launched a mosquito monitoring and surveillance program in 2001 and MIR was adopted in their program for assessing the risk of WNV. Fig. 5.2 shows the weekly WNV vector abundance and MIR in the Region Peel from 2002 to 2008. Similarly, the mosquito populations and MIR varied yearly, such as high MIR in 2002 and a huge number of mosquito populations in 2008. The data helps them to make a decision like whether to control mosquito and what action

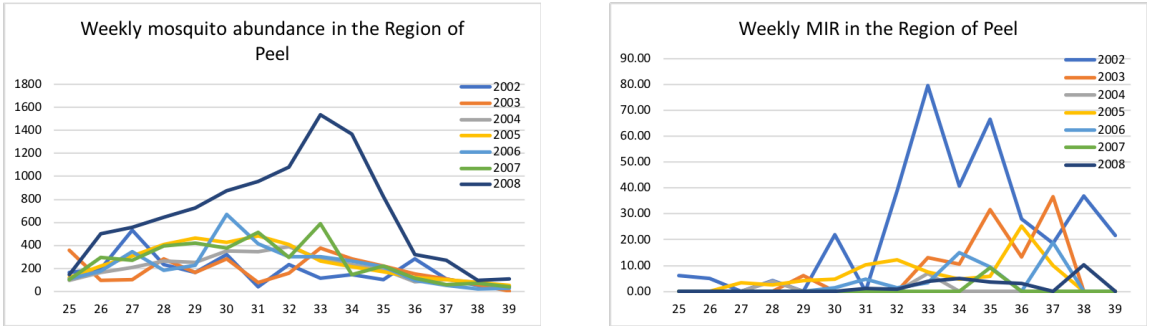

(a) (b)

Figure 5.2: Weekly mosquito abundance, weekly MIR in the Region of Peel, 2002-2008. The horizontal axis in 5.2(a) and 5.2(b) is the week number, starting from 25^{th} week and ending with 39^{th} week.

should be taken to prevent an outbreak.

In addition to the surveillance programs launched by public health, extensive research has been done to understand the transmission dynamics of WNV in compartmental models. In the literature (Thomas and Urena (2001), Wonham et al. (2004), Bowman et al. (2005), Lewis et al. (2006b), et al.), the basic reproduction number R_0 serves as a crucial threshold for the occurrence of an outbreak, in particular, R_0 being less than unity is necessary to prevent WNV prevailing, then reducing the basic reproduction number has been a goal for preventing an outbreak. Some other work (Castillo-Chavez and Song (2004), Jiang et al. (2009), Wan and Zhu (2010), Blayneh et al. (2010), Abdelrazec et al. (2014), et al.) elucidated that the basic reproduction number itself is not sufficient to describe

whether an outbreak of WNV will occur or not and to control WNV.

For public health, estimates of the IR (like MIR) they adopted are simple to carry out and applied to assess and predict the risk, however, only depending on estimates of the IR to evaluate the local WNV activity and risk of infection is not enough to provide solid and accurate results (Bustamante and Lord (2010)). How to use models and data to better characterize the transmission dynamics, the risk of infection and an early warning signal for an outbreak draws more attention. For mathematical researches, previous work has revealed that the occurrence of outbreaks greatly depends on the initial population state due to the existence of backward bifurcation, however, no real application verified the relationship between the initial population state and the occurrence of an outbreak, which needs a further and deeper study.

In our work, we establish WNV transmission models between mosquitoes and birds. We yield new insights into the applications of backward bifurcation and the threshold conditions of a WNV outbreak. Different ratios of vectors and hosts in the initial state, such as the ratio of mosquitoes and birds, the proportion of infected mosquitoes in all mosquitoes and the proportion of infected birds in all birds, will indicate the potential of a WNV outbreak. In the biological sense, the sum of indirect infection (the new bird infection) by a single bird infection and direct infection (the new mosquito infection) by a single bird infection less than the sum of two dead bird infections due to the disease will

lead to the occurrence of backward bifurcation. Also, we propose a novel index and the risk assessment criteria to characterize the potential risk of infections and an early warning for an outbreak. Moreover, we verify the results based on the risk assessment criteria for early warning of outbreaks and MIR results during 2002-2008 in the Greater Toronto Area (GTA).

5.2 Compartmental models for WNV

We start with a simplified mosquito-bird model that includes susceptible/infected mosquitoes and birds respectively, which provides a clear and deep vision of the mechanism of outbreak occurrence. Then we extend the model to a more general and comprehensive case: splitting mosquitoes population into aquatic and aerial stages, involving recovery bird populations and without the assumption of a constant mosquito population size.

5.2.1 A simplified WNV transmission model

For mosquito populations, we only consider the dynamics of female mosquitoes since only females are responsible for transmitting and spreading the virus. $S_m(t)$ and $I_m(t)$ are the population of susceptible and infectious female mosquitoes at time t respectively. Particularly, the reproduction rate is interpreted by the scaled female adult mosquitoes per capita biting rate (Rubel et al. (2008)) and the vertical transmission in mosquitoes is

ignored (Wonham et al. (2004), Fan et al. (2010)).

For bird populations, the primary hosts are birds and we denote the population of susceptible, infectious at time t as $S_b(t)$ and $I_b(t)$, and the total bird population is $N_b = (S_b + I_b)$. We regard all birds as one family for simplicity and consider the demographic dynamics of birds including migrations and reproduction. The horizontal transmission in birds is also neglected (McLean (2006)). In addition to birds, WNV mosquitoes also feed on mammals (denoted as A) like humans and horses (Abdelrazec et al. (2014)).

The cross-infection rate is interpreted using mass action incidence normalized by total host population $(N_b + A)$ and the mosquito-bird transmission dynamics is modelled as

$$\begin{cases} \frac{dS_m}{dt} = r_m(S_m + I_m) - b_m\beta_m S_m \frac{I_b}{N_b+A} - d_m S_m, \\ \frac{dI_m}{dt} = b_m\beta_m S_m \frac{I_b}{N_b+A} - d_m I_m, \\ \frac{dS_b}{dt} = r_b - b_m\beta_b I_m \frac{S_b}{N_b+A} - d_b S_b, \\ \frac{dI_b}{dt} = b_m\beta_b I_m \frac{S_b}{N_b+A} - \mu I_b - d_b I_b. \end{cases} \tag{5.1}$$

Table 5.1: Parameters in a simplified WNV transmission model (5.1)

Par.	Interpretation	Range (day^{-1})

r_m	Female mosquitoes per capita birth rate	$0.036 - 42.5$ (Wonham et al. (2004))
b_m	Female adult mosquitoes per capita biting rate	$0.03 - 0.16$ (Wonham et al. (2004))
d_m	Female mosquitoes per capita mortality rate	$0.016 - 0.07$ (Wonham et al. (2004))
r_b	Recruitment rate of birds	$800 - 1100$ (Abdelrazec et al. (2014))
β_b	WNV transmission probability from mosquitoes to birds	$0.8 - 1.0$ (Wonham et al. (2004))
μ	Birds per capita mortality rate due to WNV and the recovery	$0.125 - 0.2$ (Wonham et al. (2004))
d_b	Birds per capita natural death rate	$10^{-4} - 10^{-3}$ (Abdelrazec et al. (2014))

We assume birth rate r_m is equal to natural mortality rate of mosquitoes d_m (Abdelrazec et al. (2016)), then mosquitoes sustain a constant population size, denoted N_m. Then the

model is reduced to

$$\begin{cases} \frac{dI_m}{dt} = b_m\beta_m(N_m - I_m)\frac{I_b}{N_b+A} - d_m I_m, \\ \frac{dS_b}{dt} = r_b - b_m\beta_b I_m\frac{S_b}{N_b+A} - d_b S_b, \\ \frac{dI_b}{dt} = b_m\beta_b I_m\frac{S_b}{N_b+A} - \mu I_b - d_b I_b. \end{cases} \tag{5.2}$$

5.2.1.1 Existence and stability of equilibrium points

The disease free equilibrium is $E_0 = (0, \frac{r_b}{d_b}, 0)$. Using the next generation matrix method, the basic reproduction number is

$$R_0 = \sqrt{\frac{b_m\beta_m N_m}{(\frac{r_b}{d_b}+A)(\mu+d_b)}\frac{b_m\beta_b\frac{r_b}{d_b}}{(\frac{r_b}{d_b}+A)d_m}}. \tag{5.3}$$

Theorem 5.2.1. *For the system (5.2), the disease free equilibrium $E_0 = (0, \frac{r_b}{d_b}, 0)$ always exists. Denote $c_2 = -\mu(\mu+d_b)(b_m\beta_m d_b - d_m\mu)$, $c_1 = (\mu+d_b)((b_m\beta_m d_b - 2d_m\mu)(Ad_b + r_b) + b_m d_b\beta_b\beta_m N_m)$, $c_0 = d_m(Ad_b+r_b)^2(\mu+d_b) - N_m b_m^2 d_b r_b\beta_b\beta_m$, and $\Delta = c_1^2 - 4c_2c_0$. If we suppose $d_m\mu - b_m\beta_m d_b > 0$,*

1. If $R_0 > 1$, there exists a unique endemic equilibrium E^+.

2. If $R_0 = 1$, there exists a unique endemic equilibrium E^+ provided $c_1 < 0$; otherwise there is no endemic equilibrium.

3. If $R_0 < 1$, and

(a) if $-\frac{2c_2r_b}{\mu+d_b} + \sqrt{\Delta} < c_1 < 0$ and $\Delta > 0$, there exist two endemic equilibria E^- and E^+;

(b) if $-\frac{2c_2r_b}{\mu+d_b} < c_1 < 0$ *and* $\Delta = 0$*, these two endemic equilibria coalesce into* E^**;*

(c) otherwise, there is no endemic equilibrium.

Proof. I_b coordinates of E^- and E^+ are determined by

$$g(I_b) = c_2 I_b^2 + c_1 I_b + c_0, \tag{5.4}$$

and $S_b = \frac{r_b-(\mu+d_b)I_b}{d_b}$. We focus on the positive equilibrium and the each components of the equilibrium should be positive, then $0 < I_b < \frac{r_b}{\mu+d_b}$ needs to be satisfied.

Obviously, the roots of $g(I_b) = 0$ are

$$I_b^- = \frac{-c_1 - \sqrt{\Delta}}{2c_2},\ I_b^+ = \frac{-c_1 + \sqrt{\Delta}}{2c_2},\ with\ \Delta = c_1^2 - 4c_2c_0. \tag{5.5}$$

Adopting the expression for R_0 in (5.3), we rewrite c_0 as

$$c_0 = d_m(Ad_b + r_b)^2(\mu + d_b)(1 - R_0^2). \tag{5.6}$$

□

Theorem 5.2.2. *For the system (5.2), if there exists one simple endemic equilibrium* E^+*, it is locally stable. If there exist two simple endemic equilibria* E^- *and* E^+*, then* E^- *with low endemicity is unstable and* E^+ *with high endemicity is locally stable.*

Proof. The stability of endemic equilibrium is determined by the sign of the real part of the roots for the equation

$$h(\lambda) = \lambda^3 + a_2\lambda^2 + a_1\lambda + a_0 = 0, \tag{5.7}$$

with

$$
\begin{aligned}
a_2 &= \frac{I_b b_m \beta_m + I_m b_m \beta_b}{(N_b + A)} + 2d_b + d_m + \mu, \\
a_1 &= \frac{(d_b + \mu)(I_b b_m \beta_m + I_m b_m \beta_b - \mu I_b) + b_m(I_b d_b \beta_m + I_m d_m \beta_b)}{(N_b + A)} \\
&\quad \frac{b_m^2 \beta_m \beta_b I_b I_m}{(N_b + A)^2} + d_b(\mu + d_b + d_m), \\
a_0 &= \frac{d_b + \mu}{(N_b + A)^2}[(I_b b_m \beta_m + (N_b + A)d_m)(I_m b_m \beta_b - I_b \mu) \\
&\quad + I_b(N_b + A)(b_m \beta_m d_b - d_m \mu)].
\end{aligned} \tag{5.8}
$$

For any endemic equilibrium $\tilde{E}(\tilde{I_m}, \tilde{S_b}, \tilde{I_b})$, it is evident that $a_2 > 0$ with all positive parameters. Moreover, a_0 at $\tilde{E}$ in (5.8) can be expressed in terms of c_2 and c_1 in Theorem 5.2.1,

$$
a_0 = \frac{\tilde{I_b}(2c_2\tilde{I_b} + c_1)}{d_b(\tilde{N_b} + A)^2} \tag{5.9}
$$

If $R_0 \geq 1$, by Theorem 5.2.1 we have an unique endemic equilibrium E^+, based on (5.5), $a_0 > 0$ at E^+. Similarly, if $R_0 < 1$, taking into account Theorem 5.2.1 and (5.5), we get $a_0 < 0$ at E^- and $a_0 > 0$ at E^+. By Routh-Hurwitz criterion, not all the roots of $h(\lambda) = 0$ at E^- have negative real parts and E^- is unstable.

As for E^+ in all above cases, having known $a_0 > 0$, we still need $a_1 a_2 - a_0 > 0$ to make sure all roots of $h(\lambda) = 0$ have negative real parts.

We calculate

$$a_1a_2 - a_0 = \frac{l_1 + l_2}{(N_b^+ + A)^3},$$

where

$$\begin{aligned}
l_1 &= d_b(2d_b + d_m + \mu)(d_b + d_m + \mu)(N_b^+ + A)^3 + [I_b b_m \beta_m d_b(4d_b + 3d_m + 4\mu) \\
&\quad + I_b\mu(b_m\beta_m d_m + b_m\beta_m\mu + d_b d_m + d_m\mu) + I_m b_m \beta_b d_m(3d_b + d_m + \mu)](N_b^+ + A)^2 \\
&\quad + [I_b^2 b_m^2 \beta_m^2(2d_b + \mu) + 2I_b I_m b_m^2 \beta_m \beta_b(d_m + \mu + 2d_b) + I_m^2 b_m^2 \beta_b^2 d_m](N_b^+ + A) \\
&\quad + I_b I_m b_m^2 \beta_m \beta_b(I_b b_m \beta_m + I_m b_m \beta_b), \\
l_2 &= [d_b^2(3I_m b_m \beta_b - 2I_b\mu) + d_b\mu(4I_m b_m \beta_b - 3I_b\mu) + \mu^2(I_m b_m \beta_b - I_b\mu)](N_b^+ + A)^2 \\
&\quad + I_m b_m \beta_b(d_b + \mu)(I_m b_m \beta_b - I_b\mu)(N_b^+ + A).
\end{aligned}$$

As E^+ and all parameters are positive, $l_1 > 0$. Furthermore, $b_m\beta_m d_b - d_m\mu < 0$ (Theorem 5.2.1) and $a_0 > 0$ in (5.8) imply that $I_m b_m \beta_b - I_b\mu > 0$, accordingly $l_2 > 0$. Therefore $a_1a_2 - a_0 > 0$ and E^+ is locally stable. □

Theorem 5.2.3. *Moreover, for unstable EEP E^-, only one eigenvalue has a positive real part.*

Proof. By Routh-Hurwitz condition, the number of roots with positive real part for $h(\lambda) = 0$ (5.7) at E^- is equal to the number of sign changes in the sequence *1*, a_2, $\frac{a_1a_2 - a_0}{a_2}$, a_0. By Theorem 5.2.2, we have *1* > 0, $a_2 > 0$ and $a_0 < 0$, whatever the sign of $\frac{a_1a_2 - a_0}{a_2}$ is, the

number of sign changes is exactly one, therefore only one root of $h(\lambda) = 0$ has a positive real part. □

5.2.2 Local stable manifold of E^-

We can find the local stable manifold of unstable $E^- = (I_m^-, S_b^-, I_b^-)$ by taking the following steps.

1. Bring E^- to the origin.

   By the transformation $x = I_m - I_m^-$, $y = S_b - S_b^-$ and $z = I_b - I_b^-$, we obtain the system

$$\begin{bmatrix} \dot{x} \\ \dot{y} \\ \dot{z} \end{bmatrix} = J(E^-) \begin{bmatrix} x \\ y \\ z \end{bmatrix} + \begin{bmatrix} \sum_{i,j,k\in\mathbb{N}}^{i+j+k=2} l_{ijk} x^i y^j z^k \\ \sum_{i,j,k\in\mathbb{N}}^{i+j+k=2} p_{ijk} x^i y^j z^k \\ \sum_{i,j,k\in\mathbb{N}}^{i+j+k=2} q_{ijk} x^i y^j z^k \end{bmatrix} + \mathcal{O}(|x,y,z|^3), \tag{5.10}$$

   where

$$J(E^-) = \begin{bmatrix} -\frac{b_m\beta_m I_b^-}{N_b^-+A} - d_m & -\frac{d_m I_m^-}{N_b^-+A} & \frac{b_m\beta_m S_m^- - d_m I_m^-}{N_b^-+A} \\ -\frac{b_m\beta_b S_b^-}{N_b^-+A} & \frac{(\mu+d_b)I_b^- - b_m\beta_b I_m^-}{N_b^-+A} - d_b & \frac{(\mu+d_b)I_b^-}{N_b^-+A} \\ \frac{b_m\beta_b S_b^-}{N_b^-+A} & \frac{-(\mu+d_b)I_b^- + b_m\beta_b I_m^-}{N_b^-+A} & -\frac{(\mu+d_b)I_b^-}{N_b^-+A} - (\mu+d_b) \end{bmatrix} \tag{5.11}$$

   is Jacobian matrix at E^-.

2. Transform $J(E^-)$ to its Jordan normal form.

   Using λ to represent any eigenvalues of $J(E^-)$, we get the corresponding eigenvector is

$$V(\lambda) = \left[\frac{s(I_m^- d_m\mu + S_m^- b_m\beta_m d_b + S_m^- b_m\beta_m\lambda)}{(d_b+\mu)[I_b^- b_m + (N_b^- + A)(d_m+\lambda)]}, -\frac{s(\lambda+d_b+\mu)}{d_b+\lambda}, s\right]', \ \forall s \in \mathbb{R}.$$

   By Theorem 5.2.3, use $\lambda_1, \lambda_2 < 0$, $\lambda_3 > 0$ represent three eigenvalues of $J(E^-)$ and corresponding eigenvectors are $V_1 = V(\lambda_1)$, $V_2 = V(\lambda_2)$ and $V_3 = V(\lambda_3)$. Then let

$$\begin{bmatrix} x \\ y \\ z \end{bmatrix} = P \begin{bmatrix} X \\ Y \\ Z \end{bmatrix}, \quad P = [V_1, V_2, V_3], \tag{5.12}$$

   the system (5.10) becomes

$$\begin{bmatrix} \dot{X} \\ \dot{Y} \\ \dot{Z} \end{bmatrix} = \begin{bmatrix} \lambda_1 & 0 & 0 \\ 0 & \lambda_2 & 0 \\ 0 & 0 & \lambda_3 \end{bmatrix} \begin{bmatrix} X \\ Y \\ Z \end{bmatrix} + \begin{bmatrix} \sum\limits_{i,j,k\in\mathbb{N}}^{i+j+k=2} L_{ijk} X^i Y^j Z^k \\ \sum\limits_{i,j,k\in\mathbb{N}}^{i+j+k=2} P_{ijk} X^i Y^j Z^k \\ \sum\limits_{i,j,k\in\mathbb{N}}^{i+j+k=2} Q_{ijk} X^i Y^j Z^k \end{bmatrix} + \mathcal{O}(|X,Y,Z|^3). \tag{5.13}$$

3. Calculate the local stable manifold M^s.

   By stable manifold theorem, let

$$Z(t) = h(X(t), Y(t)) = h_{20}X(t)^2 + h_{11}X(t)Y(t) + h_{02}Y(t)^2$$

$$+ h_{30}X(t)^3 + h_{21}X(t)^2Y(t) + h_{12}X(t)Y(t)^2 + h_{03}Y(t)^3$$

$$+ \mathcal{O}(|X(t), Y(t)|^4).$$

Since M_s is invariant, we have

$$\frac{Z(t)}{dt} = \frac{dh(X(t), Y(t))}{dt},$$

that is

$$\dot{Z} = 2h_{20}X\dot{X} + h_{11}\dot{X}Y + h_{11}X\dot{Y} + 2h_{02}Y\dot{Y} + 3h_{30}X^2\dot{X} + 2h_{21}X\dot{X}Y$$

$$+ h_{21}X^2\dot{Y} + h_{12}\dot{X}Y^2 + 2h_{12}XY\dot{Y} + 3h_{03}Y^2\dot{Y} + \mathcal{O}(|X, Y|^4).$$

We simplify it as

$$\dot{Z} = (2h_{20}X + h_{11}Y + 3h_{30}X^2 + 2h_{21}XY + h_{12}Y^2)\dot{X}$$

$$+ (h_{11}X + 2h_{02}Y + h_{21}X^2 + 2h_{12}XY + 3h_{03}Y^2)\dot{Y}$$

$$+ \mathcal{O}(|X, Y|^4).$$

$\Rightarrow$

$$\lambda_3 h(X, Y) + \sum_{i,j,k\in\mathbb{N}}^{i+j+k=2} Q_{ijk}X^iY^jh(X, Y)^k + \mathcal{O}(|X, Y, h(X, Y)|^3)$$

$$= (2h_{20}X + h_{11}Y + 3h_{30}X^2 + 2h_{21}XY + h_{12}Y^2)[\lambda_1 X$$

$$+ \sum_{i,j,k\in\mathbb{N}}^{i+j+k=2} L_{ijk}X^iY^jh(X, Y)^k] + (h_{11}X + 2h_{02}Y + h_{21}X^2 + 2h_{12}XY$$

$$+ 3h_{03}Y^2)[\lambda_2 Y + \sum_{i,j,k\in\mathbb{N}}^{i+j+k=2} P_{ijk}X^iY^jh(X,Y)^k] + \mathcal{O}(|X,Y|^4).$$

$\Rightarrow$

$$\begin{aligned}
&\lambda_3[h_{20}X^2 + h_{11}XY + h_{02}Y^2 + h_{30}X^3 + h_{21}X^2Y + h_{12}XY^2 + h_{03}Y^3 \\
&+ \mathcal{O}(|X,Y|^4)] + \sum_{i,j,k\in\mathbb{N}}^{i+j+k=2} Q_{ijk}X^iY^jh(X,Y)^k + \mathcal{O}(|X,Y,h(X,Y)|^3) \\
&= (2h_{20}X + h_{11}Y + 3h_{30}X^2 + 2h_{21}XY + h_{12}Y^2)[\lambda_1 X \\
&+ \sum_{i,j,k\in\mathbb{N}}^{i+j+k=2} L_{ijk}X^iY^jh(X,Y)^k] + (h_{11}X + 2h_{02}Y + h_{21}X^2 + 2h_{12}XY \\
&+ 3h_{03}Y^2)[\lambda_2 Y + \sum_{i,j,k\in\mathbb{N}}^{i+j+k=2} P_{ijk}X^iY^jh(X,Y)^k] + \mathcal{O}(|X,Y|^4).
\end{aligned}$$

Matching coefficients of terms X^2, XY and Y^2, we have

$$X^2 : \lambda_3 h_{20} + Q_{200} = 2h_{20}\lambda_1$$

$$XY : \lambda_3 h_{11} + Q_{110} = h_{11}\lambda_1 + h_{11}\lambda_2$$

$$Y^2 : \lambda_3 h_{02} + Q_{020} = 2h_{02}\lambda_2$$

and obtain

$$h_{20} = \frac{Q_{200}}{2\lambda_1 - \lambda_3},\ h_{11} = \frac{Q_{110}}{\lambda_1 + \lambda_2 - \lambda_3},\ h_{02} = \frac{Q_{020}}{2\lambda_2 - \lambda_3}.$$

Moreover, we can obtain the expression of Q_{200}, Q_{110} and Q_{200} with calculations.

For the simplification, we introduce the notation v_{ij}, $(i = 1, 2, 3,\ j = 1, 2)$ satisfying

$$
\begin{aligned}
V_1 &= [v_{11}, v_{12}, 1]' \\
&= \left[\frac{(I_m^- d_m \mu + S_m^- b_m \beta_m d_b + S_m^- b_m \beta_m \lambda_1)}{(d_b+\mu)[I_b^- b_m + (N_b^- + A)(d_m + \lambda_1)]}, -\frac{\lambda_1 + d_b + \mu}{d_b + \lambda_1}, 1\right]', \\
V_2 &= [v_{21}, v_{22}, 1]' \\
&= \left[\frac{(I_m^- d_m \mu + S_m^- b_m \beta_m d_b + S_m^- b_m \beta_m \lambda_2)}{(d_b+\mu)[I_b^- b_m + (N_b^- + A)(d_m + \lambda_2)]}, -\frac{\lambda_2 + d_b + \mu}{d_b + \lambda_2}, 1\right]', \\
V_3 &= [v_{31}, v_{32}, 1]', \\
&= \left[\frac{(I_m^- d_m \mu + S_m^- b_m \beta_m d_b + S_m^- b_m \beta_m \lambda_3)}{(d_b+\mu)[I_b^- b_m + (N_b^- + A)(d_m + \lambda_3)]}, -\frac{\lambda_3 + d_b + \mu}{d_b + \lambda_3}, 1\right]'.
\end{aligned}
$$

Carry out transformations (5.10) and (5.12) for the system (5.2), we obtain

$$
\begin{aligned}
Q_{200} = &\frac{1}{W(N_b^- + A)}[(v_{22} - v_{12})\, b_m\, \beta_m\, v_{11} + (v_{11} - v_{21})\, b_m\, \beta_b\, v_{11}\, v_{12} \\
&+ (v_{11}\, v_{22} - v_{12}\, v_{21})\, b_m\, \beta_b\, v_{11}\, v_{12}] + \frac{(v_{12}+1)}{W\left(N_b^- + A\right)^2}\,(v_{12}\, v_{21} \\
&- v_{11}\, v_{22} - v_{11} + v_{21})\left[b_m\, \beta_b\, \left(I_m^-\, v_{12} + S_b^-\, v_{11}\right) - I_b^-\,(v_{12}+1)\,(\mu\right. \\
&\left.+ d_b)\right] + \frac{(v_{12}+1)\,(v_{22} - v_{12})}{W\left(N_b^- + A\right)^2}\left[\left(-I_b^-\, v_{11} + N_m - I_m^-\right) b_m\, \beta_m\right. \\
&\left. - (v_{12}+1)\, dm\, I_m^-\right], \\
Q_{110} = &\frac{1}{W\left(N_b^- + A\right)}[(v_{11}\, v_{22} + v_{12}\, v_{21})\,(v_{11}\, v_{22} - v_{12}\, v_{21} + v_{11} - v_{21})\, b_m\, \beta_b \\
&+ (v_{22} - v_{12})\,(v_{11} + v_{21})\, b_m\, \beta_m] + \frac{(v_{11}v_{22} - v_{12}v_{21} + v_{11} - v_{21})}{W\left(N_b^- + A\right)^2}[2(\mu
\end{aligned}
$$

$$+ d_b)(v_{22}+1)(v_{12}+1)I_b^- - b_m\beta_b I_m^-(2v_{12}v_{22}+v_{12}+v_{22})]$$

$$+ \frac{b_m\,(v_{11}\,v_{22}+v_{12}\,v_{21}+v_{11}+v_{21})}{W\left(N_b^-+A\right)^2}[(v_{12}-v_{22})\,\beta_m\,I_b^- - (v_{11}\,v_{22}$$

$$-v_{12}\,v_{21}+v_{11}-v_{21})\,\beta_b\,S_b^-\,] + \frac{(v_{12}-v_{22})}{W\left(N_b^-+A\right)^2}[2\,(v_{22}+1)\,(v_{12}$$

$$+1)\,dm\,I_m^- - (v_{22}+v_{12}+2)\left(N_m-I_m^-\right)b_m\,\beta_m],$$

$$Q_{020} = \frac{1}{W\left(N_b^-+A\right)}[(v_{22}-v_{12})\,b_m\,\beta_m\,v_{21} + (v_{11}\,v_{22}-v_{12}\,v_{21})\,b_m\,\beta_b\,v_{21}\,v_{22}]$$

$$+ \frac{(v_{22}+1)\,(v_{22}-v_{12})}{W\left(N_b^-+A\right)^2}\left[-(v_{22}+1)\,dm\,I_m^- + b_m\,\beta_m\,\left(-I_b^-v_{21}+N_m\right.\right.$$

$$\left.\left.-I_m^-\right)\right] + (v_{11}-v_{21})\,b_m\,\beta_b\,v_{21}\,v_{22} + \frac{(v_{22}+1)}{W\left(N_b^-+A\right)^2}\,(v_{12}\,v_{21}-v_{11}\,v_{22}$$

$$-v_{11}+v_{21})\left[\left(I_m^-v_{22}+S_b^-v_{21}\right)b_m\,\beta_b - I_b^-\,(v_{22}+1)\,(\mu+d_b)\right],$$

with

$$W = v_{11}\,v_{22} - v_{11}\,v_{32} - v_{12}\,v_{21} + v_{12}\,v_{31} + v_{21}\,v_{32},$$

$$N_b^- = S_b^- + I_b^-.$$

Then the local stable manifold M_s is

$$Z(t) = \frac{Q_{200}}{2\lambda_1-\lambda_3}X(t)^2 + \frac{Q_{110}}{\lambda_1+\lambda_2-\lambda_3}X(t)Y(t) + \frac{Q_{020}}{2\lambda_2-\lambda_3}Y(t)^2$$

$$+ \mathcal{O}(|X(t),Y(t)|^3). \tag{5.14}$$

Now we choose a set of parameter values $b_m = 0.2$, $\beta_m = 0.04$, $A = 5$, $d_m = 0.016$, $r_b = 2$, $\beta_b = 0.8$, $d_b = 0.001$, $\mu = 0.8$, $N_m = 1000$. Based on Theorem 5.2.1, Theorem

5.2.2 and Theorem 5.2.3, the system has a locally stable disease free equilibrium $E_0 = (0, 2000, 0)$ and two endemic equilibria, $E^- = (13.04593757, 83.128484, 2.393098023)$ is unstable and $E^+ = (130.8805745, 0.791158, 2.495891189)$ is locally stable. By (5.14), we could determine the local stable manifold M_s at E^- and it is approximated as

$$\begin{aligned}\Phi(I_m, S_b, I_b) &= 7892.203556I_m - 965.2218999S_b + 1757.114565I_b - 28208.17652 \\ &+ 8.989883276I_m^2 + 1.532643609I_mS_b - 37.45173910I_mI_b - 8.561563901I_b^2 \\ &+ 0.04625202185S_b^2 - 5.097399576S_bI_b + \mathcal{O}(|I_m, S_b, I_b|^3) = 0. \end{aligned} \tag{5.15}$$

The local stable manifold M_s separates the space $\{(I_m, S_b, I_b)|I_m > 0, S_b > 0, I_b > 0\}$ into three parts (Fig 5.4): I $= \{(I_m, S_b, I_b)|\Phi(I_m, S_b, I_b) > 0\}$, II $= \{(I_m, S_b, I_b)|\Phi(I_m, S_b, I_b) < 0\}$ and $M_s = \{(I_m, S_b, I_b)|\Phi(I_m, S_b, I_b) = 0\}$ itself.

When the initial point is in I, the trajectory will approach to endemic equilibrium E^+ (Fig. 5.5, Fig. 5.6), when the initial point is in II, the trajectory will approach the S_b-$axis$ (Fig. 5.5, Fig. 5.6), which means the disease will die out. In such a situation, we could define I as the region with high risk of infections, contrarily, II as the region with low risk of infections.

When the initial value of I_m, S_b, I_b are in I, the disease cannot be eradicated even though the basic reproduction number $R_0 < 1$. Hence the basic reproduction number is not enough to be used to measure the intensity of the virus transmission or as an indicator for evaluating the risk of infections. We develop following assessments to evaluate the

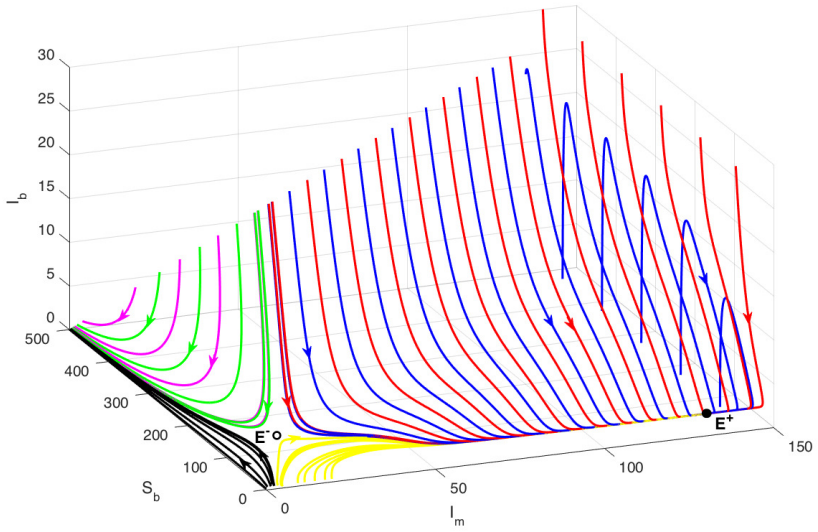

Figure 5.3: The phase portraits

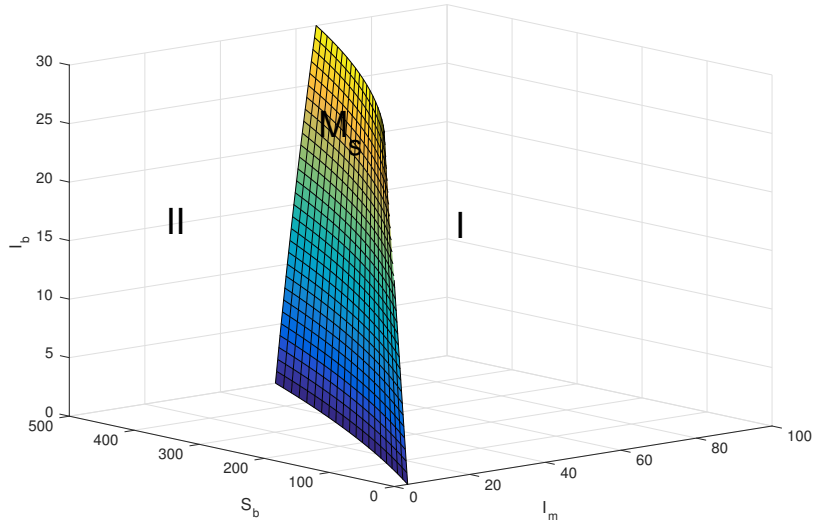

Figure 5.4: The local stable manifold, I and II

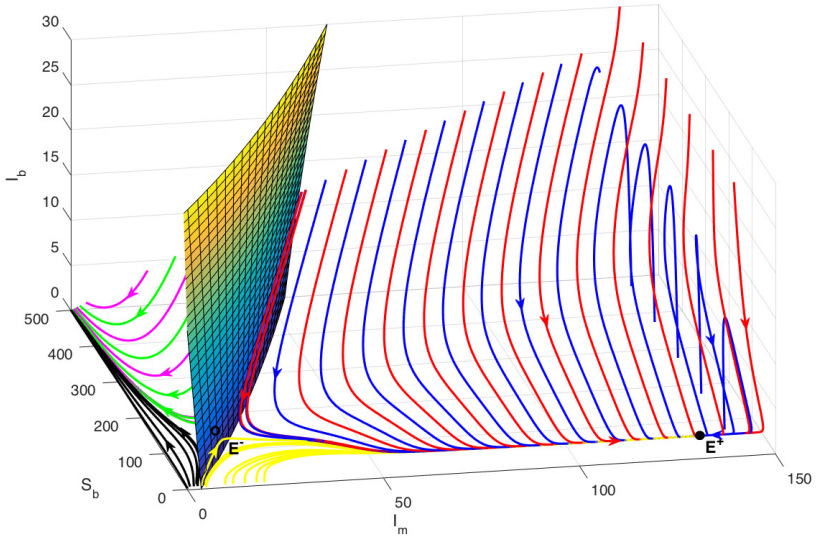

Figure 5.5: The phase portrait and the local stable manifold (1)

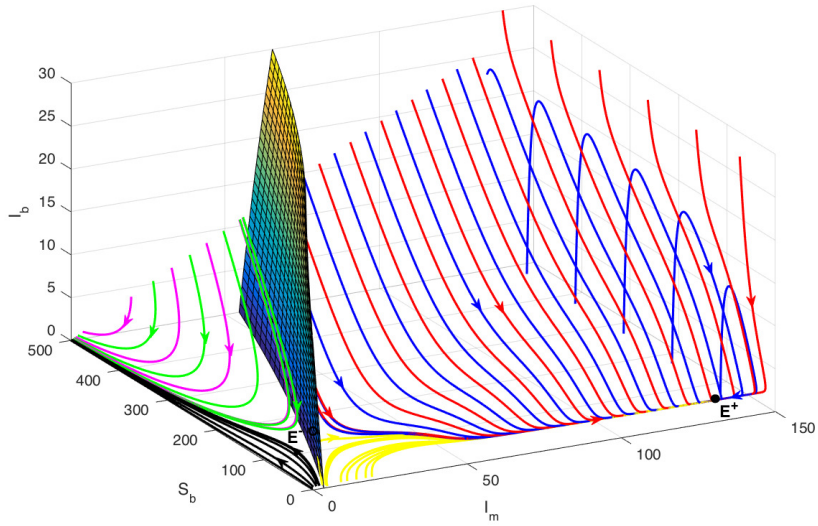

Figure 5.6: The phase portrait and the local stable manifold (2)

pattern and the risk of the disease spread.

Risk Assessment Criteria

To evaluate the intensity of the virus transmission, based on transmission model (5.2), if

1. $R_0 > 1$, the risk level is high;

2. $R_0 < 1$ & initial values are in I $= \{(I_m, S_b, I_b) | \Phi(I_m, S_b, I_b) > 0\}$, the risk level is high;

3. $R_0 < 1$ & initial values are in II $= \{(I_m, S_b, I_b) | \Phi(I_m, S_b, I_b) < 0\}$, the risk level is low.

5.3 A comprehensive WNV transmission model

We extend the simplified model to a more general case. For vector populations, we separate mosquito populations into preadult and adult two compartments and adopt mosquito population model (2.1). Particularly, we use $L(t)$ be the population of preadult WNV vector mosquitoes encompassing all aquatic stages at time t. For host populations, we also consider recovered birds and denote the population of recovered birds at time t as $R_b(t)$, then the total bird population is $N_b = (S_b + I_b + R_b)$. For the cross-infection rate between birds and mosquitoes, we assume that mosquito searching is efficient even when host densities are low, the disease transmission rate depends on the proportion of susceptible or infected birds rather than the actual density of birds (Bowman et al. (2005), Lewis et al.

(2006b)). Then the cross-infection rate is still interpreted using mass action incidence normalized by total host population $(N_b + A)$ and the transmission dynamics is

$$\begin{cases} \frac{dL}{dt} = cb_m(S_m + I_m) - \delta L - d_l L - \kappa L^2, \\ \frac{dS_m}{dt} = \delta L - b_m\beta_m S_m \frac{I_b}{N_b+A} - d_m S_m, \\ \frac{dI_m}{dt} = b_m\beta_m S_m \frac{I_b}{N_b+A} - d_m I_m, \\ \frac{dS_b}{dt} = r_b - b_m\beta_b I_m \frac{S_b}{N_b+A} - d_b S_b, \\ \frac{dI_b}{dt} = b_m\beta_b I_m \frac{S_b}{N_b+A} - \mu I_b - \gamma I_b - d_b I_b, \\ \frac{dR_b}{dt} = \gamma I_b - d_b R_b. \end{cases} \tag{5.1}$$

Table 5.2: Parameters in a comprehensive WNV transmission model (5.1)

Par.	Interpretation	Range (day^{-1})
c	the scaling factor associated with biting rate	2.325
b_m	Female adult mosquitoes per capita biting rate	$0.03 - 0.16$
δ	Mosquitos per capita maturation rate from preadult to adult	$0.051 - 0.093$
d_l	Preadult mosquitoes per capita mortality rate	$0.213 - 16.9$
κ	Intraspecific competition rate of preadult mosquitoes	$0 - 1$

β_m	WNV transmission probability from birds to mosquitoes	$0.02 - 0.24$
d_m	Female adult mosquitoes per capita mortality rate	$0.016 - 0.07$
r_b	Recruitment rate of birds	$800 - 1100$
β_b	WNV transmission probability from mosquitoes to birds	$0.8 - 1.0$
μ	Birds per capita mortality rate due to WNV	$0.125 - 0.2$
γ	Birds per capita recovery rate from WNV	$0 - 0.2$
d_b	Birds per capita natural death rate	$10^{-4} - 10^{-3}$

This model is an improved one based on our previous work (Wang et al. (2017)). To reflect that adult female mosquitoes feed on hosts to obtain proteins for egg production, the reproduction rate is proportional to mosquito biting rate. The representative aspects of intraspecific competition are extended, here the intraspecific competition can be related to any possible factors like the density of nutrients and oxygen, rather than only the size of standing water. For avian hosts, the demographic is considered, with natural birth/death and migration.

5.3.1 Disease-free equilibrium points

The model (5.1) has up to two disease-free equilibrium (DFE) points. The number of DFE points is determined by the sign of $\frac{cb_m\delta}{d_m} - (d_l + \delta)$.

If $\frac{cb_m\delta}{d_m} - (d_l + \delta) < 0$, the change rate of preadult has been negative even without considering intraspecific competition and the model has a unique equilibrium point $E_0 = (0, 0, 0, \frac{r_b}{d_b}, 0, 0)$, The E_0 has eigenvalues $-d_m$, $-d_b$(multiplicity 2), $-(\mu + \gamma + d_b)$ and the roots of the equation:

$$-\lambda^2 - (d_l + d_m + \delta)\lambda + \frac{cb_m\delta}{d_m} - (d_l + \delta) = 0. \tag{5.2}$$

All parameters are positive in a biological sense, all the roots of (5.2) have negative real parts, and DFE E_0 is locally stable.

If $\frac{cb_m\delta}{d_m} - (d_l + \delta) > 0$, that is, intraspecific competition as well as the death and the maturation reduce the change rate of L, then the model (5.1) has two DFE $E_1 = (L_0, S_{m_0}, 0, \frac{r_b}{d_b}, 0, 0)$ as well as E_0, where $L_0 = \frac{\frac{cb_m\delta}{d_m} - (d_l+\delta)}{\kappa}$, $S_{m_0} = \frac{\delta[\frac{cb_m\delta}{d_m} - (d_l+\delta)]}{d_m\kappa}$. By (5.2), E_0 has a positive real part eigenvalue and E_0 is unstable. The local stability of E_1 is determined by the basic reproduction number R_0 which can be obtained from the next generation matrix for the system (5.1).

Using the notation of van den Driessche and Watmough (2002), with the infected variables (I_m, I_b) in the model (5.1), $\mathfrak{F}$ denotes the rate of new infections and $\mathfrak{V}$ denotes the

rate of transfer between compartments,

$$\mathfrak{F} = \begin{bmatrix} b_m\beta_m S_m \frac{I_b}{N_b+A} \\ \\ b_m\beta_b I_m \frac{S_b}{N_b+A} \end{bmatrix}, \mathfrak{V} = \begin{bmatrix} d_m I_m \\ \\ (\mu+\gamma+d_b)I_b \end{bmatrix},$$

The corresponding linearized matrices at the DFE E_1 are

$$F = \begin{bmatrix} 0 & \frac{\beta_m b_m S_{m_0}}{N_{b_0}+A} \\ \\ \frac{b_m\beta_b b_m \frac{r_b}{d_B}}{N_{b_0}+A} & 0 \end{bmatrix}, V = \begin{bmatrix} d_m & 0 \\ \\ 0 & \mu+\gamma+d_b \end{bmatrix}.$$

Then the basic reproduction number R_0 is defined as the spectral radius of the matrix FV^{-1},

$$R_0 = \sqrt{\frac{b_m\beta_m \frac{S_{m_0}}{\frac{r_b}{d_b}+A}}{(\mu+\gamma+d_b)} \frac{b_m\beta_b \frac{\frac{r_b}{d_b}}{\frac{r_b}{d_b}+A}}{d_m}}, \tag{5.3}$$

where $S_{m_0} = \frac{\delta L}{d_m} = \frac{\delta[\frac{cb_m\delta}{d_m}-(d_l+\delta)]}{d_m\kappa}$.

In the biological view, R_0 gives the expected number of new infections produced by a single infective mosquito or bird when introduced into a susceptible population. The first term under the square root of R_0 performs as the spread of WNV from birds to mosquitoes; the transmission probability from birds to mosquitoes ($b_m\beta_m$) multiplied by the number of initially susceptible female mosquitoes per host ($\frac{S_{m_0}}{\frac{r_b}{d_b}+A}$) multiplied by the birds infectious lifespan ($\frac{1}{\mu+\gamma+d_b}$). The second term represents transmission of WNV from mosquitoes to birds, that is the transmission probability ($b_m\beta_b$) multiplied by the number of initially susceptible birds per host ($\frac{\frac{r_b}{d_b}}{\frac{r_b}{d_b}+A}$) times the adult female mosquito infectious lifespan ($\frac{1}{d_m}$).

The square root in R_0 provides the geometric mean for an average individual of both species combined (Wonham et al. (2004), Bowman et al. (2005), Heffernan et al. (2005)).

For system (5.1), the disease-free equilibrium E_1 is locally asymptotically stable if $R_0 < 1$ and unstable if $R_0 > 1$ (van den Driessche and Watmough (2002)).

5.3.2 Endemic equilibrium points

In order to obtain all possible endemical equilibrium points, we set the right hand side of system (5.1) equal to zero:

$$cb_m(S_m + I_m) - \delta L - d_l L - \kappa L^2 = 0 \tag{5.4}$$

$$\delta L - b_m \beta_m S_m \frac{I_b}{S_b + I_b + R_b + A} - d_m S_m = 0 \tag{5.5}$$

$$b_m \beta_m S_m \frac{I_b}{S_b + I_b + R_b + A} - d_m I_m = 0 \tag{5.6}$$

$$r_b - b_m \beta_b I_m \frac{S_b}{S_b + I_b + R_b + A} - d_b S_b = 0 \tag{5.7}$$

$$b_m \beta_b I_m \frac{S_b}{S_b + I_b + R_b + A} - \mu I_b - \gamma I_b - d_b I_b = 0 \tag{5.8}$$

$$\gamma I_b - d_b R_b = 0 \tag{5.9}$$

By (5.4), (5.5) and (5.6), we have $L = \frac{\frac{cb_m\delta}{d_m} - (d_l + \delta)}{\kappa}$ and $S_m + I_m = \frac{\delta L}{d_m}$. We explore the positive equilibria and from $L > 0$ we have $\frac{cb_m\delta}{d_m} - (d_l + \delta) > 0$. Additionally, the coordinates of an endemic equilibrium point need to satisfy

$$
\begin{aligned}
S_b =& \frac{r_b - (\mu + \gamma + d_b) I_b}{d_b}, \\
R_b =& \frac{\gamma I_b}{d_b}.
\end{aligned} \tag{5.10}
$$

We also get that

$$
\begin{aligned}
S_m =& \frac{\delta L (S_b + I_b + R_b + A)}{I_b b_m \beta_m + d_m (S_b + I_b + R_b + A)}, \\
I_m =& \frac{(r_b - d_b S_b)(S_b + I_b + R_b + A)}{b_m \beta_b S_b}.
\end{aligned} \tag{5.11}
$$

Combine with (5.6), if an endemic equation exists, the coordinate of I_b is the positive root of quadratic equation

$$
g(I_b) = c_2 I_b^2 + c_1 I_b + c_0, \tag{5.12}
$$

where

$$
\begin{aligned}
c_2 =& -(\mu + \gamma + d_b) d_m \mu (b_m \beta_m d_b - d_m \mu), \\
c_1 =& (\mu + \gamma + d_b)(b_m^2 d_b \beta_b \beta_m \delta L + d_m (b_m \beta_m d_b - 2 d_m \mu)(A d_b + r_b)), \\
c_0 =& d_m^2 (A d_b + r_b)^2 (\mu + \gamma + d_b) - L b_m^2 d_b r_b \beta_b \beta_m \delta.
\end{aligned} \tag{5.13}
$$

Adopting the expression for R_0 in (5.3), we rewrite c_0 in (5.13) as

$$
c_0 = d_m^2 (A d_b + r_b)^2 (\mu + \gamma + d_b)(1 - R_0^2). \tag{5.14}
$$

Furthermore, as we study the positive equilibrium, the positiveness of other components of the equilibrium should also be guaranteed. Accounting for (5.10) and (5.11), it also requires that the coordinate I_b satisfying the inequality

$$I_b < \frac{r_b}{\mu + \gamma + d_b}. \tag{5.15}$$

We have $d_m\mu - b_m\beta_b d_b > 0$, consequently $c_2 > 0$ and the discriminant for the quadratic equation (5.12) is

$$\begin{aligned} \Delta &= c_1^2 - 4c_2c_0 \\ &= C(e_2L^2 + e_1L + e_0), \end{aligned} \tag{5.16}$$

where

$$\begin{aligned} C &= d_b(\mu + \gamma + d_b)b_m^2\beta_m, \\ e_2 &= b_m^2 d_b\beta_b^2\beta_m\delta^2(\mu + \gamma + d_b), \\ e_1 &= 2d_m\beta_b\delta[((\mu + \gamma + d_b)(b_m\beta_m d_b - 2d_m\mu)(Ad_b + r_b) \\ &\quad + 2\mu r_b(-b_m\beta_m d_b + d_m\mu)], \\ e_0 &= d_b d_m^2\beta_m(\mu + \gamma + d_b)(Ad_b + r_b)^2. \end{aligned} \tag{5.17}$$

If $R_0 > 1$, then $c_0 < 0$ and (5.12) always has a unique positive root

$$I_b^+ = \frac{-c_1 + \sqrt{\Delta}}{2c_2}, \tag{5.18}$$

and $I_b^+ < \frac{r_b}{\mu+\gamma+d_b}$ since $g(I_b^+) > 0$, we denote the corresponding equilibrium by E^+.

If $R_0 = 1$, then $c_0 = 0$; when $c_1 < 0$, the equation has one positive root

$$I_b^+ = -\frac{c_1}{c_2}. \tag{5.19}$$

Similarly, it also meets requirement (5.15) and its corresponding equilibrium is denoted as E^+.

For $R_0 < 1$, we have $c_0 > 0$ and (5.12) has up to two positive roots when $\Delta \geq 0$.

If $\Delta > 0$ and $-\frac{c_1}{2c_2} > 0$, we obtain two positive roots

$$I_b^- = \frac{-c_1 - \sqrt{\Delta}}{2c_2},\ I_b^+ = \frac{-c_1 + \sqrt{\Delta}}{2c_2}, \tag{5.20}$$

In this case, $g(\frac{r_b}{\mu+\gamma+d_b}) > 0$ is not enough to make sure $S_b > 0$, we also needs

$$\frac{r_b}{\mu+\gamma+d_b} > -\frac{c_1}{2c_2},$$

and we use E^- and E^+ to represent corresponding two equilibria.

If $\Delta = 0$ and $-\frac{c_1}{2c_2} > 0$, these two equilibria coalesce into E^*. It is easy to get $I_b^* = -\frac{c_1}{2c_2}$ and the inequality in (5.15) is satisfied.

Theorem 5.3.1. *For the system (5.1), if we suppose $d_m\mu - b_m\beta_b d_b > 0$,*

1. The disease free equilibrium E_0 always exists.

2. If $\frac{cb_m\delta}{d_m} - (d_l + \delta) > 0$,

(1) There exists one more disease free equilibrium E_1.

(2) If $R_0 > 1$, there exists a unique endemic equilibrium E^+.

(3) If $R_0 = 1$, there exists a unique endemic equilibrium E^+ provided $c_1 < 0$; otherwise there is no endemic equilibrium.

(4) If $R_0 < 1$, and

(a) if $-\frac{2c_2r_b}{\mu+\gamma+d_b} < c_1 < 0$ and $\Delta > 0$, there exist two endemic equilibrium E^- and E^+;

(b) if $-\frac{2c_2r_b}{\mu+\gamma+d_b} < c_1 < 0$ and $\Delta = 0$, these two endemic equilibrium coalesce into E^*;

(c) otherwise, there is no endemic equilibrium.

3. Otherwise, there is no more disease-free equilibrium and no endemic equilibrium.

5.3.3 Local stability of E^- and E^+

Turning to the local stability of the endemic equilibria in the system (5.1) and by Jacobian matrix at any equilibrium point, we calculate the eigenvalues as $-d_b$ and roots of equation

$$h_1(\lambda)h_2(\lambda) = 0, \tag{5.21}$$

where

$$h_1(\lambda) = \lambda^2 + (2\kappa L + d_l + d_m + \delta)\lambda + \kappa d_m L,$$

$$
\begin{aligned}
h_2(\lambda) &= \lambda^3 + a_2\lambda^2 + a_1\lambda + a_0, \\
a_2 &= \frac{I_b b_m \beta_m + I_m b_m \beta_b}{(N_b + A)} + 2d_b + d_m + \mu + \gamma, \\
a_1 &= \frac{b_m^2 \beta_m \beta_b (I_b I_m - S_b S_m)}{(N_b + A)^2} + \frac{1}{(N_b + A)}[(\mu + \gamma + d_b)(I_b b_m \beta_m \\
&\quad + I_m b_m \beta_b - \mu I_b) + b_m(I_b d_b \beta_m + I_m d_m \beta_b)] \\
&\quad + (\mu + \gamma + d_b)(d_b + d_m) + d_m d_b, \qquad (5.22)
\end{aligned}
$$

$$
\begin{aligned}
a_0 &= \frac{1}{(N_b + A)^2}[-(b_m \beta_b S_b (S_m b_m d_b \beta_m + I_m d_m \mu)) \\
&\quad + (\mu + \gamma + d_b)(I_b b_m \beta_m + (N_b + A) d_m)(I_m b_m \beta_b \\
&\quad + (N_b + A) d_b - I_b \mu)].
\end{aligned}
$$

Apparently, the two roots of $h_1(\lambda) = 0$ have negative real parts since $L = \frac{\frac{cb_m\delta}{d_m} - (d_l + \delta)}{\kappa} > 0$. Hence, the stability of endemic equilibrium is determined by the sign of roots for the equation $h_2(\lambda) = 0$.

Theorem 5.3.2. *For the system (5.1), if there exists one simple endemic equilibrium E^+, it is locally stable. If there exist two simple endemic equilibria E^- and E^+, then E^- with low endemicity is unstable and E^+ with high endemicity is locally stable.*

Proof. The proof is achieved with the help of Routh-Hurwitz criterion. For any endemic equilibrium $\tilde{E}(\tilde{L}, \tilde{S_m}, \tilde{I_m}, \tilde{S_b}, \tilde{I_b}, \tilde{R_b})$, it is evident that $a_2 > 0$ with all positive parameters.

By (5.4), (5.5) and (5.6), a_0 at $\tilde{E}$ can be simplified as

$$a_0 = \frac{(\mu+\gamma+d_b)\tilde{I}_b}{d_b d_m(\tilde{N}_b+A)^2}[-2d_m\mu(b_m d_b\beta_m - d_m\mu)\tilde{I}_b \tag{5.23}$$

$$+ b_m^2 d_b\beta_b\beta_m\delta L + d_m(b_m d_b\beta_m - 2d_m\mu)(Ad_b + r_b)].$$

Interestingly, a_0 in (5.23) can be expressed in terms of c_2 and c_1 in (5.13)

$$a_0 = \frac{\tilde{I}_b}{d_b d_m(\tilde{N}_b+A)^2}(2c_2\tilde{I}_b + c_1). \tag{5.24}$$

If $R_0 \geq 1$, by Theorem 5.3.1 we have an unique endemic equilibrium E^+. Moreover, from (5.18) and (5.19), we obtain that $a_0 > 0$ at E^+. Similarly, if $R_0 < 1$, taking into account Theorem 5.3.1 and the I_b coordinate of E^- and E^+ in (5.20), we get $a_0 < 0$ at E^- and $a > 0$ at E^+.

By Routh-Hurwitz criterion, the roots of $h_2(\lambda) = 0$ at E^- have different signs and E^- is unstable. As for E^+ in all above cases, having known $a_0 > 0$, we still need $a_1a_2 - a_0 > 0$ to make sure all roots of $h_2(\lambda) = 0$ have negative real parts.

Still applying (5.4), (5.5) and (5.6) at E^+, we have

$$a_1a_2 - a_0 = \frac{l_1 + l_2 + l_3}{(N_b^+ + A)^3},$$

where

$$l_1 = [I_m^+ b_m\beta_b(I_b^+ b_m\beta_m + d_m(N_b^+ + A)) + I_b^+ b_m\beta_m(N_b^+ + A)(2d_b + \mu + \gamma)$$

$$+ d_b d_m (N_b^+ + A)^2][I_b^+ b_m \beta_m + I_m^+ b_m \beta_b + (N_b^+ + A)(2d_b + d_m + \mu + \gamma)],$$

$$l_2 = (N_b^+ + A)(d_b + \mu + \gamma)[I_m^+ b_m \beta_b + (N_b^+ + A)d_b - I_b^+ \mu][I_m^+ b_m \beta_b$$

$$+ (N_b^+ + A)(2d_b + \mu + \gamma)],$$

$$l_3 = S_b b_m \beta_b (N_b^+ + A)(S_m^+ b_m d_b \beta_m + I_m^+ d_m \mu).$$

As E^+ and all parameters are positive, $l_1 > 0$ and $l_3 > 0$. Furthermore, $a_0 > 0$ in (5.22) implies that $I_m^+ b_m \beta_b + (N_b^+ + A)d_b - I_b^+ \mu > 0$, accordingly $l_2 > 0$. Therefore $a_1 a_2 - a_0 > 0$ and E^+ is locally stable. □

5.3.4 Backward bifurcation

By Theorem 5.3.1 and setting the discriminant Δ equal to zero, one can solved for the critical value of R_0, and denote $R_0^c = R_0|_{\Delta=0,\ \frac{-2r_b c_2}{\mu+\gamma+d_b} < c_1 < 0}$, then we get

$$R_0^c = \sqrt{\frac{r_b \beta_m^2 d_b^2 b_m^2}{M}}, \tag{5.25}$$

where

$$M = (\mu + \gamma + d_b)[2d_m(2d_m\mu - b_m d_b \beta_m)(Ad_b + r_b) - b_m^2 d_b \beta_m \beta_b \delta L]$$

$$+ 4d_m \mu r_b (b_m d_b \beta_m - d_m \mu)$$

$$> 0.$$

Further from $R_0^c < R_0 < 1$, we can obtain

$$\kappa \in \left(\frac{2e_2\left[\frac{cb_m\delta}{d_m} - (d_l+\delta)\right]}{-e_1+\sqrt{e_1^2-4e_2e_0}}, \frac{2e_2\left[\frac{cb_m\delta}{d_m} - (d_l+\delta)\right]}{-e_1-\sqrt{e_1^2-4e_2e_0}} \right), \tag{5.26}$$

where e_2, e_1 and e_0 are expressed in (5.17), $e_1 < 0$ from $M > 0$ and $-e_1 - \sqrt{e_1^2 - 4e_2e_0} > 0$.

Theorem 5.3.3. *For the system (5.1), consider all the parameters are positive. When bifurcation parameter $R_0 = 1$, the system (5.1) undergoes a backward bifurcation if*

$$b_m\beta_m \frac{S_{m_0}}{(\frac{r_b}{d_b}+A)d_m}\frac{b_m\beta_b}{d_b} + \frac{b_m\beta_m}{d_m} < 2\frac{\mu}{d_b}. \tag{5.27}$$

From the biological point of view, the sum of indirect infection (the new bird infection) by a single bird infection and direct infection (the new mosquito infection) by a single bird infection is less than the the sum of two dead bird infections due to the disease. For the indirect infection, the transmission probability from birds to mosquitoes ($b_m\beta_m$) multiplied by the number of initially susceptible female mosquitoes per host ($\frac{S_{m_0}}{\frac{r_b}{d_b}+A}$) multiplied by the mosquito infectious lifespan ($\frac{1}{d_m}$), then these new infectious mosquitoes $b_m\beta_m\frac{S_{m_0}}{(\frac{r_b}{d_b}+A)d_m}$ transmit the virus ($b_m\beta_b$) to birds multiplied by bird lifespan ($\frac{1}{d_b}$). The direct infection is an infected bird multiplied by the transmission probability from birds to mosquitoes ($b_m\beta_m$) and the mosquito infectious lifespan ($\frac{1}{d_m}$).

Proof. We apply the Theorem 4.1 in Castillo-Chavez and Song (2004) to show the occurrence of the backward bifurcation for the system (5.1).

Using the same notation as in Castillo-Chavez and Song (2004), let $x_1 = L$, $x_2 = S_m$, $x_3 = I_m$, $x_4 = S_b$, $x_5 = I_b$, $x_6 = R_b$. Then the system (5.1) can be written as $\frac{dX}{dt} = F(X)$, with $X = (x_1,\ x_2,\ x_3,\ x_4,\ x_5,\ x_6)'$ and $F = (f_1,\ f_2,\ f_3,\ f_4,\ f_5,\ f_6)'$. Further, we denote

$$\phi = \beta_m b_m^2 \delta \beta_b r_b d_b L - d_m^2(\mu + \gamma + d_b)(Ad_b + r_b)^2,$$

accordingly $\phi \geq 0$ if and only if $R_0 \geq 1$, and $\phi < 0$ if and only if $R_0 < 1$.

Then we can obtain following the Jacobian matrix of the system (5.1) at E_1 (denoting $X_1 = E_1$) with condition $\phi = 0$,

$$\begin{pmatrix} -\frac{2d_m^2\kappa(Ad_b+r_b)^2(\mu+\gamma+d_b)}{b_m^2 d_b r_b \beta_b \beta_m \delta} - d_l - \delta & cb_m & cb_m & 0 & 0 & 0 \\ \delta & -d_m & 0 & 0 & -\frac{d_m(Ad_b+r_b)(\mu+\gamma+d_b)}{b_m r_b \beta_b} & 0 \\ 0 & 0 & -d_m & 0 & \frac{d_m(Ad_b+r_b)(\mu+\gamma+d_b)}{b_m r_b \beta_b} & 0 \\ 0 & 0 & -\frac{\beta_b b_m r_b}{Ad_b+r_b} & -d_b & 0 & 0 \\ 0 & 0 & \frac{\beta_b b_m r_b}{Ad_b+r_b} & 0 & -\mu-\gamma-d_b & 0 \\ 0 & 0 & 0 & 0 & \gamma & -d_b \end{pmatrix}.$$

From the Jacobian matrix, a straightforward calculation yields the characteristic equation

$$\begin{aligned} P(\lambda) = \lambda(\lambda + d_b)^2[\lambda + (d_b + d_m + \mu + \gamma)][\lambda^2 \\ + (\frac{2cb_m\delta}{d_m} - d_l - \delta + d_m)\lambda + d_m(\frac{cb_m\delta}{d_m} - d_l - \delta)]. \end{aligned}$$

Apparently, the Jacobian matrix has a simple zero eigenvalue and the rest eigenvalues

have negative real parts due to $\frac{cb_m\delta}{d_m} - (d_l + \delta) > 0$. Thus we can adopt the Theorem in Castillo-Chavez and Song (2004) to analyze the dynamics of the system (5.1).

One can get that the Jacobian matrix has a right eigenvector ω and a left eigenvector ν associated with 0 eigenvalue respectively. Particularly, for any positive ω_6 and nu_3,

$$\begin{aligned}
\omega = \ & (0,\ -\frac{d_b(\mu+\gamma_d-b)(Ad_b+r_b)\omega_6}{b_m r_b\beta_b\gamma},\ \frac{d_b(\mu+\gamma_d-b)(Ad_b+r_b)\omega_6}{b_m r_b\beta_b\gamma},\\
& -\frac{(\mu+\gamma+d_b)\omega_6}{\gamma},\ \frac{d_b\omega_6}{\gamma},\ \omega_6)',\\
\nu = \ & (0,\ 0,\ \nu_3,\ 0,\ \frac{d_m(Ad_b+r_b)\nu_3}{\beta_b b_m r_b},\ 0).
\end{aligned}$$

Let a and b be the coefficients defined in Theorem 4.1 (Castillo-Chavez and Song (2004)) in the form

$$\begin{aligned}
a &= \sum_{k,i,j}^{6} \nu_k\omega_i\omega_j \frac{\partial^2 f_k}{\partial x_i \partial x_j}(X_1, 0),\\
b &= \sum_{k,i}^{6} \nu_k\omega_i \frac{\partial^2 f_k}{\partial x_i \partial \phi}(X_1, 0).
\end{aligned}$$

By straightforward calculation, we have

$$\begin{aligned}
a =& -\frac{2d_b^2\omega_6^2\nu_3[d_m(\mu+\gamma+d_b)(Ad_b+r_b)+r_b(b_m d_b\beta_m-2d_m\mu)]}{b_m\beta_b\gamma^2 r_b^2},\\
b =& \frac{d_b^2\omega_6\nu_3}{r_b b_m\beta_b d_m\gamma(Ad_b+r_b)} > 0.
\end{aligned}$$

Figuring out that coefficient b is always positive, the system (5.1) will undergo a backward bifurcation if the coefficient $a > 0$ as well, that is the following condition needs to

be satisfied,

$$d_m(\mu+\gamma+d_b)(Ad_b+r_b)+r_b(b_m d_b \beta_m - 2d_m\mu) < 0, \tag{5.28}$$

furthermore, it can be rewritten as

$$1+\frac{r_b b_m \beta_m}{d_m(\mu+\gamma+d_b)(A+\frac{r_b}{d_b})} < \frac{2\frac{r_b}{d_b}\mu}{(\mu+\gamma+d_b)(A+\frac{r_b}{d_b})}. \tag{5.29}$$

Combining with $R_0 = 1$, we have

$$\frac{b_m\beta_m\frac{S_{m_0}}{\frac{r_b}{d_b}+A}}{(\mu+\gamma+d_b)}\frac{b_m\beta_b\frac{\frac{r_b}{d_b}}{\frac{r_b}{d_b}+A}}{d_m}+\frac{r_b b_m\beta_m}{d_m(\mu+\gamma+d_b)(A+\frac{r_b}{d_b})} < \frac{2\frac{r_b}{d_b}\mu}{(\mu+\gamma+d_b)(A+\frac{r_b}{d_b})}, \tag{5.30}$$

reorganizing the (5.30), we obtain

$$b_m\beta_m\frac{S_{m_0}}{(\frac{r_b}{d_b}+A)d_m}\frac{b_m\beta_b}{d_b}+\frac{b_m\beta_m}{d_m} < 2\frac{\mu}{d_b}. \tag{5.31}$$

□

Theorem 5.3.4. *When $R_0^c < R_0 < 1$, only one eigenvalue of E^- has a positive real part.*

Proof. To verify the number of eigenvalues with positive real part at E^- is one, we need to check the sign of real parts for all eigenvalues. we have shown that E^- has eigenvalues $-d_b$ and two roots with negative real parts of $h_1(\lambda) = 0$ in (5.21), the rest are the roots of $h_2(\lambda) = 0$ in (5.22). By Routh-Hurwitz condition, the number of roots with positive real part for $h_2(\lambda) = 0$ is equal to the number of sign changes in the sequence *1*, a_2, $\frac{a_1a_2-a_0}{a_2}$, a_0. By Theorem 5.3.2, one can get *1* > 0, $a_2 > 0$ and $a_0 < 0$, whatever the sign of $\frac{a_1a_2-a_0}{a_2}$

is, the number of sign changes is exactly one, therefore only one root of $h_2(\lambda) = 0$ has a positive real part. □

5.3.5 Local stable manifold of E^-

We can obtain the local stable manifold at E^- with following steps.

1. Bring E^- to the origin.

   By the transformation $y_1 = L - L^-$, $y_2 = S_m - S_m^-$, $y_3 = I_m - I_m^-$, $y_4 = S_b - S_b^-$, $y_5 = I_b - I_b^-$, $y_6 = R_b - R_b^-$ and denote $Y = [y_1, y_2, y_3, y_4, y_5, y_6]'$, we obtain the system

   $$\dot{Y} = J(E^-)Y + G_1(|Y|^2) + \mathcal{O}(|Y|^3), \tag{5.32}$$

   where $J(E^-)$ is Jacobian matrix at E^-,

   $$G_1(|Y|^2) = \left[\sum_{i\in\mathbb{K}, j_i\in\mathbb{N}}^{\sum j_i=2} l_{\{J_I\}}\Pi y_i^{j_i}, \sum_{i\in\mathbb{K}, j_i\in\mathbb{N}}^{\sum j_i=2} m_{\{J_I\}}\Pi y_i^{j_i}, \sum_{i\in\mathbb{K}, j_i\in\mathbb{N}}^{\sum j_i=2} n_{\{J_I\}}\Pi y_i^{j_i}, \right.$$
   $$\left. \sum_{i\in\mathbb{K}, j_i\in\mathbb{N}}^{\sum j_i=2} o_{\{J_I\}}\Pi y_i^{j_i}, \sum_{i\in\mathbb{K}, j_i\in\mathbb{N}}^{\sum j_i=2} p_{\{J_I\}}\Pi y_i^{j_i}, \sum_{i\in\mathbb{K}, j_i\in\mathbb{N}}^{\sum j_i=2} q_{\{J_I\}}\Pi y_i^{j_i} \right]',$$

   with set $\mathbb{K} = \{1, 2, 3, 4, 5, 6\}$, $\{J_I\} = j_1 j_2 j_3 j_4 j_5 j_6$.

2. Transform $J(E^-)$ to its Jordan normal form.

   By Theorem 5.2.3, use λ_1, λ_2, λ_3, λ_4, $\lambda_5 < 0$, $\lambda_6 > 0$ represent six eigenvalues of

$J(E^-)$ and corresponding eigenvectors are $V_i = V(\lambda_i),\ (i = 1, ..., 6)$. Then let

$$Y = PZ,\ Z = [z_1, z_2, z_3, z_4, z_5, z_6]',\ P = [V_1, V_2, V_3, V_4, V_5, V_6], \tag{5.33}$$

the system (5.10) becomes

$$\dot{Z} = \begin{bmatrix} \lambda_1 & 0 & 0 & 0 & 0 & 0 \\ 0 & \lambda_2 & 0 & 0 & 0 & 0 \\ 0 & 0 & \lambda_3 & 0 & 0 & 0 \\ 0 & 0 & 0 & \lambda_4 & 0 & 0 \\ 0 & 0 & 0 & 0 & \lambda_5 & 0 \\ 0 & 0 & 0 & 0 & 0 & \lambda_6 \end{bmatrix} Z + G_2(|Z|^2) + \mathcal{O}(|Z|^3), \tag{5.34}$$

where

$$G_2(|Z|^2) = \Bigg[\sum_{i\in\mathbb{K}, j_i\in\mathbb{N}}^{\sum j_i=2} L_{\{J_I\}}\Pi z_i^{j_i}, \sum_{i\in\mathbb{K}, j_i\in\mathbb{N}}^{\sum j_i=2} M_{\{J_I\}}\Pi z_i^{j_i}, \sum_{i\in\mathbb{K}, j_i\in\mathbb{N}}^{\sum j_i=2} N_{\{J_I\}}\Pi z_i^{j_i}, \sum_{i\in\mathbb{K}, j_i\in\mathbb{N}}^{\sum j_i=2} O_{\{J_I\}}\Pi z_i^{j_i}, \sum_{i\in\mathbb{K}, j_i\in\mathbb{N}}^{\sum j_i=2} P_{\{J_I\}}\Pi z_i^{j_i}, \sum_{i\in\mathbb{K}, j_i\in\mathbb{N}}^{\sum j_i=2} Q_{\{J_I\}}\Pi z_i^{j_i} \Bigg]',$$

with set $\mathbb{K} = \{1, 2, 3, 4, 5, 6\}$, $\{J_I\} = j_1 j_2 j_3 j_4 j_5 j_6$.

3. Calculate the local stable manifold M^s.

   By stable manifold theorem, let

$$
\begin{aligned}
z_6(t) &= H(z_1(t), z_2(t), z_3(t), z_4(t), z_5(t)) \\
&= h_{20000} z_1(t)^2 + h_{02000} z_2(t)^2 + h_{00200} z_3(t)^2 + h_{00020} z_4(t)^2 + h_{00002} z_5(t)^2 \\
&\quad + h_{11000} z_1(t) z_2(t) + h_{10100} z_1(t) z_3(t) + h_{10010} z_1(t) z_4(t) + h_{10001} z_1(t) z_5(t) \\
&\quad + h_{01100} z_2(t) z_3(t) + h_{01010} z_2(t) z_4(t) + h_{01001} z_2(t) z_5(t) + h_{00110} z_3(t) z_4(t) \\
&\quad + h_{00101} z_3(t) z_5(t) + h_{00011} z_4(t) z_5(t) + \mathcal{O}(|z_1(t), z_2(t), z_3(t), z_4(t), z_5(t)|^3).
\end{aligned}
$$

Since M_s is invariant, we have

$$
\frac{z_6(t)}{dt} = \frac{dH(z_1(t), z_2(t), z_3(t), z_4(t), z_5(t))}{dt},
$$

then match the coefficients of each term on the both sides of equal sign, we could obtain $h_{k_1 k_2 k_3 k_4 k_5} (k_{i\{i=1,\ldots,5\}} \in \mathbb{N} \,\&\, \sum_{i=1}^{5} k_i = 2)$ in term of $\lambda_i (i = 1, ..., 6)$ and $Q_{\{j_1 j_2 j_3 j_4 j_5 j_6\}} (j_i \in \mathbb{N} \,\&\, \sum_{i=1}^{6} j_i = 2)$:

$$
\begin{aligned}
&h_{20000} = \tfrac{Q_{200000}}{2\,\lambda_1 - \lambda_6}, \quad h_{02000} = \tfrac{Q_{020000}}{2\,\lambda_2 - \lambda_6}, \quad h_{00200} = \tfrac{Q_{002000}}{2\,\lambda_3 - \lambda_6}, \\
&h_{00020} = \tfrac{Q_{000200}}{2\,\lambda_4 - \lambda_6}, \quad h_{00002} = \tfrac{Q_{000020}}{2\,\lambda_5 - \lambda_6}, \quad h_{11000} = \tfrac{Q_{110000}}{\lambda_1 + \lambda_2 - \lambda_6}, \\
&h_{10100} = \tfrac{Q_{101000}}{\lambda_1 + \lambda_3 - \lambda_6}, \quad h_{10010} = \tfrac{Q_{100100}}{\lambda_1 + \lambda_4 - \lambda_6}, \quad h_{10001} = \tfrac{Q_{100010}}{\lambda_1 + \lambda_5 - \lambda_6}, \\
&h_{01100} = \tfrac{Q_{011000}}{\lambda_2 + \lambda_3 - \lambda_6}, \quad h_{01010} = \tfrac{Q_{010100}}{\lambda_2 + \lambda_4 - \lambda_6}, \quad h_{01001} = \tfrac{Q_{010010}}{\lambda_2 + \lambda_5 - \lambda_6}, \\
&h_{00110} = \tfrac{Q_{001100}}{\lambda_3 + \lambda_4 - \lambda_6}, \quad h_{00101} = \tfrac{Q_{001010}}{\lambda_3 + \lambda_5 - \lambda_6}, \quad h_{00011} = \tfrac{Q_{000110}}{\lambda_4 + \lambda_5 - \lambda_6}.
\end{aligned}
\tag{5.35}
$$

Then the local stable manifold M_s is

$$
\begin{aligned}
z_6(t) = {} & \frac{Q_{200000}}{2\,\lambda_1 - \lambda_6} z_1(t)^2 + \frac{Q_{020000}}{2\,\lambda_2 - \lambda_6} z_2(t)^2 + \frac{Q_{002000}}{2\,\lambda_3 - \lambda_6} z_3(t)^2 + \frac{Q_{000200}}{2\,\lambda_4 - \lambda_6} z_4(t)^2 \\
& + \frac{Q_{000020}}{2\,\lambda_5 - \lambda_6} z_5(t)^2 + \frac{Q_{110000}}{\lambda_1 + \lambda_2 - \lambda_6} z_1(t) z_2(t) + \frac{Q_{101000}}{\lambda_1 + \lambda_3 - \lambda_6} z_1(t) z_3(t) \\
& + \frac{Q_{100100}}{\lambda_1 + \lambda_4 - \lambda_6} z_1(t) z_4(t) + \frac{Q_{100010}}{\lambda_1 + \lambda_5 - \lambda_6} z_1(t) z_5(t) + \frac{Q_{011000}}{\lambda_2 + \lambda_3 - \lambda_6} z_2(t) z_3(t) \\
& + \frac{Q_{010100}}{\lambda_2 + \lambda_4 - \lambda_6} z_2(t) z_4(t) + \frac{Q_{010010}}{\lambda_2 + \lambda_5 - \lambda_6} z_2(t) z_5(t) + \frac{Q_{001100}}{\lambda_3 + \lambda_4 - \lambda_6} z_3(t) z_4(t) \\
& + \frac{Q_{001010}}{\lambda_3 + \lambda_5 - \lambda_6} z_3(t) z_5(t) + \frac{Q_{000110}}{\lambda_4 + \lambda_5 - \lambda_6} z_4(t) z_5(t) \\
& + \mathcal{O}(|z_1(t), z_2(t), z_3(t), z_4(t), z_5(t)|^3). \qquad (5.36)
\end{aligned}
$$

Now we choose a set of parameter values $c = 3$, $b_m = 0.2$, $\delta = 0.53$, $d_l = 0.6$, $\kappa = 0.011$, $\beta_m = 0.04$, $A = 5$, $d_m = 0.018$, $r_b = 1.3$, $\beta_b = 0.8$, $d_b = 0.0001$, $\mu = 0.15$, $\gamma = 0.1$. By Theorem 5.3.1 and Theorem 5.3.2, the system has a locally stable disease free equilibrium $E_1 = (1503.333334, 44264.81482, 0, 13000, 0, 0)$ and two endemic equilibria, $E^- = (1503.333334, 44262.94641, 1.86842, 10296.04958, 1.081147708, 1081.147708)$ is unstable and $E^+ = (1503.333334,\ 44260.1706,\ 4.64423,\ 7329.212192,\ 2.26740816,\ 2267.40816)$ is locally stable. By (5.36), we could determine the local stable manifold M_s at E^- and it is approximated as

$$
\begin{aligned}
\widetilde{\Phi}(L, S_m, I_m, S_b, I_b, R_b) = {} & -2.097324027 \times 10^{-7} I_b I_m - 5.243309986 \times 10^{-7} I_m R_b \\
& - 5.499881399 \times 10^{4} I_b - 1.764578440 \times 10^{-8} L + 1.357368031 \times 10^{-12} L S_b
\end{aligned}
$$

$$
\begin{aligned}
&- 9.8081782918 \times 10^{-20} I_m L - 1.140726416 \times 10^{-4} S_m - 5.499881422 \times 10^{4} S_b \\
&- 2.097323995 \times 10^{-7} I_m S_b + 10.57669504 R_b S_b + 1.357368028 \times 10^{-12} I_b L \\
&- 3.66040946 \times 10^{-23} L S_m + 10.576695 \times I_b R_b - 1.37497035510^{5} R_b \\
&+ 2.115339009 S_b^2 - 6.429287425 \times 10^{-23} L^2 + 8.774818569 \times 10^{-11} I_b S_m \\
&+ 2.115338991 I_b^2 - 6.32165998 \times 10^{-18} I_m S_m - 7.772186201 \times 10^{-15} I_m^2 \\
&+ 13.2208688 R_b^2 - 1.106445065 \times 10^{-21} S_m^2 + 2.726521193 \times 10^{-3} I_m \\
&+ 2.193704647 \times 10^{-10} R_b S_m + 8.774818586 \times 10^{-11} S_b S_m + 4.230678 I_b S_b \\
&+ 3393.420078 L R_b + 3.574922924 \times 10^{8} + \mathcal{O}(|L, S_m, I_m, S_b, I_b, R_b|^3) = 0. \qquad (5.37)
\end{aligned}
$$

The local stable manifold M_s separates the space $\{(L, S_m, I_m, S_b, I_b, R_b) | L > 0, S_m > 0, I_m > 0, S_b > 0, I_b > 0, R_b > 0\}$ into three parts: I $= \{(L, S_m, I_m, S_b, I_b, R_b) | (L, S_m, I_m, S_b, I_b, R_b) > \mathbf{0}$ & $\widetilde{\Phi}(L, S_m, I_m, S_b, I_b, R_b) > 0\}$, II $= \{(L, S_m, I_m, S_b, I_b, R_b) | (L, S_m, I_m, S_b, I_b, R_b) > \mathbf{0}$ & $\widetilde{\Phi}(L, S_m, I_m, S_b, I_b, R_b) < 0\}$ and $M_s = \{(L, S_m, I_m, S_b, I_b, R_b) | (L, S_m, I_m, S_b, I_b, R_b) > \mathbf{0}$ & $\widetilde{\Phi}(L, S_m, I_m, S_b, I_b, R_b) = 0\}$ itself.

When the initial point is in I, the trajectory will go to endemic equilibrium E^+, when the initial point is in II, the trajectory will approach the S_b-$axis$, which means the disease will die out. Then we could define I as the region with high risk of infections, contrarily, II as the region with low risk of infections.

Risk Assessment Criteria

To evaluate the intensity of the virus transmission, based on transmission model (5.1), if

1. $R_0 > 1$, the risk level is high;

2. $R_0 < 1$ & initial values are in $\text{I} = \{(L, S_m, I_m, S_b, I_b, R_b) | (L, S_m, I_m, S_b, I_b, R_b) > \mathbf{0}$ & $\widetilde{\Phi}(L, S_m, I_m, S_b, I_b, R_b) > 0\}$, the risk level is high;

3. $R_0 < 1$ & initial values are in $\text{II} = \{(L, S_m, I_m, S_b, I_b, R_b) | (L, S_m, I_m, S_b, I_b, R_b) > \mathbf{0}$ & $\widetilde{\Phi}(L, S_m, I_m, S_b, I_b, R_b) < 0\}$, the risk level is low.

5.4 Risk assessments

True Infection Rate (IR) can be determined by testing individual mosquitoes but this is time-consuming and expensive. Instead, testing sets of pooled mosquitoes of the same species is an easier and more cost-effective approach. A common practice of testing sets of pooled mosquitoes is using Minimum infection rate (MIR) to estimate infection rate (Condotta et al. (2004)). MIR is calculated (Rao and Durvasula (2013), Mullen and Durden (2009), Centers for Disease Control and Prevention (2015b), Public Health Ontario (2018)):

$$MIR = \frac{Number\ of\ positive\ pools}{Number\ of\ mosquitoes\ tested} \times 1000.$$

It is the simplest estimate and by definition, MIR aims at defining the lower limit of infection rate. When infection rates are low and/or pool size small, MIR provides good

estimates of the true infection rate because one makes an assumption that a positive pool contains only one infected mosquito or the chance of more than one infected individual in a positive pool is negligible (Centers for Disease Control and Prevention (2015b), Gu et al. (2004), Walter et al. (1980), Gu et al. (2003)). MIR has been widely used for WNV by public health and researchers (Centers for Disease Control and Prevention (2015b), Bernard et al. (2001), Kulasekera et al. (2001), Rutledge et al. (2003), Gu and Novak (2004), etc).

The basic reproduction number R_0 of WNV gives the expected number of new infections produced by a single infective mosquito or bird when introduced into a susceptible population, and is used to measure the transmission potential of a disease (van den Driessche and Watmough (2002), Bowman et al. (2005), Bacaer (2007), Dietz (1993), etc). The magnitude of R_0 allows one to determine the amount of effort which is necessary either to prevent an epidemic or to eliminate an infection from a population (Dietz (1993)).

By (5.3), we have known the first term under the square root of R_0 represents the number of susceptible mosquitoes become infected when introducing one infective bird (denoted as $1_{I_{b_0}}$), the second term represents the number of bird infections by one infective mosquito (denoted as $1_{I_{m_0}}$). R_0 is calculated at disease free equilibrium, that is at initial time $t = 0$, all birds and all mosquitoes are susceptible, namely $N_{b_0} = \frac{r_b}{d_b} = S_{b_0}$ and

$N_{m_0} = S_{m_0}$. Then we can rewrite the basic reproduction number as

$$R_0 = \sqrt{\frac{1_{I_{b_0}} b_m \beta_m \frac{S_{m_0}}{N_{b_0}+A}}{(\mu+\gamma+d_b)} \frac{1_{I_{m_0}} b_m \beta_b \frac{S_{b_0}}{N_{b_0}+A}}{d_m}}, \tag{5.1}$$

5.4.1 Novel risk index $R_{risk}(t)$

Analogously, we develop a novel index serving as an indicator of risk of infection at any time t. Furthermore, $I_m(t)$, $I_b(t)$ are infective mosquitoes and birds at time t respectively, $N_b(t)$ is total number of birds at time t. One susceptible mosquito and bird are denoted as 1_{s_m} and 1_{s_b} respectively.

$$\begin{aligned} R_{risk}(t) &= \sqrt{\frac{I_b(t) b_m \beta_m \frac{1_{s_m}}{N_b(t)+A}}{(\mu+\gamma+d_b)} \frac{I_m(t) b_m \beta_b \frac{1_{s_b}}{N_b(t)+A}}{d_m}}, \\ &= \sqrt{\frac{I_b(t) b_m \beta_m}{(\mu+\gamma+d_b)(N_b(t)+A)} \frac{I_m(t) b_m \beta_b}{d_m (N_b(t)+A)}}. \end{aligned} \tag{5.2}$$

$R_{risk}(t)$ can be served to describe the expected number of infections distributed to infect a single susceptible individual, namely to evaluate the potential of an individual becoming an infection at time t. The first term under the square root represents that one susceptible mosquito in what manner to become infectious when there are $I_b(t)$ infectious birds. The second term performs as the potential of a susceptible bird getting infected when surrounded by $I_m(t)$ number infectious mosquitoes. Then the square root provides the geometric mean for an average individual of both species combined.

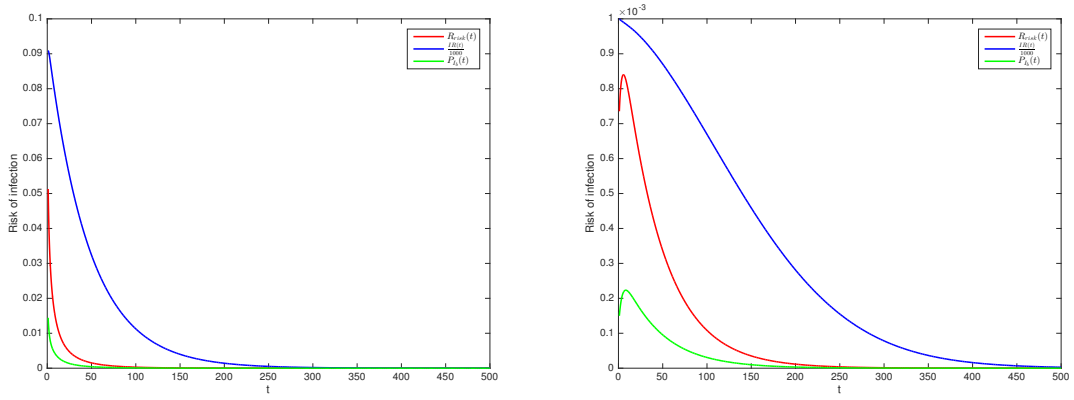

(a) Case 1 (b) Case 2

Figure 5.7: Comparison of $R_{risk}(t)$ and $IR(t)$

Here we will compare $R_{risk}(t)$ and $IR(t)$ based on model (5.1). Apparently by definition, $IR(t) = \frac{I_m(t)}{N_m(t)}$, where $N_m(t)$ is total female mosquito population. We also introduce WNV infection in the bird population, i.e. proportion of infectious birds $P_{I_b}(t) = \frac{I_b(t)}{N_b(t)}$.

Fig. 5.7(a) indicates that $R_{risk}(t)$ and $IR(t)$ have the same trend to depict the risk of WNV transmission, that is the risk declines as time goes on. Also, the proportion of infectious birds $P_{I_b}(t)$ has this decreasing trend. In Fig. 5.7(b), the overall trend of $R_{risk}(t)$, same as $IR(t)$, is decreasing. However, at the initial time period, $IR(t)$ declines directly, while $R_{risk}(t)$ increases first, then it begins to decrease, in accordance with the trend of $P_{I_b}(t)$. Facing the situation that the infection rate of mosquitoes mildly decrease while the percentage of infectious birds increases sharply, it is improper to come to the conclusion that the risk of WNV infection is decreasing. Hence only the infection rate

being an indicator of risk is not enough.

By the definition (5.2) and simulation (Fig. 5.7), one can figure out that the novel index $R_{risk}(t)$ reveals the information of the prevalence of WNV infection in both mosquito and bird populations. Furthermore, rewrite $R_{risk}(t)$ in the form

$$R_{risk}(t) = \sqrt{\frac{b_m^2 \beta_m \beta_b}{d_m(\mu+\gamma+d_b)} \frac{I_m(t)}{N_m(t)} \frac{I_b(t)}{N_b(t)+A} \frac{N_m(t)}{N_b(t)+A}},$$

and denote $\alpha = \frac{b_m^2 \beta_m \beta_b}{d_m(\mu+\gamma+d_b)}$, $r_{I_b h}(t) = \frac{I_b(t)}{N_b(t)+A}$ and $r_{mh}(t) = \frac{N_m(t)}{N_b(t)+A}$, the relationship between $R_{risk}(t)$ and $IR(t)$ is

$$R_{risk}(t) = \sqrt{\alpha \cdot IR(t) \cdot r_{I_b h}(t) \cdot r_{mh}(t)}. \tag{5.3}$$

For $R_{risk}(t)$, $IR(t)$ is used in conjunction with parameter α, the ratio of infectious birds to total hosts $r_{I_b h}(t)$ and the ratio of total female mosquitoes to total hosts $r_{mh}(t)$ when evaluating local WNV activity patterns. $R_{risk}(t)$, a more informative index, can also serve as a public health measure to evaluate WNV severity.

Usually, public health use MIR to estimate the infection rate IR. Replacing $IR(t)$ in (5.3) by $MIR(t)$, we obtain a special case

$$\mathbf{R}_{risk}(t) = \sqrt{\alpha \cdot MIR(t) \cdot r_{I_b h}(t) \cdot r_{mh}(t)}. \tag{5.4}$$

5.4.2 Risk assessment criteria

Another approach to evaluate the severity of WNV transmission is based on the risk assessment criteria in Section 5.3.5, we apply the risk assessment criteria to the GTA to verify the occurrence of the WNV outbreaks. In particular, the criteria is carried out based on the comprehensive model (5.1) and corresponding $\widetilde{\Phi}(L, S_m, I_m, S_b, I_b, R_b)$ in (5.37) is used. The sign of $\widetilde{\Phi}(L, S_m, I_m, S_b, I_b, R_b)$ depends on the values of L, S_m, I_m, S_b, I_b and R_b.

To obtain the sign of $\widetilde{\Phi}(L, S_m, I_m, S_b, I_b, R_b)$, the ideal situation is directly substitute collected data of each compartment. However, this cannot be realized due to the lack of available data for all compartments. We deal with this case by using ratios among mosquitoes and birds. Denote $N_m : N_b = p_{mb}$, $L : N_m = p_{lm}$, $I_m : N_m = p_{im}$, $I_b : N_b = p_{ib}$ and $R_b : N_b = p_{rb}$, then the local stable manifold M_s (5.37) is equivalent to

$$\widetilde{\Phi}(N_b, p_{mb}, p_{lm}, p_{im}, p_{ib}, p_{rb}) = 0 \tag{5.5}$$

with

$$\widetilde{\Phi}(N_b, p_{mb}, p_{lm}, p_{im}, p_{ib}, p_{rb}) \tag{5.6}$$

$$\begin{aligned} &= 9.804517882 \times 10^{-5}\, p_{im}\, p_{lm} {p_{mb}}^2 Nb^2 - 2.036052047 \times 10^{3}\, p_{lm}\, p_{mb} p_{rb}\, Nb^2 \\ &\quad + 3.147302214 \times 10^{8}\, p_{im}\, p_{mb} p_{rb}\, Nb^2 - 1.316222788 \times 10^{5}\, p_{rb} p_{mb}\, Nb^2 \\ &\quad + 6.429287425 \times 10^{-8}\, {p_{lm}}^2 {p_{mb}}^2 Nb^2 - 2.727661919 \times 10^{12}\, p_{im}\, p_{mb}\, Nb \end{aligned} \tag{5.7}$$

$$+ 0.631944709 \times 10^{-2}\, p_{im}\, {p_{mb}}^2 Nb^2 + 3.21414\, p_{ib}\, p_{im}\, p_{mb} Nb^2 - 8.7748186 \times 10^5 p_{mb} N_b^2$$

$$+ 2.098201477 \times 10^8\, p_{im}\, p_{mb}\, Nb^2 + 1.106445065 \times 10^{-6}\, {p_{mb}}^2 Nb^2 + 1.8 \times 10^7\, p_{ib}\, Nb^2$$

$$- 4.759512769 \times 10^{15}\, {p_{rb}}^2 Nb^2 - 6.346017022 \times 10^{15}\, p_{rb}\, Nb^2 - 2.3 \times 10^{11}\, p_{ib}\, Nb$$

$$- 1.357368031 \times 10^3\, p_{lm}\, p_{mb}\, Nb^2 - 2.115339009 \times 10^{15}\, Nb^2 + 2.2 \times 10^7\, p_{ib} p_{rb}\, Nb^2$$

$$+ 7.765865647\, {p_{im}}^2 {p_{mb}}^2 Nb^2 + 1.76457844 \times 10^7\, p_{lm}\, p_{mb}\, Nb + 1.7 \times 10^{-4}\, p_{ib} p_{mb}\, Nb^2$$

$$+ 1.140726416 \times 10^9\, p_{mb}\, Nb + 8.249822128 \times 10^{19}\, p_{rb}\, Nb + 5.499881422 \times 10^{19}\, Nb$$

$$+ 3 \times 10^{-6}\, p_{ib}\, p_{lm}\, p_{mb} Nb^2 + 3.66040946 \times 10^{-8}\, p_{lm}\, {p_{mb}}^2 Nb^2 - 3.574922924 \times 10^{23}$$

$$+ \mathcal{O}(|p_{lm} p_{mb} N_b, (1 - p_{im}) p_{mb}\, Nb, p_{im}\, p_{mb}\, Nb, (1 - p_{ib} - p_{rb}) N_b, p_{ib} N_b, p_{rb} N_b|^3).$$

Usually, the ratio of mosquito population to bird population, the ratio of preadult mosquitoes to adult mosquitoes and the total population size of bird in a region during the same time period (such as July) are not change much year. Then we fix these three variables and obtain the following local stable manifold M_s

$$\widetilde{\Phi}(p_{im}, p_{ib}, p_{rb}) = 0 \tag{5.8}$$

with

$$\widetilde{\Phi}(p_{im}, p_{ib}, p_{rb})$$

$$= 2.832571993 \times 10^{23} p_{im} p_{rb} - 3.25491161 \times 10^{24} p_{rb} + 1.078963694 \times 10^{23} p_{im}$$

$$+ 6.989279082 \times 10^{21} {p_{im}}^2 - 4.283561492 \times 10^{24} {p_{rb}}^2 + 1.98 \times 10^{16} p_{ib} p_{rb}$$

$$- 6.125136134 \times 10^{23} + 9.327153 \times 10^{15} p_{ib} + 2.892726 \times 10^{15} p_{ib} p_{im}. \qquad (5.9)$$

By the Risk Assessment Criteria, when $R_0 < 1$, we need to check the sign of $\widetilde{\Phi}(p_{im}, p_{ib}, p_{rb})$ (5.9), where both mosquito data as well as bird data is needed. Then we verify the criteria using seven years data from 2002 to 2008 since no bird data is available after 2008. To use the risk assessment criteria, the results greatly depend on the initial states of variables. Here, we use the mosquito and bird data in July as the initial values since the increase of mosquito population noticeably starts in July (Wang et al. (2017)) and infected mosquito data is first collected in July. The proportion of recovered birds are relatively small (since vectors begin to increase and are not enough to transmit WNV in July, the infected birds are relative less, let alone recovered birds), then we assign a very small value for the ratio of the recoveries birds to the total bird population. Then we use data in July in Fig. 5.8 and the risk assessment criteria to predict the WNV outbreak, where the positive sign of $\widetilde{\Phi}$ (when $R_0 < 1$) serves as an early warning signal for the WNV outbreaks.

From Fig. 5.8, both bird and mosquito infections in 2002 and 2005 are apparently more than the other years, the basic reproduction number can be greater than one in other modellings, directly indicating the occurrence of WNV outbreaks. While for the other years (2003, 2004, 2006-08), R_0 is not enough to be used for early warning of outbreaks, then predictions need to be made by the sign of $\widetilde{\Phi}$ based on the second case of the risk assessment criteria. Here, our model is set up with the basic reproduction $R_0 < 1$, and we

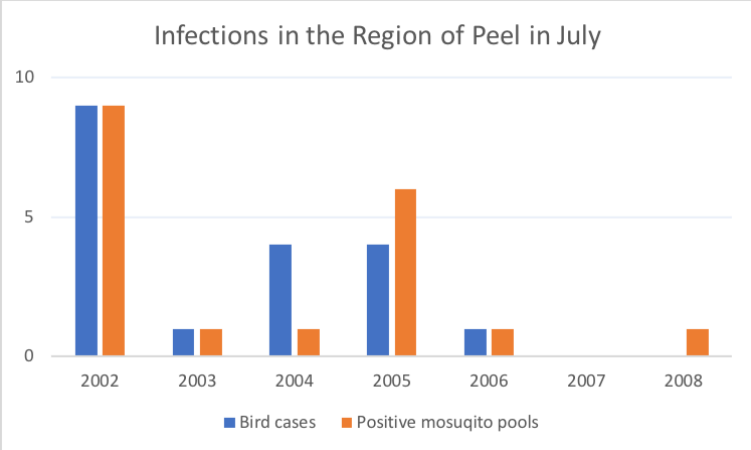

Figure 5.8: Yearly WNV bird infections and positive mosquito pools in July, Region of Peel, 2002-2008

will do predictions based on the sign of $\widetilde{\Phi}$ for all seven years (including 2002 and 2005) and results is shown by sign function in terms of $\widetilde{\Phi}$ (Fig. 5.9).

The results indicate the high risk that WNV outbreaks would occur in 2002, 2003 and 2005, which is consistent in the real situations that outbreaks really occurred in these four years (shown in Fig. 5.10, where mosquito data and bird data is stacked each year providing a more apparent verification). Hence the risk assessment criteria are a good tool to predict and serving as an early warning signal for the WNV outbreaks. Even though the initial infection states in the year 2003, 2004 and 2006 and 2008 are very similar, the predicted results obtained using the Risk Assessment Criteria are different. Our criteria not only reflects the dependence on the initial states but also characterizes the mechanism

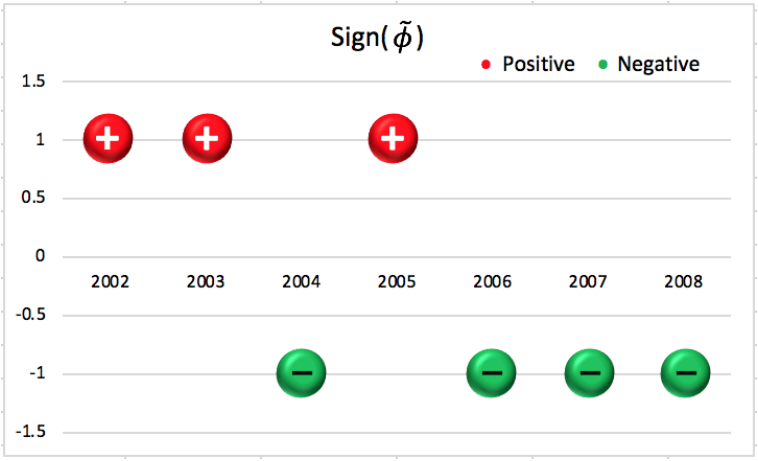

Figure 5.9: The sign of $\widetilde{\Phi}$ using data in July as initial values, Region of Peel, 2002-2008; red bubble represents $\widetilde{\Phi} > 0$ and indicates the risk level of outbreak occurring is high, green bubble represents $\widetilde{\Phi} < 0$ and indicates the risk level of outbreak occurring is low.

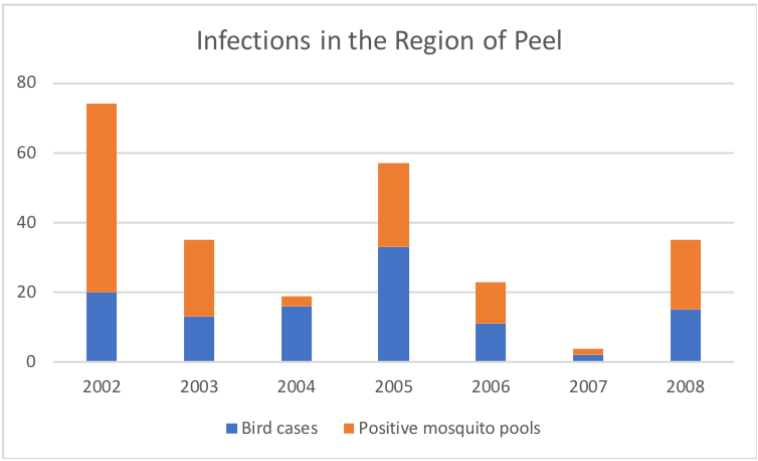

Figure 5.10: Yearly WNV bird infections and positive mosquito pools (stacked column), Region of Peel, 2002-2008

of outbreaks occurring, its predicted results are accurate and can be regarded as a new reliable tool in the WNV surveillance program.

Moreover, we apply the risk assessment criteria to all five regions in the GTA and compare the results with corresponding annual MIR from 2002 to 2008 (Fig. 5.11). Usually, positive mosquitoes are detected and collected in July and can be directly used, with some exception, such as Halton region's in 2004. For these cases, the initial values based on July's is not enough, the data of a week in which positive mosquitoes are first collected is used by averaging it. For instance, the first collected positive mosquito data (denoted as M_{+H04}) in 2004 in Halton was obtained in the third week of August, then the initial value of positive mosquitoes for Halton region in 2004 is chosen as $M_{+H04}/3$. Each region has its own risk assessment criteria due to the difference in abundance and distribution of vectors and hosts, thus we can compare the results for the same region in different years. Based on the risk assessment criteria, the positive sign of $\widetilde{\Phi}$ indicates a high level for the occurrence of an outbreak, generally in accordance with a larger MIR result correspondingly. There are some exceptions, for the Region of York in 2003, the MIR result and annual infections (Fig. 5.12(d)) reveal a high WNV intensity, while the risk assessment criteria result is not. One possible reason is that the lack of initial positive mosquito data in July and August in 2003 in York leading to this inaccurate indication. In the year of 2007 in the city Toronto, the Region of Halton and the Region of Peel, the results based

Region / Year	Toronto		Durham		Halton		Peel		York	
	$sign(\tilde{\phi})$	MIR	$sign(\tilde{\phi})$	MIR	$sign(\tilde{\phi})$	MIR	$sign(\tilde{\phi})$	MIR	$sign(\tilde{\phi})$	MIR
2002	+	36.75	+	66.67	+	11.68	+	18.63	+	9.1
2003	+	11.87	+	50	+	10.23	+	16.82	−	8.7
2004	+	5.51	+	4.27	−	5.74	−	5.46	−	0
2005	+	13.96	+	13.64	+	12.64	+	5.89	+	8.06
2006	+	7.67	+	13.07	−	5.74	−	5.41	+	4.38
2007	−	7.93	−	0	−	13.3	−	9.09	−	0
2008	−	3.29	−	0	−	4.75	−	2.83	−	3.55

Figure 5.11: The comparison of the results based on risk assessment criteria and yearly MIR in five regions of the GTA, 2002-2008

on the risk assessment criteria indicate a low risk level for an outbreak occurring, while the MIR results (compared with other years' results) are relatively large. To look into the contradictory results, we present annual infections in these three regions in Fig. 5.12(a) - Fig. 5.12(c), we obtain that infections in these regions in 2007 are in small numbers, hence our risk assessment criteria provides more accurate results.

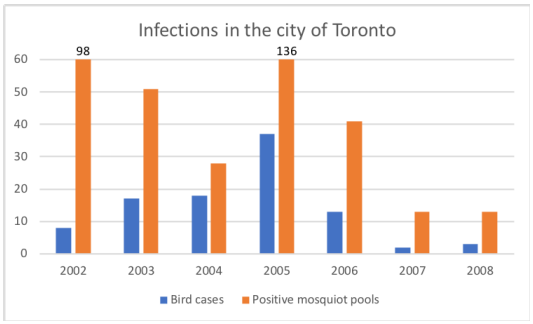

(a)

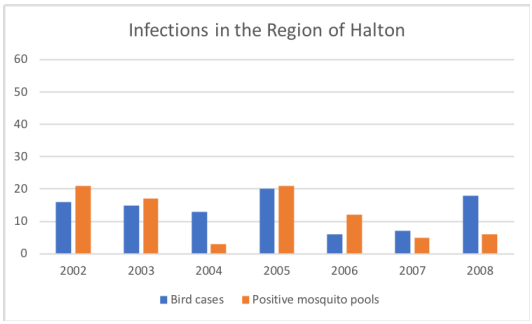

(b)

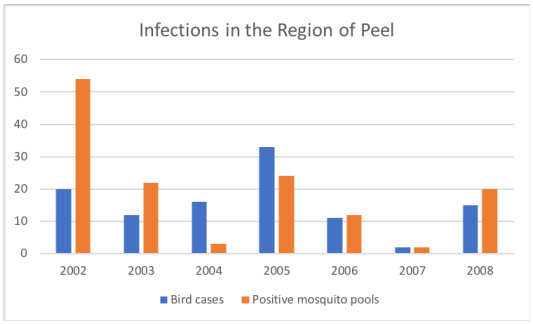

(c)

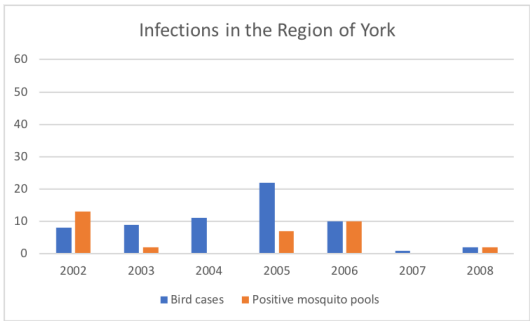

(d)

Figure 5.12: Yearly WNV bird infections and positive mosquito pools in the GTA, 2002-2008.

6 Conclusions and future work

Mosquito-borne diseases, such as WNV, dengue, and Zika virus, have become a significant global health burden for human society. Complex factors, including weather conditions, anthropogenic land use and vector-virus-host interactions, greatly affect the mosquito abundance and distribution, and the disease transmission process as well. Thus studying the mosquito population dynamics and transmission dynamics of MBDs, understanding how these factors play roles in the MBDs is of great significance. We use WNV and *Culex* mosquitoes (WNV vectors) in the Region of Peel, Ontario, Canada, as an example for this research study.

We introduce the background of MBDs, particularly WNV, and current mathematical modelling of mosquitoes and transmissions in Chapter 1. In Chapter 2, we study single-species population models for the mosquito and the bird respectively. For mosquitoes, the blood resources are indispensable for the reproduction, which is worth considering to estimate mosquito abundance. We first summarize the host feeding preferences of mosquitoes, then we propose a general aquatic-aerial two stages mosquito population model. In the

model, we take into account the contribution of the mosquito feeding preference to the oviposition rate and the intraspecific competition among preadult mosquitoes. We obtained that relative high birth rate can ensure the survival of mosquitoes and intraspecific competition exerts an opposite effect for the growth and development of mosquitoes. For birds, we summarize the role of birds in the transmission of WNV, in particular, the impacts of bird species, migration and age states on the transmission. To explore the influence of WNV on bird populations, we build a bird population model considering the horizontal transmission of WNV and reveal that positive equilibrium exists and is locally stable when the basic reproduction number is greater than one.

For the model estimating the population size of *Culex* mosquitoes in Chapter 3, we define an effective trapping zone of a CDC light trap and propose a model to predict real mosquito populations in the surrounding area. In our model, we consider the trapping mechanism of a CDC light trap and collecting procedure and used the trap counts in the Region of Peel to develop and validate the model. This type of modelling is useful for predictions of the mosquito population for control measures in public health practice. This work has also considered the temperature, precipitation, and mosquito feeding preference factors.

In Chapter 4, we establish single-season WNV transmission dynamical models and find that moderate temperature and precipitation will increase the potential of the basic

reproduction number being greater than one, increasing the mosquito population and consequently the potential for an outbreak of WNV. On the contrary, an excess of precipitation will control the vector population and reduce the peak value of infectious mosquitoes and birds. A smaller intraspecific competition rate (an indicator of the SWMP properties) leads to a larger mosquito population and more infectious birds and mosquitoes. This work can be used to guide WNV programs in local health units where monitoring standing water and larviciding is often used to control mosquito populations and the spread of WNV.

Based on the WNV transmission model in the previous chapter, we improve and build compartmental models to investigate backward bifurcation and threshold dynamics for the WNV outbreaks in Chapter 5. The existence of backward bifurcation reveals that the basic reproduction number less than one is not enough to prevent the WNV outbreak occurring. Then we propose new approaches to characterize the potential risk of infections and an early warning for an outbreak. We develop a novel risk index R_{risk}, a more comprehensive tool compared to infection rate, to evaluate the local WNV activity patterns. In addition, we set up a risk assessment criteria: the basic reproduction number R_0 greater than one still indicates a high risk level for the occurrence of WNV outbreaks; when R_0 is less than one, there are two possible results as well, that is, the high level or the low level. Whether the level is high or low is determined by the initial states of vectors and hosts, whether they enter into the high risk region I or in the low risk region II, in other words, risk levels

depend on the sign of $\widetilde{\Phi}$ we established. Then we apply the risk assessment criteria to the GTA and verify the evaluation results based on the criteria is consistent with MIR results. In the end, we conclude the entire research dissertation and give some prospective points for the future work of this research in Chapter 6.

In the dissertation, using the WNV as an example, we have modelled, analyzed, predicted and controlled the transmission dynamics of mosquito-borne diseases. In addition to what we have done, there still are some extensions and improvements are worth taking into account in the future work.

Firstly, besides temperature and precipitation, other factors influence mosquito abundance and WNV transmission. For example, wind patterns, elevation and landscape impact the efficiency of traps, the mosquito abundance as well as the transmission. These factors will be considered in the model estimating mosquito population in Chapter 2 and the WNV transmission model in Chapter 3 and Chapter 4 in the future.

Secondly, we will make collaboration with the Wild Life to provide a better estimation of mosquito populations. When the data of host distribution and the population is available, we can incorporate bird data as well as traps count data into the mosquito population model in Chapter 3 to predict true mosquito abundance in different regions. Also, the model output in Chapter 4 is not validated due to the lack of available infection data for birds, additional research needs to be conducted in the future to overcome this issue.

Thirdly, an extension of bird migration such as seasonal migratory movements of birds, more than just constant migration is worth further investigations in Chapter 2 and Chapter 5. The classification of birds based on their capability of transmitting virus or age states needs to be considered as well.

Fourthly, we will enhance the collaboration with public health, using our models and surveillance program data for the predictions and helping them make decisions on the control of vectors and prevention of diseases. Also, we will use the observed surveillance data to improve the accuracy of our models.

Lastly, the extending of the mosquito model and transmission models to estimate the population of other mosquito species such as *Anopheles* and *Aedes* species, to study other mosquito-borne diseases such as Malaria, Zika and Dengue fever can be taken into account.

Bibliography

Abdelrazec, A., Bélair, J., Shan, C., and Zhu, H. (2016). Modeling the spread and control of dengue with limited public health resources. *Mathematical Biosciences*, 271:136–145.

Abdelrazec, A., Lenhart, S., and Zhu, H. (2014). Transmission dynamics of West Nile virus in mosquitoes and corvids and non-corvids. *Journal of Mathematical Biology*, 68(6):1553–1582.

Agnew, P., Haussy, C., and Michalakis, Y. (2000). Effects of density and larval competition on selected life history traits of *Culex pipiens quinquefasciatus* (Diptera: Culicidae). *J. Med. Entomol*, 37(5):732–735.

Agnew, P., Hide, M., Sidobre, C., and Michalakis, Y. (2002). A minimalist approach to the effects of density-dependent competition on insect life-history traits. *Ecological Entomology*, 27(4):396–402.

Amundsen, P.-A., Knudsen, R., and Klemetsen, A. (2007). Intraspecific competition and density dependence of food consumption and growth in Arctic charr. *Journal of Animal Ecology*, 76(1):149–158.

Bacaer, N. (2007). Approximation of the basic reproduction number R_0 for vector-borne diseases with a periodic vector population. *Bulletin of Mathematical Biology*, 69(3):1067–1091.

Begon, M., Townsend, C. R., and Harper, J. L. (2006). *Ecology: from individuals to ecosystems*. Number Sirsi) i9781405111171.

Bennett, R. S., Cress, C. M., Ward, J. M., Firestone, C.-Y., Murphy, B. R., and Whitehead, S. S. (2008). La Crosse virus infectivity, pathogenesis, and immunogenicity in mice and monkeys. *Virology Journal*, 5(1):25.

Bernard, K. A., Maffei, J. G., Jones, S. A., Kauffman, E. B., Ebel, G., Dupuis 2nd, A., Ngo, K. A., Nicholas, D. C., Young, D. M., Shi, P.-Y., et al. (2001). West Nile virus infection in birds and mosquitoes, New York State, 2000. *Emerging Infectious Diseases*, 7(4):679.

Blayneh, K. W., Gumel, A. B., Lenhart, S., and Clayton, T. (2010). Backward bifurcation and optimal control in transmission dynamics of West Nile virus. *Bulletin of Mathematical Biology*, 72(4):1006–1028.

Bowman, C., Gumel, A., van den Driessche, P., Wu, J., and Zhu, H. (2005). A mathematical model for assessing control strategies against West Nile virus. *Bulletin of Mathematical Biology*, 67(5):1107–1133.

Brown, H. E., Paladini, M., Cook, R. A., Kline, D., Barnard, D., and Fish, D. (2008). Effectiveness of mosquito traps in measuring species abundance and composition. *Journal of Medical Entomology*, 45(3):517–521.

Burkett, D. A., Lee, W. J., Lee, K. W., Kim, H. C., Lee, H. I., Lee, J. S., Shin, E., Wirtz, R. A., Cho, H. W., Claborn, D. M., et al. (2001). Light, carbon dioxide, and octenol-baited mosquito trap and host-seeking activity evaluations for mosquitoes in a malarious area of the Republic of Korea. *Journal of the American Mosquito Control Association*, 17(3):196–205.

Burkett-Cadena, N. D., Graham, S. P., Hassan, H. K., Guyer, C., Eubanks, M. D., Katholi, C. R., and Unnasch, T. R. (2008). Blood feeding patterns of potential arbovirus vectors of the genus *Culex* targeting ectothermic hosts. *The American Journal of Tropical Medicine and Hygiene*, 79(5):809–815.

Bustamante, D. M. and Lord, C. C. (2010). Sources of error in the estimation of mosquito infection rates used to assess risk of arbovirus transmission. *The American Journal of Tropical Medicine and Hygiene*, 82(6):1172–1184.

Caillout, K., Robertson, C., Wheeler, D., Komar, N., and Bulluck, L. (2013a). Vector contact rates on Eastern bluebird nestlings do not indicate West Nile virus transmission in Henrico County, Virginia, USA. *International Journal of Environmental Research and Public Health*, 10(12):6366–6379.

Caillout, K. A., Riggan, A. E., Bulluck, L. P., Carlson, J. C., and Sabo, R. T. (2013b). Nesting bird " host funnel " increases mosquito-bird contact rate. *Journal of Medical Entomology*, 50(2):462–466.

Campbell, G. L., Marfin, A. A., Lanciotti, R. S., and Gubler, D. J. (2002). West Nile virus. *The Lancet Infectious Diseases*, 2(9):519–529.

Caraballo, H. and King, K. (2014). Emergency department management of mosquito-borne illness: malaria, dengue, and West Nile virus. *Emergency Medicine Practice*, 16(5):1–23.

Castillo-Chavez, C. and Song, B. (2004). Dynamical models of tuberculosis and their applications. *Mathematical Biosciences and Engineering*, 1(2):361–404.

Centers for Disease Control and Prevention (2015a). Mosquito light trap. Available at `https://www.cdc.gov/museum/history/mosquito.html`.

Centers for Disease Control and Prevention (2015b). Mosquito surveillance software. Available at `https://www.cdc.gov/westnile/resourcepages/mosqsurvsoft.html`.

Centers for Disease Control and Prevention (2015c). West Nile virus & dead birds. Available at `https://www.cdc.gov/westnile/faq/deadbirds.html`.

Centers for Disease Control and Prevention (2016a). Emerging infectious diseases. Available at `https://wwwnc.cdc.gov/eid/article/22/10/16-1082_article`.

Centers for Disease Control and Prevention (2016b). Other mosquito-borne diseases. Available at `https://www.cdc.gov/niosh/topics/outdoor/mosquito-borne/other.html`.

Centers for Disease Control and Prevention (2018). Mosquito-borne diseases. Available at `https://www.cdc.gov/niosh/topics/outdoor/mosquito-borne/default.html`.

Centers for Disease Control and Prevention and others (2015). Species of dead birds in which West Nile virus has been detected, United States,1999-2012. *CDC, Atlanta, Georgia: http://www. cdc. gov/westnile/resources/pdfs/birdspecies1999-2012. pdf Accessed*, 20.

Chilaka, N., Perkins, E., and Tripet, F. (2012). Visual and olfactory associative learning in the malaria vector *Anopheles gambiae* sensu stricto. *Malaria Journal*, 11(1):27.

Cianci, D., Broek, J. V. D., Caputo, B., Marini, F., Torre, A. D., Heesterbeek, H., and Hartemink, N. (2013). Estimating mosquito population size from mark–release–recapture data. *Journal of Medical Entomology*, 50(3):533–542.

Ciota, A. T., Drummond, C. L., Ruby, M. A., Drobnack, J., Ebel, G. D., and Kramer, L. D. (2012). Dispersal of *Culex* mosquitoes (Diptera: Culicidae) from a wastewater treatment facility. *Journal of Medical Entomology*, 49(1):35–42.

Condotta, S. A., Hunter, F. F., and Bidochka, M. J. (2004). West Nile virus infection rates in pooled and individual mosquito samples. *Vector-Borne & Zoonotic Diseases*, 4(3):198–203.

Cruz-Pacheco, G., Esteva, L., Montaño-Hirose, J. A., and Vargas, C. (2005). Modelling the dynamics of West Nile Virus. *Bulletin of Mathematical Biology*, 67(6):1157–1172.

Curtis Dyna-fog (2013). CDC Light Trap 2506 Manual. Available at `http://www.dynafog.com/wp-content/uploads/2015/07/Light-Trap-2506-Manual-June-12-2013.pdf`.

De Meillon, B., Sebastian, A., and Khan, Z. (1967). The duration of egg, larval and pupal stages of *Culex pipiens* fatigans in Rangoon, Burma. *Bulletin of the World Health Organization*, 36(1):7.

Dietz, K. (1993). The estimation of the basic reproduction number for infectious diseases. *Statistical Methods in Medical Research*, 2(1):23–41.

Dodson, B. L. and Rasgon, J. L. (2017). Vector competence of *Anopheles* and *Culex* mosquitoes for Zika virus. *PeerJ*, 5:e3096.

Dohm, D. J., O'Guinn, M. L., and Turell, M. J. (2002). Effect of environmental temperature on the ability of *Culex pipiens* (Diptera: Culicidae) to transmit West Nile virus. *Journal of Medical Entomology*, 39(1):221–225.

Dusek, R. J., McLean, R. G., Kramer, L. D., Ubico, S. R., II, A. P. D., Ebel, G. D., and Guptill, S. C. (2009). Prevalence of West Nile virus in migratory birds during spring and fall migration. *American Journal of Tropical Medicine and Hygiene*, 81(6):1151–1158.

Edman, J. D. and Taylor, D. J. (1968). *Culex nigripalpus*: seasonal shift in the bird-mammal feeding ratio in a mosquito vector of human encephalitis. *Science*, 161:67–68.

Epopa, P. S., Millogo, A. A., Collins, C. M., North, A., Tripet, F., Benedict, M. Q., and Diabate, A. (2017). The use of sequential mark-release-recapture experiments to estimate population size, survival and dispersal of male mosquitoes of the *Anopheles gambiae* complex in Bana, a west African humid Savannah Village. *Parasites & Vectors*, 10(1).

Epstein, P. R. (2001). West Nile virus and the climate. *Journal of Urban Health: Bulletin of the New York Academy of Medicine*, 78(2):367–371.

Fan, G., Liu, J., van den Driessche, P., Wu, J., and Zhu, H. (2010). The impact of maturation delay of mosquitoes on the transmission of West Nile virus. *Mathematical Biosciences*, 228(2):119–126.

Farajollahi, A., Fonseca, D. M., Kramer, L. D., and Kilpatrick, A. M. (2011). "Bird biting" mosquitoes and human disease: A review of the role of *Culex pipiens complex* mosquitoes in epidemiology. *Infection, Genetics and Evolution*, 11(7):1577–1585.

Farfán-Ale, J. A., Blitvich, B. J., Loroño-Pino, M. A., Marlenee, N. L., Rosado-Paredes, E. P., García-Rejón, J. E., Flores-Flores, L. F., Chulim-Perera, L., López-Uribe, M., Pérez-Mendoza, G., Sánchez-Herrera, I., Santamaría, W., Moo-Huchim, J., Gubler, D. J., Cropp, B. C., Calisher, C. H., and Beaty, B. J. (2004). Longitudinal studies of West Nile virus infection in avians, Yucatán State, México. *Vector-Borne and Zoonotic Diseases*, 4(1):3–14.

Florida Coordinating Council on Mosquito Control (1998). The state of the mission as defined by mosquito controllers, regulators, and environmental managers.

Gardner, A. M., Hamer, G. L., Hines, A. M., Newman, C. M., Walker, E. D., and Ruiz, M. O. (2012). Weather variability affects abundance of larval *Culex* (Diptera: Culicidae) in storm water catch basins in Suburban Chicago. *Journal of Medical Entomology*, 49(2):270–276.

Gill, F. B. (1994). *Ornithology*. Macmillan.

Gong, H., DeGaetano, A. T., and Harrington, L. C. (2011). Climate-based models for West Nile *Culex* mosquito vectors in the Northeastern US. *International Journal of Biometeorology*, 55(3):435–446.

Government of Canada (2006). Historical climate data. Toronto Lester B. Pearson IntL A. Available at `http://climate.weather.gc.ca/index_e.html`.

Government of Canada (2011). Historical climate data. Toronto Lester B. Pearson IntL A. Available at `http://climate.weather.gc.ca/index_e.html`.

Government of Canada (2015). Treatment of West Nile virus. *West Nile virus. Diseases and conditions.* Available at `http://healthycanadians.gc.ca/diseases-conditions-maladies-affections/disease-maladie/west-nile-nil-occidental/treatment-traitement-eng.php`.

Government of Canada (2018). Surveillance of West Nile virus. Available at https://www.canada.ca/en/public-health/services/diseases/west-nile-virus/surveillance-west-nile-virus.html.

Greenberg, J. A., DiMenna, M. A., Hanelt, B., and Hofkin, B. V. (2012). Analysis of post-blood meal flight distances in mosquitoes utilizing zoo animal blood meals. *Journal of Vector Ecology*, 37(1):83–89.

Griffing, S. M., Kilpatrick, A. M., Clark, L., and Marra, P. P. (2007). Mosquito landing rates on nesting American robins (Turdus migratorius). *Vector-Borne and Zoonotic Diseases*, 7(3):437–443.

Gu, W., Lampman, R., and Novak, R. (2004). Assessment of arbovirus vector infection rates using variable size pooling. *Medical and Veterinary Entomology*, 18(2):200–204.

Gu, W., Lampman, R., and Novak, R. J. (2003). Problems in estimating mosquito infection rates using minimum infection rate. *Journal of Medical Entomology*, 40(5):595–596.

Gu, W. and Novak, R. J. (2004). Detection probability of arbovirus infection in mosquito populations. *The American Journal of Tropical Medicine and Hygiene*, 71(5):636–638.

Gubler, D. J. (2007). The continuing spread of West Nile virus in the western hemisphere. *Clinical Infectious Diseases*, 45(8):1039–1046.

Guedes, D. R., Paiva, M. H., Donato, M. M., Barbosa, P. P., Krokovsky, L., dos S Rocha, S. W., Saraiva, K. L., Crespo, M. M., Rezende, T. M., Wallau, G. L., Barbosa, R. M., Oliveira, C. M., Melo-Santos, M. A., Pena, L., Cordeiro, M. T., de O Franca, R. F., de Oliveira, A. L., Peixoto, C. A., Leal, W. S., and Ayres, C. F. (2017). Zika virus replication in the mosquito *Culex quinquefasciatus* in Brazil. *Emerging Microbes & Infections*, 6(8):e69.

Hamer, G. L., Anderson, T. K., Donovan, D. J., Brawn, J. D., Krebs, B. L., Gardner, A. M., Ruiz, M. O., Brown, W. M., Kitron, U. D., Newman, C. M., Goldberg, T. L., and Walker, E. D. (2014). Dispersal of adult *Culex* mosquitoes in an urban West Nile virus hotspot: a mark-capture study incorporating stable isotope enrichment of natural larval habitats. *PLoS Neglected Tropical Diseases*, 8(3):e2768.

Hamer, G. L., Chaves, L. F., Anderson, T. K., Kitron, U. D., Brawn, J. D., Ruiz, M. O., Loss, S. R., Walker, E. D., and Goldberg, T. L. (2011). Fine-scale variation in vector host use and force of infection drive localized patterns of West Nile virus transmission. *PLoS ONE*, 6(8):e23767.

Hamer, G. L., Kitron, U. D., Goldberg, T. L., Brawn, J. D., Loss, S. R., Ruiz, M. O., Hayes, D. B., and Walker, E. D. (2009). Host selection by *Culex pipiens* mosquitoes and West Nile virus amplification. *The American Journal of Tropical Medicine and Hygiene*, 80(2):268–278.

Hamer, G. L., Walker, E. D., Brawn, J. D., Loss, S. R., Ruiz, M. O., Goldberg, T. L., Schotthoefer, A. M., Brown, W. M., Wheeler, E., and Kitron, U. D. (2008). Rapid amplification of West Nile virus: the role of hatch-year birds. *Vector-Borne and Zoonotic Diseases*, 8(1):57–68.

Hassan, H. K., Cupp, E. W., Hill, G. E., Katholi, C. R., Klingler, K., and Unnasch, T. R. (2003). Avian host preference by vectors of Eastern Equine Encephalomyelitis virus. *The American Journal of Tropical Medicine and Hygiene*, 69(6):641–647.

Heffernan, J., Smith, R., and Wahl, L. (2005). Perspectives on the basic reproductive ratio. *Journal of The Royal Society Interface*, 2(4):281–293.

Hemingway, J. and Ranson, H. (2000). Insecticide resistance in insect vectors of human disease. *Annual Review of Entomology*, 45(1):371–391.

Jiang, J., Qiu, Z., Wu, J., and Zhu, H. (2009). Threshold conditions for West Nile virus outbreaks. *Bulletin of Mathematical Biology*, 71(3):627–647.

Karki, S., Hamer, G. L., Anderson, T. K., Goldberg, T. L., Kitron, U. D., Krebs, B. L., Walker, E. D., and Ruiz, M. O. (2016). Effect of trapping methods, weather, and landscape on estimates of the *Culex* vector mosquito abundance. *Environmental Health Insights*, 10:EHI.S33384.

Kilpatrick, A. M., Daszak, P., Jones, M. J., Marra, P. P., and Kramer, L. D. (2006a). Host heterogeneity dominates West Nile virus transmission. *Proceedings of the Royal Society B: Biological Sciences*, 273(1599):2327–2333.

Kilpatrick, A. M., Kramer, L. D., Campbell, S. R., Alleyne, E. O., Dobson, A. P., and Daszak, P. (2005). West Nile virus risk assessment and the bridge vector paradigm. *Emerging Infectious Diseases*, 11(3):425–429.

Kilpatrick, A. M., Kramer, L. D., Jones, M. J., Marra, P. P., and Daszak, P. (2006b). West Nile virus epidemics in North America are driven by shifts in mosquito feeding behavior. *PLoS Biology*, 4(4):e82.

Kilpatrick, A. M., Kramer, L. D., Jones, M. J., Marra, P. P., Daszak, P., and Fonseca, D. M. (2007). Genetic influences on mosquito feeding behavior and the emergence of zoonotic pathogens. *The American Journal of Tropical Medicine and Hygiene*, 77(4):667–671.

Kipp, A. M., Lehman, J. A., Bowen, R. A., Fox, P. E., Stephens, M. R., Klenk, K., Komar, N., and Bunning, M. L. (2006). West Nile virus quantification in feces of experimentally infected American and fish crows. *The American Journal of Tropical Medicine and Hygiene*, 75(4):688–690.

Koenig, W. D., Marcus, L., Scott, T. W., and Dickinson, J. L. (2007). West Nile virus and California breeding bird declines. *EcoHealth*, 4(1):18–24.

Komar, N., Burns, J., Dean, C., Panella, N. A., Dusza, S., and Cherry, B. (2001). Serologic evidence for West Nile virus infection in birds in Staten Island, New York, after an outbreak in 2000. *Vector-Borne and Zoonotic Diseases*, 1(3):191–196.

Komar, N., Langevin, S., Hinten, S., Nemeth, N., Edwards, E., Hettler, D., Davis, B., Bowen, R., and Bunning, M. (2003a). Experimental infection of North American birds with the New York 1999 strain of West Nile virus. *Emerging Infectious Diseases*, 9(3):311.

Komar, O., Robbins, M. B., Klenk, K., Blitvich, B. J., Marlenee, N. L., Burkhalter, K. L., Gubler, D. J., Gonzálvez, G., Peña, C. J., Peterson, A. T., and Komar, N. (2003b). West Nile virus transmission in resident birds, Dominican Republic. *Emerging Infectious Diseases*, 9(10):1299–1302.

Kopp, A., Gillespie, T. R., Hobelsberger, D., Estrada, A., Harper, J. M., Miller, R. A., Eckerle, I., Müller, M. A., Podsiadlowski, L., Leendertz, F. H., et al. (2013). Provenance and geographic spread of St. Louis Encephalitis virus. *MBio*, 4(3).

Kramer, L. D., Styer, L. M., and Ebel, G. D. (2008). A global perspective on the epidemiology of West Nile virus. *Annual Review of Entomology*, 53(1):61–81.

Kulasekera, V. L., Kramer, L., Nasci, R. S., Mostashari, F., Cherry, B., Trock, S. C., Glaser, C., and Miller, J. R. (2001). West Nile virus infection in mosquitoes, birds, horses, and humans, Staten Island, New York, 2000. *Emerging Infectious Diseases*, 7(4):722.

Ladd B, F. J. (2003). Management of ponds, wetlands, and other water reservoirs to minimize mosquitoes. *Purdue Extension Water Quality Team*.

Lampman, R. L., Krasavin, N. M., Ward, M. P., Beveroth, T. A., Lankau, E. W., Alto, B. W., Muturi, E., and Novak, R. J. (2013). West Nile virus infection rates and avian serology in East-Central Illinois. *Journal of the American Mosquito Control Association*, 29(2):108–122.

Landesman, W. J., Allan, B. F., Langerhans, R. B., Knight, T. M., and Chase, J. M. (2007). Inter-annual associations between precipitation and human incidence of West Nile virus in the United States. *Vector-Borne and Zoonotic Diseases*, 7(3):337–343.

Langevin, S. A., Bunning, M., Davis, B., and Komar, N. (2001). Experimental infection of chickens as candidate sentinels for West Nile virus. *Emerging Infectious Diseases*, 7(4):726.

Levine, R. S., Hedeen, D. L., Hedeen, M. W., Hamer, G. L., Mead, D. G., and Kitron, U. D. (2017). Avian species diversity and transmission of West Nile virus in Atlanta, Georgia. *Parasites & Vectors*, 10(1).

Lewis, M., Rencławowicz, J., and van den Driessche, P. (2006a). Traveling waves and spread rates for a West Nile virus model. *Bulletin of Mathematical Biology*, 68(1):3–23.

Lewis, M. A., Rencławowicz, J., van den Driessche, P., and Wonham, M. (2006b). A comparison of continuous and discrete-time West Nile virus models. *Bulletin of Mathematical Biology*, 68(3):491–509.

Lindgren, C. J., Postey, R., Smet, K. D., Higgs, C., and Thompson, A. B. (2009). West Nile virus as a cause of death among endangered Eastern Loggerhead Shrikes, Lanius ludovicianus migrans, in West St. Paul, Manitoba. *The Canadian Field-Naturalist*, 123(1):7.

Lines, J., Curtis, C., Wilkes, T., and Njunwa, K. (1991). Monitoring human-biting mosquitoes (Diptera: Culicidae) in Tanzania with light-traps hung beside mosquito nets. *Bulletin of Entomological Research, Cambridge Univ Pres*, 81:77–84.

Lončarić, Ž. and Hackenberger, B. K. (2013). Stage and age structured *Aedes vexans* and *Culex pipiens* (Diptera: Culicidae) climate-dependent matrix population model. *Theoretical Population Biology*, 83:82–94.

Loss, S. R., Hamer, G. L., Goldberg, T. L., Ruiz, M. O., Kitron, U. D., Walker, E. D., and Brawn, J. D. (2009). Nestling passerines are not important hosts for amplification of West Nile virus in Chicago, Illinois. *Vector-Borne and Zoonotic Diseases*, 9(1):13–18.

Mahmood, F., Chiles, R. E., Fang, Y., Barker, C. M., and Reisen, W. K. (2004). Role of nestling mourning doves and house finches as amplifying hosts of St. Louis Encephalitis virus. *Journal of Medical Entomology*, 41(5):965–972.

Mandal, S., Sarkar, R., and Sinha, S. (2011). Mathematical models of malaria - a review. *Malaria Journal*, 10(1):202.

Marino, S., Hogue, I. B., Ray, C. J., and Kirschner, D. E. (2008). A methodology for performing global uncertainty and sensitivity analysis in systems biology. *Journal of Theoretical Biology*, 254(1):178–196.

Mboera, L., Kihonda, J., Braks, M., and Knols, B. (1998). Short report: Influence of centers for disease control light trap position, relative to a human-baited bed net, on catches of *Anopheles gambiae* and *Culex quinquefasciatus* in Tanzania. *The American Journal of Tropical Medicine and Hygiene*, 59(4):595–596.

McKee, E. M., Walker, E. D., Anderson, T. K., Kitron, U. D., Brawn, J. D., Krebs, B. L., Newman, C., Ruiz, M. O., Levine, R. S., Carrington, M. E., McLean, R. G., Goldberg, T. L., and Hamer, G. L. (2015). West Nile virus antibody decay rate in free-ranging birds. *Journal of Wildlife Diseases*, 51(3):601–608.

McLaughlin, R. and Focks, D. (1990). Effects of cattle density on New Jersey light trap mosquito captures in the rice/cattle agroecosystem of southwestern Louisiana. *Journal of the American Mosquito Control Association*, 6(2):283–286.

McLean, R. G. (2006). West Nile virus in North American birds. *Ornithological Monographs*, pages 44–64.

McLean, R. G., Ubico, S. R., Docherty, D. E., Hansen, W. R., Sileo, L., and McNamara, T. S. (2001). West Nile virus transmission and ecology in birds. *Annals of the New York Academy of Sciences*, 951(1):54–57.

Michigan Mosquito Control Association (2018). Mosquito Surveillance. Available at `http://www.cdc.gov/malaria/about/disease.html`.

Miller, B. R., Godsey, M. S., Crabtree, M. B., Savage, H. M., Al-Mazrao, Y., Al-Jeffri, M. H., Abdoon, A.-M. M., Al-Seghayer, S. M., Al-Shahrani, A. M., and Ksiazek, T. G. (2002). Isolation and genetic characterization of Rift Valley fever virus from *Aedes vexans arabiensis*, Kingdom of Saudi Arabia. *Emerging Infectious Diseases*, 8(12):1492–1494.

Molaei, G., Andreadis, T. G., Armstrong, P. M., Anderson, J. F., and Vossbrinck, C. R. (2006). Host feeding patterns of *Culex* mosquitoes and West Nile virus transmission, northeastern United States. *Emerging Infectious Diseases*, 12(3):468.

Møller, A. P. (2013). Long-term trends in wind speed, insect abundance and ecology of an insectivorous bird. *Ecosphere*, 4(1):art6.

Moore, C. G., McLean, R., Mitchell, C. J., Nasci, R., Tsai, T., Calisher, C., Marfin, A., Moore, P., and Gubler, D. (1993). *Guidelines for arbovirus surveillance programs in the United States*, volume 500. US Department of Health and Human Services, Public Health Service, Centers for Disease Control and Prevention, National Center for Infectious Diseases, Division of Vector-Borne Infectious Diseases.

Mpho, M., Holloway, G., and Callaghan, A. (2000). Fluctuating wing asymmetry and larval density stress in *Culex quinquefasciatus* (Diptera: Culicidae). *Bulletin of Entomological Research*, 90(03).

Mullen, G. R. and Durden, L. A. (2009). *Medical and veterinary entomology*. Academic Press.

Nash, D., Mostashari, F., Fine, A., Miller, J., O'Leary, D., Murray, K., Huang, A., Rosenberg, A., Greenberg, A., Sherman, M., Wong, S., Campbell, G. L., Roehrig, J. T., Gubler, D. J., Shieh, W.-J., Zaki, S., Smith, P., and Layton, M. (2001). The outbreak of West Nile virus infection in the New York City area in 1999. *New England Journal of Medicine*, 344(24):1807–1814.

Nemeth, N., Gould, D., Bowen, R., and Komar, N. (2006). Natural and experimental West Nile virus infection in five raptor species. *Journal of Wildlife Diseases*, 42(1):1–13.

Nemeth, N. M., Oesterle, P. T., and Bowen, R. A. (2009). Humoral immunity to West Nile virus is long-lasting and protective in the house sparrow (Passer domesticus). *The American Journal of Tropical Medicine and Hygiene*, 80 5:864–9.

Newhouse, V. F., Chamberlain, R., Johnston, J., Sudia, W. D., et al. (1966). Use of dry ice to increase mosquito catches of the CDC miniature light trap. *Mosq. News*, 26:30–35.

Otero, M., Solari, H. G., and Schweigmann, N. (2006). A stochastic population dynamics model for *Aedes aegypti*: formulation and application to a city with temperate climate. *Bulletin of Mathematical Biology*, 68(8):1945–1974.

Petersen, L. R. and Marfin, A. A. (2002). West Nile virus: a primer for the clinician. *Annals of Internal Medicine*, 137(3):173.

Peterson, A. T., Vieglais, D. A., and Andreasen, J. K. (2003). Migratory birds modeled as critical transport agents for West Nile virus in North America. *Vector-Borne and Zoonotic Diseases*, 3(1):27–37.

Public Health Ontario (2014). Eastern Equine Encephalitis virus. Available at https://www.publichealthontario.ca/en/eRepository/Eastern_Equine_Encephalitis_Virus_Report_2014.pdf.

Public Health Ontario (2018). Definitions for vector surveillance reports. Available at https://www.publichealthontario.ca/en/DataAndAnalytics/Documents/WNV%20surveillance%20reports%20definitions.pdf.

Qi, R., Zhang, L., and wu Chi, C. (2008). Biological characteristics of dengue virus and potential targets for drug design. *Acta Biochimica et Biophysica Sinica*, 40(2):91–101.

Rajagopalan, P., Yasuno, M., Menon, P., et al. (1976). Density effect on survival of immature stages of *Culex pipiens fatigans* in breeding sites in Delhi villages. *Indian Journal of Medical Research*, 64(5):688–708.

Rao, V. S. H. and Durvasula, R. (2013). *Dynamic models of infectious diseases*, volume 1. Springer.

Rappole, J. (2000). Migratory birds and spread of West Nile virus in the western hemisphere. *Emerging Infectious Diseases*, 6(4):319–328.

Reed, K. D., Meece, J. K., Henkel, J. S., and Shukla, S. K. (2003). Birds, migration and emerging zoonoses: West Nile virus, lyme disease, influenza A and enteropathogens. *Clinical Medicine & Research*, 1(1):5–12.

Region of Peel (2002). West Nile virus in the region of Peel. Available at https://www.peelregion.ca/health/vbd/files/technical-report-2002/adult-mosquito-surveillance.pdf.

Region of Peel (2006). Adult Mosquito Surveillance. *West Nile virus in the Region of Peel*. Available at https://www.peelregion.ca/health/vbd/pdfs/2006-report/2006-wnv-tr-adult-mosq.pdf.

Region of Peel (2011). Vector-borne disease prevention plan. Available at https://www.peelregion.ca/health/vbd/pdf/2011-vbd%20plan.pdf.

Region of Peel (2012). The 2011 vector-borne disease in the Region of Peel. *Adult Mosquito Surveillance*. Available at https://www.peelregion.ca/health/vbd/pdfs/2012/vbd-report2011-june14-2012.pdf.

Region of Peel (2013). Vector-borne disease report 2012. Available at https://www.peelregion.ca/health/vbd/pdfs/2012/2012-vbd-report-may-2013.pdf.

Region of Peel (2015). Vector-borne disease prevention plan. Available at http://www.peelregion.ca/health/vbd/resources/pdf/vbd-2015.pdf.

Region of Peel (2016). West Nile virus in Peel, September 25 September 30, 2006. Available at http://www.peelregion.ca/health/vbd/updates/pdf/2016/peel-wnv-update-sept-25.pdf.

Reisen, W. K. (1995). Effect of temperature on *Culex tarsalis* (Diptera: Culicidae) from the Coachella and San Joaquin Valleys of California. *Journal of Medical Entomology*, 32(5):636–645.

Reisen, W. K., Barker, C. M., Carney, R., Lothrop, H. D., Wheeler, S. S., Wilson, J. L., Madon, M. B., Takahashi, R., Carroll, B., Garcia, S., Fang, Y., Shafii, M., Kahl, N., Ashtari, S., Kramer, V., Glaser, C., and Jean, C. (2006a). Role of corvids in epidemiology of West Nile virus in Southern California. *Journal of Medical Entomology*, 43(2):356–367.

Reisen, W. K., Fang, Y., and Martinez, V. M. (2006b). Effects of temperature on the transmission of West Nile virus by *Culex tarsalis* (Diptera: Culicidae). *Journal of Medical Entomology*, 43(2):309–317.

Reisen, W. K., Meyer, R. P., Cummings, R. F., and Delgado, O. (2000). Effects of trap design and CO2 presentation on the measurement of adult mosquito abundance using Centers for Disease Control-style miniature light traps. *Journal of the American Mosquito Control Association*, 16(1):13–18.

Reisen, W. K., Wheeler, S., Armijos, M. V., Fang, Y., Garcia, S., Kelley, K., and Wright, S. (2009). Role of communally nesting ardeid birds in the epidemiology of West Nile virus revisited. *Vector-Borne and Zoonotic Diseases*, 9(3):275–280.

Reiskind, M. H., Walton, E. T., and Wilson, M. L. (2004). Nutrient-dependent reduced growth and survival of larval *Culex restuans* (Diptera: Culicidae): laboratory and field experiments in Michigan. *Journal of Medical Entomology*, 41(4):650–656.

Ringia, A. M., Blitvich, B. J., Koo, H.-Y., de Wyngaerde, M. V., Brawn, J. D., and Novak, R. J. (2004). Antibody prevalence of West Nile virus in birds, Illinois, 2002. *Emerging Infectious Diseases*, 10(6):1120–1124.

Rizzoli, A., Bolzoni, L., Chadwick, E. A., Capelli, G., Montarsi, F., Grisenti, M., de la Puente, J. M., Muñoz, J., Figuerola, J., Soriguer, R., Anfora, G., Luca, M. D., and Rosà, R. (2015). Understanding West Nile virus ecology in Europe: *Culex pipiens* host feeding preference in a hotspot of virus emergence. *Parasites & Vectors*, 8(1).

Ross, R. (1915). Some a priori pathometric equations. *British Medical Journal, BMJ Group*, 1:546.

Rozendaal, J. A. (1997). *Vector control: methods for use by individuals and communities*. World Health Organization.

Rubel, F., Brugger, K., Hantel, M., Chvala-Mannsberger, S., Bakonyi, T., Weissenbck, H., and Nowotny, N. (2008). Explaining Usutu virus dynamics in Austria: model development and calibration. *Preventive Veterinary Medicine*, 85(3-4):166–186.

Rueda, L. M., Patel, K. J., Axtell, R. C., and Stinner, R. E. (1990). Temperature-dependent development and survival rates of *Culex quinquefasciatus* and *Aedes aegypti* (Diptera: Culicidae). *Journal of Medical Entomology*, 27(5):892–898.

Ruiz, M. O., Chaves, L. F., Hamer, G. L., Sun, T., Brown, W. M., Walker, E. D., Haramis, L., Goldberg, T. L., and Kitron, U. D. (2010). Local impact of temperature and precipitation on West Nile virus infection in *Culex* species mosquitoes in northeast Illinois, USA. *Parasites & Vectors*, 3(1):19.

Rutledge, C. R., Day, J. F., Lord, C. C., Stark, L. M., and Tabachnick, W. J. (2003). West Nile virus infection rates in *Culex nigripalpus* (Diptera: Culicidae) do not reflect transmission rates in Florida. *Journal of Medical Entomology*, 40(3):253–258.

Savage, H. M., Aggarwal, D., Apperson, C. S., Katholi, C. R., Gordon, E., Hassan, H. K., Anderson, M., Charnetzky, D., McMillen, L., Unnasch, E. A., and Unnasch, T. R. (2007). Host choice and West Nile virus infection rates in blood-fed mosquitoes, including members of the *Culex pipiens complex*, from Memphis and Shelby County, Tennessee, 2002–2003. *Vector-Borne and Zoonotic Diseases*, 7(3):365–386.

Schaeffer, B., Mondet, B., and Touzeau, S. (2008). Using a climate-dependent model to predict mosquito abundance: application to *Aedes (Stegomyia) africanus* and *Aedes (Diceromyia) furcifer* (Diptera: Culicidae). *Infection, Genetics and Evolution*, 8(4):422–432.

Service, M. W. (1980). Effects of wind on the behaviour and distribution of mosquitoes and blackflies. *International Journal of Biometeorology*, 24:347–353.

Service, M. W. (2008). *Medical entomology for students*. Cambridge University Press.

Shaman, J. (2002). Using a dynamic hydrology model to predict mosquito abundances in flood and swamp water. *Emerging Infectious Diseases*, 8(1):8–13.

Shaman, J. and Day, J. F. (2007). Reproductive phase locking of mosquito populations in response to rainfall frequency. *PLoS ONE*, 2(3):e331.

Shaman, J., Spiegelman, M., Cane, M., and Stieglitz, M. (2006). A hydrologically driven model of swamp water mosquito population dynamics. *Ecological Modelling*, 194(4):395–404.

Sharpe, P. J. and DeMichele, D. W. (1977). Reaction kinetics of poikilotherm development. *Journal of Theoretical Biology*, 64(4):649–670.

Simpson, J. E., Hurtado, P. J., Medlock, J., Molaei, G., Andreadis, T. G., Galvani, A. P., and Diuk-Wasser, M. A. (2012). Vector host-feeding preferences drive transmission of multi-host pathogens: West Nile virus as a model system. *Proceedings of the Royal Society B: Biological Sciences*, 279(1730):925–933.

Takeda, T., Whitehouse, C. A., Brewer, M., Gettman, A. D., and Mather, T. N. (2003). Arbovirus surveillance in Rhode Island: assessing potential ecologic and climatic correlates. *Journal of the American Mosquito Control Association*, 19 3:179–89.

Takken, W. and Verhulst, N. O. (2013). Host preferences of blood-feeding mosquitoes. *Annual Review of Entomology*, 58(1):433–453.

Tejerina, E. F., Almeida, F. F. L., and Almirón, W. R. (2009). Bionomics of *Aedes aegypti subpopulations* (Diptera: Culicidae) from Misiones Province, northeastern Argentina. *Acta Tropica*, 109(1):45–49.

Thiemann, T. C., Wheeler, S. S., Barker, C. M., and Reisen, W. K. (2011). Mosquito host selection varies seasonally with host availability and mosquito density. *PLoS Neglected Tropical Diseases*, 5(12):e1452.

Thomas, D. and Urena, B. (2001). A model describing the evolution of West Nile-like encephalitis in New York City. *Mathematical and Computer Modelling*, 34(7-8):771–781.

Toronto and Region Conservation Authority (2014). West Nile virus monitoring. Available at `http://trca.on.ca/the-living-city/monitoring/west-nile-virus-monitoring-program.dot`.

Toronto and Region Conservation Authority and CH2M Hill Canada Ltd. (2016). Inspection and maintenance guide for stormwater management ponds and constructed wetlands. Available at https://sustainabletechnologies.ca/app/uploads/2018/04/SWMFG2016_Guide_April-2018.pdf.

Toronto Water (2015). Landscape design guidelines for stormwater management ponds. Available at https://www.toronto.ca/wp-content/uploads/2017/11/913f-ecs-specs-landscape-Landscape_Design_Guidelines_SWM_Ponds_Sep2015.pdf.

Townson, H. and Nathan, M. B. (2008). Resurgence of chikungunya. *Transactions of the Royal Society of Tropical Medicine and Hygiene*, 102(4):308–309.

Tsoularis, A. and Wallace, J. (2002). Analysis of logistic growth models. *Mathematical Biosciences*, 179(1):21–55.

Tun-Lin, W., Burkot, T. R., and Kay, B. H. (2000). Effects of temperature and larval diet on development rates and survival of the dengue vector *Aedes aegypti* in north Queensland, Australia. *Medical and Veterinary Entomology*, 14(1):31–37.

van den Driessche, P. and Watmough, J. (2002). Reproduction numbers and sub-threshold endemic equilibria for compartmental models of disease transmission. *Mathematical Biosciences*, 180(1-2):29–48.

VanDalen, K. K., Hall, J. S., Clark, L., McLean, R. G., and Smeraski, C. (2013). West Nile virus infection in American robins: new insights on dose response. *PLoS ONE*, 8(7):e68537.

Villela, D. A. M., de Azambuja Garcia, G., and de Freitas, R. M. (2017). Novel inference models for estimation of abundance, survivorship and recruitment in mosquito populations using mark-release-recapture data. *PLOS Neglected Tropical Diseases*, 11(6):e0005682.

Walter, S. D., Hildreth, S. W., and Beaty, B. J. (1980). Estimation of infection rates in populations of organisms using pools of variable size. *American Journal of Epidemiology*, 112(1):124–128.

Wan, H. and Zhu, H. (2010). The backward bifurcation in compartmental models for West Nile virus. *Mathematical Biosciences*, 227(1):20–28.

Wan, H. and Zhu, H. (2014). A new model with delay for mosquito population dynamics. *Mathematical Biosciences and Engineering*, 11(6):1395–1410.

Wang, J., Ogden, N. H., and Zhu, H. (2011). The Impact of weather conditions on *Culex pipiens* and *Culex restuans* (Diptera: Culicidae) abundance: a case study in Peel Region. *Journal of Medical Entomology*, 48(2):468–475.

Wang, Y., Pons, W., Fang, J., and Zhu, H. (2017). The impact of weather and storm water management ponds on the transmission of West Nile virus. *Royal Society Open Science*, 4(8):170017.

Wheye, P., Dobkin, D., and Ehrlich, D. (1988). The birder's handbook: a field guide to the natural history of North American birds. *Fireside, New York, NY*.

Wilke, A. B. B. and Marrelli, M. T. (2015). Paratransgenesis: a promising new strategy for mosquito vector control. *Parasites & Vectors*, 8(1).

Wonham, M. J., de Camino-Beck, T., and Lewis, M. A. (2004). An epidemiological model for West Nile virus: invasion analysis and control applications. *Proceedings of the Royal Society B: Biological Sciences*, 271(1538):501–507.

Work, T. H., Hurlbut, H. S., and Taylor, R. (1955). Indigenous wild birds of the Nile delta as potential West Nile virus circulating reservoirs. *Am J Trop Med Hyg*, 4:872–88.

World Health Organization (2016). West Nile virus. *Media centre*. Available at `http://www.who.int/mediacentre/factsheets/fs354/en/`.

World Health Organization (2017). Vector-borne diseases. *Media centre*. Available at `http://www.who.int/news-room/fact-sheets/detail/vector-borne-diseases`.

World Health Organization (2018). Mosquito-borne diseases. *Neglected tropical diseases*. Available at `http://www.who.int/neglected_diseases/vector_ecology/mosquito-borne-diseases/en/`.

Yasuno, M. and Tonn, R. J. (1970). A study of biting habits of *Aedes aegypti* in Bangkok, Thailand. *World Health Organ.*, 43:319.

Zimmer, P. (2005). West Nile virus national report on dead bird surveillance. *Canadian Cooperative Wildlife Health Centre*.